Characterization of PdpC, a protein encoded by the *Francisella* pathogenicity island

by

Eli Beauford Nix
B.Sc., Lakehead University, 2004

A Dissertation Submitted in Partial Fulfillment of the
Requirements for the Degree of

DOCTOR OF PHILOSOPHY

in the Department of Biochemistry and Microbiology

Supervisory Committee

Characterization of PdpC, a protein encoded by the *Francisella* pathogenicity island

by

Eli Beauford Nix
B.Sc., Lakehead University, 2004

Supervisory Committee:

Dr. Francis E. Nano, (Department of Biochemistry and Microbiology)
Supervisor

Dr. Stephen V. Evans, (Department of Biochemistry and Microbiology)
Departmental Member

Dr. Terry Pearson, (Department of Biochemistry and Microbiology)
Departmental Member

Dr. Real Roy, (Department of Biology)
Outside Member

Abstract

Supervisory Committee:
Dr. Francis E. Nano, (Department of Biochemistry and Microbiology)
Supervisor
Dr. Stephen V. Evans, (Department of Biochemistry and Microbiology)
Departmental Member
Dr. Terry Pearson, (Department of Biochemistry and Microbiology)
Departmental Member
Dr. Real Roy, (Department of Biology)
Outside Member

Tularemia is a zoonotic disease caused by the bacterial pathogen *Francisella*. A major virulence determinant of *Francisella* is the ability to survive and multiply within macrophages. Previous research identified a genetic element of approximately 30 kb in length, which possessed characteristics typical of a pathogenicity island. In *F. novicida,* the *Francisella* pathogenicity island (FPI) is composed of 18 genes. Initial studies revealed that several FPI-encoded genes are required for intramacrophage growth. The FPI contains several homologues of a newly described type six secretion system (T6SS).

I developed a chicken embryo infection model to provide a simple, low-cost assay to evaluate the virulence of *Francisella* strains. The results demonstrate that this assay is able to discriminate large differences in virulence among *Francisella* strains. Further, this system can facilitate large-scale experiments to quickly survey mutant collections for virulence, while reducing animal suffering.

Next, I adapted a genetic technique called co-transformation for use in *Francisella*. This technique facilitates the introduction of mutant or wild type DNA into the chromosome, without requiring the introduction of antibiotic resistance markers or negative selection markers. I also

developed two new *Francisella* shuttle vectors for use in complementation studies. I demonstrated that these vectors are compatible with other pFNL-10-based *Francisella* shuttle vectors. They also permit tri-parental mating, allowing researchers to circumvent the restriction modification system in *F. novicida*. Finally, conjugation removes the need for electroporation equipment, which can create aerosols. These aerosols can represent a potential health risk for researchers studying highly virulent *Francisella* strains.

The FPI gene *pdpC* was investigated for its role in virulence and intramacrophage growth. We found that *pdpC* was dispensable for growth in macrophages but required for virulence in two animal models. Microscopy studies using epitope tagged *pdpC* suggest that the protein may be secreted during macrophage infection. Quantitative microscopy provides evidence that PdpE (the gene immediately downstream of PdpC) is secreted in a T6SS dependent manner.

Additional mutations in the *pdpC* gene revealed an effect upon the expression of the Igl proteins located in the minor FPI operon. The mechanism linking *pdpC* to *iglA-D* expression is unknown, but it is unlikely to be post-translational in nature. The genetic basis for this effect has been difficult to define, but we have developed a working hypothesis. We propose that two genetic mutations in *pdpC* are required; the first consists of a defined deletion in the N-terminal-half of the gene, while the second consists of an undefined region located at the C-terminal end.

Table of Contents

Supervisory Committee ii
Abstract iii
Table of Contents v
List of Tables ix
List of Figures x
List of Abbreviations xii
Acknowledgements xviii
Dedication xix

Chapter 1: Introduction 1
1.1 *Francisella tularensis* 1
1.1.1 Discovery of Bacterium *tularensis* 2
1.1.2 The disease tularemia 3
1.1.3 Relevant strains of *Francisella* 3
1.1.4 *Francisella* as a biological weapon 5
1.1.5 Tularemia vaccines 7
1.1.6 Treatment of tularemia 8
1.2 Mechanisms of bacterial genomic evolution 9
1.2.1 Mutations and genetic transfer 9
1.2.2 Genomic islands 11
1.2.3 Pathogenicity islands 12
1.2.4 The Francisella pathogenicity island 15
1.3 Type VI secretion 17
1.3.1 Discovery of the Type VI secretion system 17
1.4 Intracellular lifestyle of *Francisella* 21
1.4.1 Uptake of *Francisella* by macrophages 21
1.4.2 Escape from the phagosome 25
1.4.3 Intramacrophage signalling 27

Chapter 2: Virulence of *Francisella* spp. in Chicken Embryos 29
2.1 Introduction 29

2.2 Materials and methods 31
2.2.1 Bacterial strains and growth conditions 31
2.2.2 Chicken embryo infections 31
2.2.3 Microscopy 32
2.3 Results and discussion 33
2.3.1 Growth of *F. tularensis* in 7-day-old chicken embryos 33
2.3.2 Virulence of *F. novicida* 34
2.3.3 Virulence of LVS 35
2.3.4 Virulence of mutants of *F. novicida* 36
2.3.5 *F. tularensis* in chicken embryonic tissue 40

Chapter 3: Genetic elements for deletion mutagenesis and complementation in *Francisella* spp. 45
3.1 Introduction 45
3.2 Materials and methods 45
3.2.1 Bacterial strains and growth conditions 45
3.2.2 Transformation and conjugation 46
3.3 Results 47
3.3.1 Deletion mutagenesis via co-transformation with plasmid DNA 47
3.3.2 Engineered broad-host-range plasmids 49
3.4 Discussion 51

Chapter 4: PdpC, a *Francisella* T6SS protein, is required for full virulence but not for intracellular growth. 53
4.1 Introduction 53
4.2 Materials and methods 55
4.2.1 Bacterial strains and plasmids 56
4.2.2 PCR and primer design 56
4.2.3 Recombinant DNA techniques 57
4.2.4 Targeted integration of 3xFLAG tag into the *F. novicida* chromosome 58
4.2.5 Chemical transformation of *F. novicida* 59
4.2.6 SDS-PAGE and immunoblotting 59
4.2.7 Macrophage growth assay 60
4.2.8 Chicken embryo and mouse infections 61

4.2.9 Organ burden assays 62
4.2.10 Immunofluorescence microscopy 62
4.3 Results 63
4.3.1 PdpC is expressed in *F. novicida* and LVS 63
4.3.2 *pdpC* is required for virulence in embryonated chicken eggs 65
4.3.3 *pdpC* is required for full virulence in mice 66
4.3.4 *pdpC* is not required for intramacrophage growth 67
4.3.5 Reduced virulence of the Δ*pdpC* is not due to effects on *pdpE* 68
4.3.6 Reduced accumulation of *pdpC* mutants in the liver of chicken embryos 70
4.3.7 PdpC is localized to the host cells during infection 71
4.3.8 PdpE is secreted in a *pdpB* dependent manner 76
4.4 Discussion 79

Chapter 5: Mutagenesis of the FPI gene *pdpC* alters expression of intracellular growth locus genes ABCD. 82
5.1 Introduction 82
5.2 Materials and methods 84
5.2.1 Bacterial strains and plasmids 84
5.2.2 Polymerase chain reaction and primer design 86
5.2.3 Recombinant DNA techniques 87
5.2.4 Chemical transformation of *F. novicida* 87
5.2.5 Deletion mutagenesis 88
5.2.6 Restoration of mutant to wild type genotype 89
5.2.7 DNA sequence and analysis 89
5.2.8 SDS-PAGE and immunoblotting 89
5.2.9 Macrophage growth assay 90
5.2.10 Chicken embryo infections 91
5.2.11 Subcellular fractionation 91
5.2.12 NADH oxidase assay 92
5.3 Results 93
5.3.1 Membrane association of PdpC 93
5.3.2 Intramacrophage growth phenotypes of *pdpC* mutant strains 95
5.3.3 Correlation of PdpC production with intramacrophage growth 97
5.3.4 Virulence of *pdpC* mutants in a chicken embryo model of infection 98

5.3.5 In a *pdpC*Δ4 background IglABCD are undetectable..... 101

5.3.6 Restoration of *pdpC*Δ4 lesion lead to IglB protein production and wild type phenotype..... 103

5.3.7 The *pdpC*Δ4 phenotype is not ascribed solely to the genetic deletion 4 lesion.... 106

The *pdpC* mutant strains differ in sequence within the intergenic region upstream of *pdpC* 106

5.3.8 Selective marking and transfer of *pdpC*Δ4 DNA into an IglC permissive strain blocks IglC expression..... 108

5.4 Discussion 111

Chapter 6: Conclusions and future studies..... 117

Chapter 7: Bibliography..... 120

List of Tables

Table 1. *Francisella* sp. strains used in the development of a chicken embryo model of infection. 38

Table 2. Bacterial strains and plasmids used to develop mutagenesis and complementation strategies in *Francisella*. 47

Table 3. Bacterial strains and plasmids used to characterize PdpC. 57

Table 4. Virulence of *F. novicida* strains following intradermal infection of BALB/c mice. 67

Table 5. Bacterial strains and plasmids used to investigate *pdpC* mutant phenotypes. 85

List of Figures

Figure 1. General structure of pathogenicity islands. 14

Figure 2. Diagrammatic representation of the *Francisella* pathogenicity island..... 17

Figure 3. Type I-V secretion systems in Gram-negative bacteria..... 19

Figure 4. Morphology of uptake of various bacterial intracellular pathogens by human macrophages. 23

Figure 5. Growth of LVS and *F. novicida* in chicken embryos..... 34

Figure 6. Reproducibility of the time to death induced by *F. novicida* U112. 35

Figure 7. Virulence of LVS in chicken embryos. 36

Figure 8. Levels of virulence of *F. novicida* strains in chicken embryos. 39

Figure 9. Immunofluorescence of *F. novicida* U112 in chicken embryonic tissues..... 41

Figure 10. Immunofluorescent localization of LVS in chicken embryonic tissues. 43

Figure 11. Deletion mutagenesis in *F. novicida* via co-transformation..... 48

Figure 12. Organization of plasmids pEN1 and pEN2. 50

Figure 13. Identification of PdpC with anti-peptide antibody. 64

Figure 14. Virulence of *F. novicida* Δ*pdpC* mutant during the infection of chicken embryos. .. 66

Figure 15. Intramacrophage growth of Δ*pdpC*. 68

Figure 16. Mutants with insertions in the *pdpE* gene. 70

Figure 17. Poor accumulation of Δ*pdpC* mutant strain in the liver of chicken embryos..... 71

Figure 18. *In trans* PdpC-3xFLAG tag expression during infection of J774A.1 cells. 72

Figure 19. PdpC-3xFLAG expressed from the bacterial chromosome..... 74

Figure 20. Time course of PdpC detection within infected J774A.1 macrophage-like cells..... 76

Figure 21. pKH16 in wild type and a Δ*pdpB* background during infection of J774A.1 cells. 78

Figure 22. Detection of PdpC in subcellular fractions of *F. novicida* in broth-grown versus macrophage-grown cultures. 94

Figure 23. Intramacrophage growth of *F. novicida pdpC* mutants. 95

Figure 24. Diagrammatic representation of the *pdpC* deletion mutants. 97

Figure 25. Western immunoblot probed against PdpC in representative mutant strains. 98

Figure 26. of *F. novicida pdpC* mutants during infection of chicken embryos. 100

Figure 27. Western immunoblot probed for IglA in subcellular fractions of *pdpC*Δ4. 101

Figure 28. Western Immunoblot probed against IglABCD in select mutant strains. 103

Figure 29. Restoration of *pdpC*Δ4 to the wild type phenotype..... 105

Figure 30. *IglJ-pdpC* intergenic consensus sequence. 108

Figure 31. Diagrammatic representation of *pdpC* and *pdpE* transponson mutants accompanied by corresponding Western immunoblots. 110

List of Abbreviations

anmK	anhydro-N-acetylmuramic acid kinase
Ap	ampicillin
Bcl-2	B-cell lymphoma 2
Bid	Bcl-2 interacting domain
BMDM	bone marrow-derived macrophage
ca	circa
CD	cluster of differentiation
cDMEM	complete Dulbecco's modified eagle medium
CFU	colony forming units
Cm	chloramphenicol
DAPI	4',6-diamidino-2-phenylindole
DMEM	Dulbecco's modified eagle medium
DNA	deoxyribonucleic acid
dotU	defect in organelle trafficking U
DPBS	Dulbecco's phosphate buffered saline
DR	direct repeat

EEA1	early endosome antigen 1
Em	erythromycin
Em^R	erythromycin resistance
FBS	fetal bovine serum
FCV	*Francisella*-containing vacuole
FPI	*Francisella* pathogenicity island
FTB	*Francisella* transformation buffer
G + C	guanine + cytosine
GI	genomic island
gp	gene product
GTPase	guanosine triphosphate hydrolase
Hcp	hemolysin co-regulated protein
Hyg	hygromycin
Hyg^R	hygromycin resistance
IAHP	*icmF* associated homologous proteins
icmF	intracellular multiplication gene F
igl	intracellular growth locus

IL	interleukin
int	integrase
IS	insertion element
IS_c	complete insertion element
IS_d	defective insertion element
kb	kilobase
kDa	kilodalton
Kdp	histidine kinase D
Km	kanamycin
Km^R	kanamycin resistance
LAMP	lysosome associated membrane protein
LB	Luria Bertani
LC3-II	light chain 3-II
Lcr	low calcium response
LD	lethal dose
LEE	locus of enterocyte effacement
LPS	lipopolysaccharide

LVS	live vaccine strain
mgl	macrophage growth locus
min	minute
MOI	multiplicity of infection
mRNA	messenger ribonucleic acid
NADH	nicotinamide adenine dinucleotide
NF-κβ	nuclear factor kappa beta
ng	nanogram
nt	nucleotide
ori	origin of replication
PAI	pathogenicity island
PAMP	pathogen associated molecular patterns
PBS	phosphate buffered saline
PCR	polymerase chain reaction
pdp	pathogenesis determinant protein
P_{FT}	*Francisella tularensis* promoter
PI3K	phosphoinositide-3-kinase

PRR	pattern recognition receptors
RNA	ribonucleic acid
RPM	revolutions per minute
RtxA	repeats-in-toxin A
SDS-PAGE	sodium dodecyl sulphate polyacrylamide gel electrophoresis
Sec	secretion
sRNA	small non coding regulatory ribonucleic acid
SSAS	secretion substrate acceptor site
Ssp	stringent starvation protein
T1SS	Type I secretion system
Tat	twin-arginine translocation
TLR	Toll-like receptor
TNF-α	tumor necrosis factor alpha
tRNA	transfer ribonucleic acid
TSA	trypticase soy agar
TSB	trypticase soy broth
ug	microgram

UN	United Nations
US	United States
VAS	virulence-associated secretion
vasK	virulence-associated secretion gene K
vgrG	valine-glycine repeat G
Yop	*Yersinia* outer proteins
Ysc	Yop secretion system

Acknowledgements

I am very lucky to have had the opportunity to study in Dr. Nano's laboratory. He is a supervisor who is always challenging his students to improve, and genuinely wants them to succeed, both in the laboratory and beyond it. Fran, thank you very much for your patience and guidance.

I would also like everyone who worked in the laboratory. Na and Karen for helping me get started and kindly answering any questions I had. Crystal, O.D.B., Ralph, and Barry for listening, trouble shooting, and being good friends. Thanks to Bill, Nancy, Sarah, and Sheila for helping to edit this manuscript.

None of this would have been possible without the love and support of my parents Nancy and Chester and grandparents Gladys and Richard. I am looking forward to living close by again.

Dedication

To my wife Sarah, I love you.

Chapter 1: Introduction

Truly the Earth belongs to the microbes and not man. Consider that the age of the Earth is estimated at 4.5 billion years and that 3.5 billion years ago microbial life was already flourishing (195). During this time bacteria have colonized an amazing variety of ecological niches, from vents near the rim of volcanoes over 6,000 meters above sea level to 1,600 meters beneath the ocean floor (179). Humans have not been overlooked either; it has been reported that the number of microbes persisting in and on our bodies actually outnumber the total human cells by at least a factor of 10, and the bacteria found in our intestinal track alone accounts for an average of one kilogram of our body weight (15). The diversity of bacterial species that have colonized our bodies is remarkable. So far over 500 species have been identified exclusively from the oral cavity and it is estimated that this number could double before a complete survey is finished (224). Given our constant exposure to such a high number and wide variety of bacteria, it is fortunate indeed that only a miniscule fraction of the kingdom Bacteria cause disease in humans. Of those pathogenic bacteria, an even smaller proportion is able to subvert host immune cells such as the macrophage. These bacteria use a variety of specialized adaptations and survival strategies to subvert and overcome the human immune response, surviving against all odds.

1.1 *Francisella tularensis*

Francisella tularensis is a small, Gram-negative, non motile, aerobic coccobacillus. The bacterium causes tularemia, a zoonotic febrile disease, and infects a wide variety of animals

(101). It is frequently associated with aquatic environments and although non-spore forming, the organism can remain viable for years in contaminated mud water suspensions (73, 157). Further as a facultative intracellular pathogen, *Francisella tularensis* possesses the rare ability to replicate within macrophages (7).

1.1.1 Discovery of Bacterium *tularense*

In 1911, McCoy and Chapin discovered the causative agent of what they described as a "plague-like disease of rodents". They named the organism *Bacterium tularense* since their first samples were from Tulare County California (135). Chapin was later stricken with a fever-illness that kept him from work for twenty-eight days, after which his serum tested positive for the presence of antibodies against *Bacterium tularense.* In spite of what would appear to be an obvious connection, the link between the Chapin's illness and the rodent disease was not established. At the same time, in Utah, Pearse clinically described a human disease known as deer-fly fever. It was his belief that the bite of the deer-fly *Chrysops discalis* caused the disease (161). Ten years later, Edward Francis isolated *Bacterium tularense* from several cases of deer-fly fever and local jack rabbits in Utah. He subsequently named the disease tularemia (78). Francis then demonstrated that *Chrysops discalis* could transmit *Bacterium tularense* to laboratory animals (79). Thus it was established that the disease affecting both California ground squirrels and humans in Utah had the same etiology, as well as share an arthropod agent that could transmit it. The bacterium would be placed in the genus *Pasteurella* and then provisionally moved to *Brucella* (155). In 1947 it was suggested that the bacteria should be assigned to a new genus: *Francisella*, in honour of Dr. Edward Francis (57).

1.1.2 The disease tularemia

The clinical manifestation of tularaemia depends upon a number of factors: the strain one is infected with, the route of infection and the dose of infection (54). Generally, symptoms begin to present 3-5 days post-infection and usually include fever and chills, body aches, unproductive cough and nausea (199). Diagnosis of tularemia is challenging since many of the symptoms are non specific and resemble a number of less serious ailments. Infection through the skin or mucus membranes results in ulceroglandular tularemia, which accounts for approximately 80% of total cases (72). A bite from an insect usually initiates infection in this form of the disease, and an ulcer forms at the site of the bite. Remarkably, the ulcer can persist for months. The bacteria disseminate to the regional lymph nodes, which become swollen, and from there, the bacteria can spread to the liver, spleen, lungs, kidneys, central nervous system, intestines and skeletal muscle (66). Mortality rates are reported at less than 3%, however if untreated, recovery can be quite lengthy and relapse can occur (69). Rarely, the eyes are inoculated, usually by infected fingertips causing oculoglandular tularemia, characterized by the appearance of nodules on the ocular surface followed by dispersion to the local lymph nodes (108, 172). Ingestion of infected foodstuffs can lead to oropharyngeal or gastrointestinal tularemia (205). Inhalation of as few as 10 colony forming units (CFU) can cause pneumonoic tularemia. Diagnosis of this form can be difficult since patients often do not show signs typical of a respiratory disease (190).

1.1.3 Relevant strains of *Francisella*

Originally classified within the family Pasteurellaceae, the advent of DNA sequencing revealed that genus *Francisella* was sufficiently unique to warrant its own family designation: Francisellaceae. Currently the family is divided into three species; *noatunensis, philomiragia* and *tularensis.* *F. noatunensis* is a pathogen that affects many fish species, including economically important ones, such as Atlantic salmon and cod (154). *F. philomiragia* is an opportunistic pathogen associated with water that can infect immunocompromised humans (132). *F. tularensis* is further divided into four subspecies; *tularensis, holarctica, mediasiatica* and *novicida*. Although the four subspecies share greater than 95% similarity at the nucleotide level, there are striking differences among them both in terms of geographical distribution and virulence to animals (36).

F. tularensis ssp. *tularensis* (referred to as *F. tularensis* for the remainder of this manuscript) is found nearly exclusively in North America, and causes the most acute and lethal form of tularemia in humans. If untreated, the respiratory form of the disease caused by this strain has a mortality rate between 30-60% (55, 105, 190, 191). *F. tularensis* ssp. *holarctica* (referred to as *F. holarctica* for the remainder of this manuscript) is found throughout the northern hemisphere. It causes a milder disease that is rarely fatal. An attenuated version of this strain was produced by the Soviet Union in the 1940s by repeated passage *in vitro* and through mice by an intraperitoneal route (60). The resultant live vaccine strain (LVS) has been widely used as a model to study the pathogenesis of tularemia. It is an attractive model due to its inability to cause disease in healthy humans, yet still induce a disease in animals that closely resembles human tularemia (188). *F. tularensis* ssp. *mediasiatica* is confined to Central Asia and has not been studied extensively, although in virulence it appears to resemble *F. holarctica* both in humans and lagomorphs (152). *F. tularensis* ssp. *novicida,* (referred to as *F. novicida* for

the remainder of this manuscript) once believed to be distributed exclusively in North America has recently been isolated in Australia, giving credence to the notion that *Francisella* may be more widespread than previously assumed (221). This strain is highly attenuated in humans, with only a handful of reports attributing it to disease and then only in severely immunocompromised individuals (98). As is the case with LVS, *F. novicida* has also been used commonly to study the pathogenesis of tularemia, since its virulence in mice approaches that of *F. tularensis* in humans (162).

1.1.4 *Francisella* as a biological weapon

The great and frightening potential of *F. tularensis* as a biological weapon did not go unnoticed by world powers of the twentieth century. Several characteristics of the pathogen make it an ideal candidate for offensive use. Firstly, it is one of the most infectious agents known to man, with an exceedingly low dose (<10 cells) required to cause disease by inhalation (190). Secondly, tularaemia is not communicable between humans; therefore, an attack would be limited to the initial target zone. Thirdly, in view of the pathogen's ability to persist in a multitude of animal hosts, it is likely that local reservoirs of the disease would be established leading to recurring outbreaks (66).

During the occupation of Manchuria by Japanese forces from 1932 to 1942, Dr. Ishii Shiro directed biological weapons research on many biowarfare agents including *F. tularensis* (211). Ishii and others experimented on unwilling humans and conducted field tests on Chinese villages (6). Shockingly, with the conclusion of the war, scientists directly involved were not tried for crimes against humanity. Instead, in exchange for the data generated inhumanely a

cover up was arranged by the American occupation authorities, and as a result, no high-ranking Japanese biological weapons expert was ever charged with a crime. Many of the scientists involved were recruited by the Soviet Union and United States (US) to further their own programs (96).

In 1969, Nixon terminated the US offensive biological weapons program ceasing any further research and destroying their biological arsenal which included weaponized *Francisella* (43). The 1974 United Nations (UN) convention on biological weapons prohibited the development, possession and stockpiling of pathogens in quantities that could not be justified for prophylactic or other peaceful purposes. Over 100 nations signed the treaty including Iraq and the Soviet Union, however, in practice both nations continued activities prohibited by the convention. After the first Persian Gulf War, Iraqi officials admitted to having an offensive biological weapons program (227). Evidence for a continued Soviet biological weapons program appeared in 1979 when an anthrax epidemic occurred among people who lived within four kilometres of a Soviet military microbiology facility at Ekaterinberg, Russia. Initially, Soviet officials insisted the cause was ingestion of contaminated meat, but in 1992, Yeltsin admitted that the facility was part of an offensive biological weapons program and the epidemic had been caused by the accidental release of anthrax spores. As recently as 1995, a report by the UN estimated that Russia had up to 30,000 people working on its biological warfare program (43).

The UN estimates that dispersal of fifty kilograms of aerosolized *F. tularensis* over a city with a population of five million would result in 250,000 incapacitated casualties and 19,000 deaths. Sickness would be expected to last for several weeks with frequent relapses occurring for months after the initial attack (1). The US Centres for Disease Control and Prevention

estimates the cost of a bioterrorist attack using *F. tularensis* at least 5.4 billion US dollars per 100,000 individuals exposed (109).

Clearly, history has demonstrated that we cannot rely solely upon international treaties or the ethics of scientists to prevent a bioweapon attack. Considering how little bacteriological skill is required to propagate many of the dangerous agents, the major hurdles one would face in the orchestration of a terrorist attack are the acquisition of the strain and method of delivery. Unfortunately due to the expertise left behind from the cold war, it is far more likely that we shall face a biological, rather than nuclear terrorist attack.

1.1.5 Tularemia vaccines

It had been observed that once an individual recovered from a case of tularemia they developed a high degree of natural immunity, even against massive exposures (76). This phenomenon was encouraging since it suggested that a vaccine could likely provide formidable protection. Lee Foshay and coworkers developed a heat-killed vaccine that was used by American laboratory workers in the 1940s, but this vaccine provoked severe side effects. To be well tolerated, the dosage had to be scaled back to the point where daily injections over months were required before agglutination titres approached that of naturally immune individuals (76). This regime was plausible for a small number of laboratory workers but not large-scale vaccinations.

Live attenuated strains derived from *F. holarctica* have been used to vaccinate approximately 60 million people in the former Soviet Union between 1930 and 1960. In 1956 one of these strains was brought to the US, where it was designated LVS (live vaccine strain) and

it was used to vaccinate laboratory workers (201). With the advent of this vaccine, cases of pneumonic tularaemia in laboratory workers decreased sharply, and although the number of cases of ulceroglandular tularaemia was unchanged, the severity was decreased (190).

Numerous studies have demonstrated that LVS vaccination provides good protection in both humans and animals against *F. tularensis* (61, 137, 212, 222, 225). At one point, LVS was given new investigational drug status by the American Food and Drug Administration. This status has been revoked and applications to license the vaccine were rejected. This rejection was based on several factors. First when cultivated, LVS spontaneously produces two phenotypes that differ in their opacity, known as "blue" and "grey" variants. The parental LVS strain is a blue variant, but grey variants arise at a rate of 10^{-3}- 10^{-4} per generation (59). The grey variant is poorly immunogenic and could make up as much as 20% of batch preparations for vaccine production (182). The basis of attenuation was unknown in LVS; therefore the risk of a reversion back to a virulent form could not be calculated (156). Recently, Salomonsson *et al.* identified the two virulence loci responsible for the attenuation of LVS. The genes encode a putative type IV pilin called *pilA* and an outer membrane protein designated FTT0918 (180). Second, vaccination does not provide protection in some individuals and can actually cause a tularemia like infection at a rate of up to 3% (212).

1.1.6 Treatment of tularemia

Historically, the most prevalent antibiotic used in the treatment of tularemia was the aminoglycoside streptomycin. Although clinical trials have never been conducted to evaluate its efficacy, there are over 200 cases of its therapeutic use in the literature. Streptomycin treatment

resulted in a recovery rate greater than 95%; however due to toxicity issues, it is rarely used today (67). Antibiotics which have a bacteriostatic effect, such as tetracycline and chloramphenicol are rarely used because they have often been associated with a relapse. Chloramphenicol has been associated with the condition aplastic anemia (158). Currently, the fluoroquinolone ciprofloxacin is the preferred therapy. In cases where the drug was administered within two weeks of infection, no treatment failures have been reported (123, 164). Ciprofloxacin is a bactericidal drug that prevents bacterial DNA replication by interfering with gyrase and topoisomerase IV resulting in DNA damage (40).

1.2 Mechanisms of bacterial genomic evolution

1.2.1 Mutations and genetic transfer

Bacterial genomes need to change over time in order to cope with alterations to the environment; this process is known as genomic evolution. Genomic change can occur via three basic mechanisms: mutations, deletion or rearrangement of genes, and horizontal gene transfer. Although technically, any heritable change in the DNA qualifies as a mutation, here the term is used in the context of a small discrete change in the DNA. The consequences of small intragenic mutations can be described in three ways: missense, nonsense and frameshift. When a missense mutation occurs, one of the amino acids in the protein is replaced by another. Often this change does not result in the inactivation of the protein since the substituted amino acid may have similar properties or the residue may be superfluous. Nonsense mutations arise when a stop codon is introduced into the open reading frame; this type of mutation almost always results in the inactivation of the gene product. Frameshift mutations take place when DNA sequence is

added or subtracted from the open reading frame that is not a multiple of three. As a result of this change, all codons downstream of the mutation will be different, and thus every amino acid after the mutation will be wrong. This type of mutation often truncates the protein due to the appearance of a stop codon, and nearly always inactivates the protein. All three types of mutation can occur spontaneously, but are not irreversible since a subsequent mutation can cause a reversion to wild-type.

Deletions take place between two regions on the chromosome that are identical or nearly identical, causing a recombination that removes the sequence in between. Genetic rearrangement includes duplications or inversions of parts of the chromosome, and these inversions can cause changes in the expression of affected genes or they can cause a fusion between two genes. Duplications can give rise to additional copies of one or more genes, which is important from an evolutionary perspective since a gene cannot usually change without a loss in its original function. This provides an opportunity for changes to take place, while the other gene provides the original function.

Horizontal gene transfer can be described as the movement of genetic material between bacteria in any method other than by descent, usually occurring between, but not limited to, a phylogenetically distant donor and recipient (121). There are three general methods by which horizontal gene transfer can occur; transformation, conjugation and transduction.

Transformation involves the uptake of naked DNA by a recipient. For this process to happen the cell must first reach a physiological state called “competence”. Some species like *Bacillus subtilis* are naturally prone to transformation of DNA from any source. Others such as *Haemophillus influenzae* only efficiently take up DNA that has a specific recognition sequence.

By virtue of the very high frequency of the recognition sequence in their genomes, a strong bias towards uptake from closely related species is created (202). Environmental stress can also induce competence. For instance, in response to DNA damage caused by an antibiotic, the SOS response increases the competence of the cell, which in turn promotes the spread of antibiotic resistance genes (169).

In conjugation, the exchange of DNA is usually mediated by a plasmid during direct cell to cell contact between a donor and recipient. A tube-like structure known as a pilus facilitates contact in Gram-negative bacteria, while in Gram-positive bacteria this is accomplished by surface-associated adhesions (41). Transduction takes place when a phage acts as the agent for genetic transfer between bacteria. The amount of DNA transferred is limited by the size of the phage head.

1.2.2 Genomic islands

Mutations and the rearrangement of genes usually represent a relatively slow means of alteration. While horizontal gene transfer can represent a “quantum leap” as it can facilitate the acquisition of one or more functional genes from a single event (91). As more bacterial genomes have become sequenced it has became apparent that DNA in a genome can be subdivided into two broad categories. The majority of a genome's sequence (70-80%) is highly conserved, consisting of genes essential to cellular function. This core genome is also characterized by a homogeneous G + C content typical to that bacterial species (82). The remaining sequence (20-30%) forms a discordant jumble of foreign DNA scattered throughout the genome of which large portions contain distinct G + C content. This portion of the genome formed a flexible gene pool

made up of mobile or formerly mobile genetic elements, including large unstable regions designated as "genomic islands" (93).

Broadly speaking, genomic islands (GIs) can be described as discrete DNA segments which differ between closely related species and are associated with some sort of mobile element (107). Bioinformatic studies show that GIs tend to code more "novel" (no detectable homologues in other species) genes than are found in the rest of the genome they are associated with (103). The coding capacities of GIs are very diverse and include traits such as symbiosis, metabolism, resistance, fitness and pathogenesis among others (81, 92, 106, 116, 207).

Despite the expansive nature of GIs, there are various attributes that distinguish them from other genetic elements. They are usually between 10 and 200 kilobases (kb) of DNA in length; and for those smaller than 10 kb, the term genomic "islet" is used (93). GIs usually have different nucleotide statistics than the rest of the genome such as G + C content or codon usage. Often GIs are inserted at tRNA genes and are flanked by 16-20 base pairs (bp) of perfect or near perfect direct repeats which can act as recognition sequences for their enzymatic excision (194). GIs may contain genes or pseudogenes related to plasmid conjugation systems, or phages implicated in promoting their transfer between genomes. Additionally, GIs often harbour insertion elements or transposons that function to add or delete sequence from the GI (31). Finally, GIs contain genes which offer some kind of selective advantage to the genomes in which they reside.

1.2.3 Pathogenicity islands

Pathogenicity islands (PAIs) constitute a subgroup of GIs which encode virulence factors (Fig. 1). The virulence factor must be pathogen enabling to qualify; for instance, an iron uptake system encoded in a soil bacterium that does not confer pathogenicity would be termed a fitness island. The same iron uptake system laterally transferred to another bacterium could represent the final requirement for survival by facilitating iron scavenging in a mammalian host where a paucity of bioavailable iron exists. The latter constitutes a PAI because in that context it is required for pathogenicity. PAIs have been observed to encode a wide variety of virulence factors including toxins, adhesions, invasions, modulins, effectors, superantigens, antibiotic resistance, protein secretion systems I through VI, siderophores, proteases, lipases, O antigen synthesis, serum resistance, and capsule synthesis to name a few (93, 194). Many PIs also encode gene products of unknown function which will likely lead to the discovery of new virulence factors (165, 193).

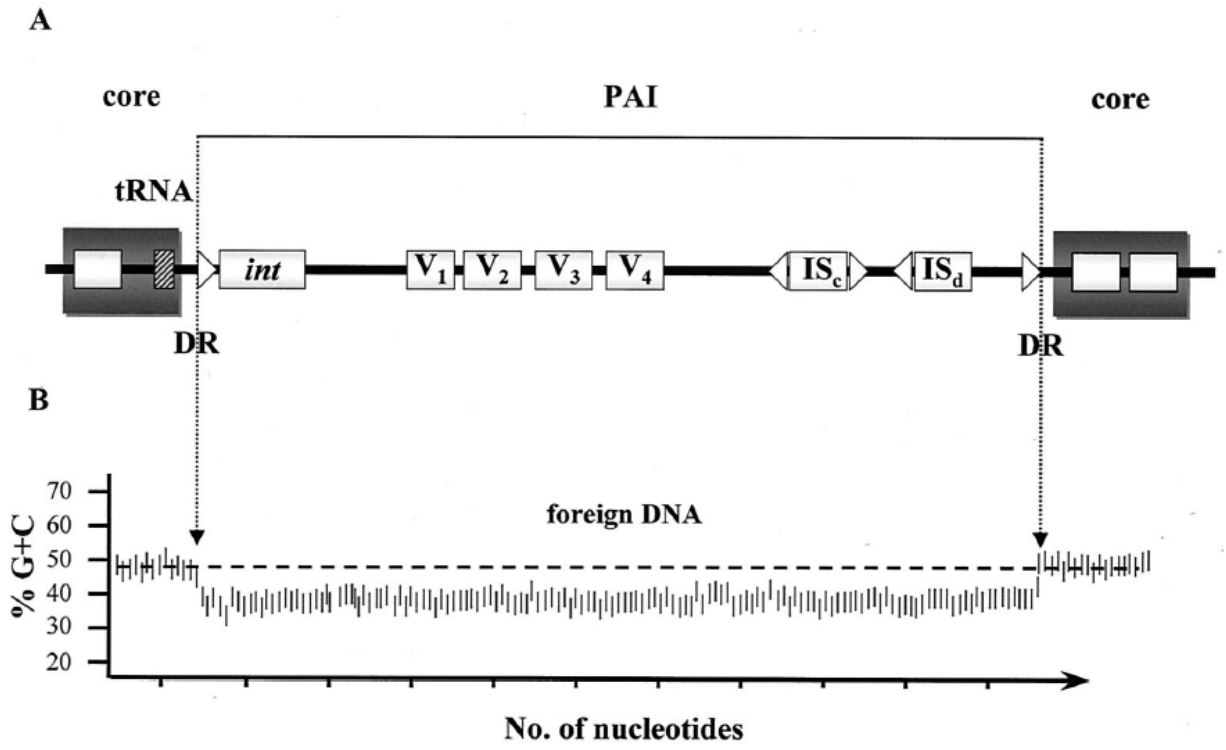

Figure 1. General structure of pathogenicity islands.

(A) Typical PAIs are distinct regions of DNA that are present in the genome of pathogenic bacteria but absent in non-pathogenic strains of the same or related species. PAIs are mostly inserted in the backbone genome of the host strain (dark grey bars) in specific sites that are frequently tRNA or tRNA-like genes (hatched grey bar). Mobility genes, such as integrases (*int*), are frequently located at the beginning of the island, close to the tRNA locus or the respective attachment site. PAIs harbour one or more genes that are linked to virulence (V1 to V4) and are frequently interspersed with other mobility elements, such as IS elements (ISc, complete insertion element) or remnants of IS elements (ISd, defective insertion element). The PAI boundaries are frequently determined by direct repeats (DR) (triangle), which are used for insertion and deletion processes. (B) A characteristic feature of PAIs is a G+C content different from that of the core genome. Adapted from Schmidt, H. and M. Hensel 2004.

As more pathogenic bacteria are sequenced we find a growing number have PAIs associated with them. This is not surprising, if the assortment of virulence factors, along with the speed of transfer in evolutionary terms, is taken into account. It is curious to note the

absence of PAIs from many important pathogens such as *Chlamydia* spp., *Mycobacterium* spp., the spirochetes and most streptococcal species, among others (194). Pathogens that harbour PAIs tend to be flexible about what kind of host they occupy and often are able to survive living free of a host in the environment. The ability to persist in the environment provides extensive opportunities for acquiring foreign genetic material. This suggests that PAIs, and more generally GIs, provide opportunities for habitat expansion. In contrast, pathogens that lack PAIs tend to be highly adapted and specialized, and consequently evolved towards a loss of flexibility. Often specialization is concurrent with genome reduction, which could act to remove horizontally acquired DNA (204). These mechanisms do not explain the lack of identification of PAIs in many streptococcal species that do have a high degree of host flexibility and are free living. One possible explanation is that the high rate of recombination possessed by streptococcal species causes genome rearrangements breaking large genomic blocks into mosaics which no longer fit classical PAI characteristics (95).

1.2.4 The *Francisella* pathogenicity island

In 2004, the Nano laboratory discovered a 30 kb region of *F. novicida* DNA which contained several genes required for virulence (147). Bioinformatic analysis revealed that the region exhibited many classical PAI features, ergo it was designated the *Francisella* pathogenicity island (FPI). The *F. novicida* genome has an average G + C content of 32.5% which is considered uncommonly low for bacteria (146). With a G + C average of 28.1%, the FPI is 4.4% below genome average. As previously mentioned, G + C content that deviates from the genome average is a hallmark of PAIs. Additionally the FPI harbours genes linked to

virulence. It is flanked by 16 bp of direct repeats and has an Ile tRNA gene immediately upstream of it. *F. novicida* contains a single copy of the FPI, however all the clinically relevant strains contain two identical copies (147). The fact that two copies of the FPI are present in many strains provides evidence it was mobile at some point in the phylogeny of *Francisella*.

Usually PAIs are associated with pathogenic strains and missing from closely related non pathogenic strains (82). For example, the locus of enterocyte effacement (LEE) PAI is present in many enteropathogenic *Escherichia coli* strains but missing from the non pathogenic laboratory strain *E. coli* K-12. The LEE contains the genes required to attach to host epithelium and efface microvilli (65). When *E. coli* K-12 was transformed with LEE it acquired the attachment and effacement phenotype (136). Presently, all sequenced *Francisellae* genomes possess at least one copy of the FPI- so where are the closely related strains lacking the FPI? There are several possible explanations: Nearly all our isolates of *Francisella* have been obtained from a host rather than free living in the environment. It is well documented that only a tiny fraction of the Earth's bacterial fauna have been identified and even fewer cultured, therefore, perhaps benign PAI-negative *Francisella* have simply not been discovered yet (126). The FPI may have been acquired early on in the phylogeny of *Francisella*, and ancestors previous to that event may no longer exist.

The FPI is composed of 18 genes organized into two polycistronic operons (Fig. 2). Most of these genes are required for macrophage intracellular growth, including pathogenicity determinant protein A (*pdpA*), *pdpB*, intracellular growth locus A (*iglA*), *iglBCDEFGHIJ* valine-glycine repeat G (*vgrG*) gene and finally, defect in organelle trafficking U gene (*dotU*) (21, 52, 87, 89, 147, 193). Although *pdpD* is not required for *in vitro* macrophage intracellular growth, it is required for full virulence in both a chicken embryo and mouse infection model.

The Anhydro-N-acetylmuramic acid kinase (*anmK*) gene is also not required for intracellular growth but has been shown to contribute marginally to virulence in the chicken embryo infection model (127). The final gene of the *pdpA* operon, *pdpE*, is not required for virulence or intramacrophage growth. The largest open reading frame in the FPI, *pdpC*, is not required for intracellular growth but is absolutely required for virulence in a mouse model of infection (This work).

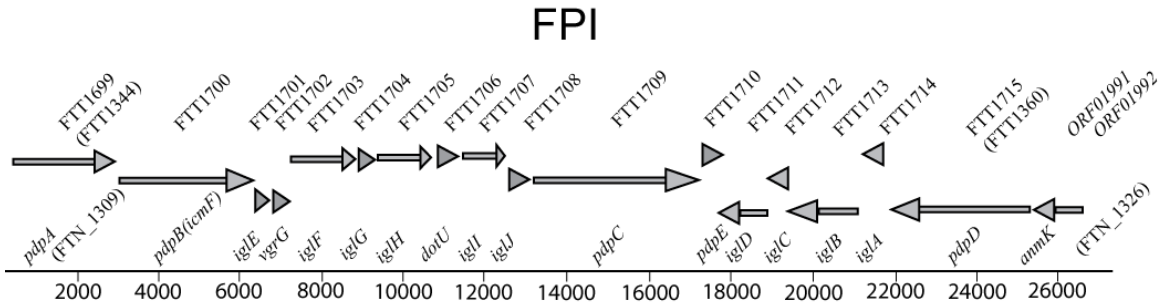

Figure 2. Diagrammatic representation of the *Francisella* pathogenicity island.
The arrows indicating open reading frames. Above the arrows are the locus tags for *F. tularensis*, below are the common gene names in *F. novicida*. Below the arrows flanking the FPI are reference locus tags for *F. novicida*, and the units of the scale are kilobase.

1.3 Type VI secretion

1.3.1 Discovery of the Type VI secretion system

Bacteria have developed a number of mechanisms in order to facilitate the transport of proteins across cellular envelopes. The type VI secretion system (T6SS) represents the latest of such molecular machines to be described. T6SSs contain two homologous genes of the *Legionella pneumophila* type IV secretion system (T4SS): intracellular multiplication gene F (*icmF*) and defect in organelle trafficking gene U (*dotU*). This observation led to the initial classification of prototypical T6SSs as a subset of the T4SS. More gene clusters were identified

which contained homologues of *icmF* and *dotU* but lacked any other T4SS genes. The genes associated with *icmF* and *dotU* were conserved between clusters to various degrees and were thus termed *icmF* associated homologous proteins (IAHP) (51). In *L. pneumophila* these genes play an accessory role and do not form a crucial part of the core apparatus (216). Whereas in a T6SS context, *icmF* and *dotU* form essential structural components of the secretion machine (159).

In 2006, Pukatzki and coworkers described the first prototypic T6SS while studying *Vibrio cholera* using a *Dictyostelium discoideum* amoebae host model system. They identified genes required for resistance to amoebae predation using a transposon mutagenesis approach. Two of the genes subsequently identified showed a high degree of similarity to *icmF and dotU*. By comparing the supernatants of wild type to those of a virulence-associated secretion gene K (*vasK*) (an *icmF* homologue) mutant, they identified four proteins that were secreted in a *vasK* dependant manner, namely hemolysin co-regulated protein (Hcp), and three valine-glycine repeat proteins (VgrG)-1, VgrG-2, and VgrG-3. There were several characteristics of these secreted proteins that led Pukatzki to describe them as a new secretion system. For instance, normally a signal peptide is required for type II and type V secretion systems, which secrete proteins in a two-step process. In the first step, the secretion (Sec) pathway translocates proteins (recognized by their signal peptide) from the cytoplasm into the periplasm (27). None of the four secreted proteins from Pukatski's *V. cholera* T6SS contained a canonical secretion signal peptide. The lack of signal peptide is consistent with the type I, III, and type IV secretion systems, which translocate proteins in a one step process from the cytoplasm directly to the extracellular milieu without using the Sec pathway, and thus do not require a secretion signal peptide (Fig. 3) (71). Normally the type I secretion system (T1SS) is composed of three components. In *V. cholerae*, a

T1SS containing four components was previously identified, and since the gene cluster investigated by Pukatzki contains eighteen genes, the possibility of an additional T1SS was dismissed (28). Complete genome sequencing of the experimental strain V52 demonstrated the absence of a T4SS. Finally, the V52 strain only encodes a T3SS typical of flagella biosynthesis, and no attenuated mutants contained insertions within the T3SS. After demonstrating that the secretion system they had begun to characterize did not fit into any known system they named the genes involved virulence-associated secretion (VAS) genes and proposed that they encoded part of a new type of secretion system (171).

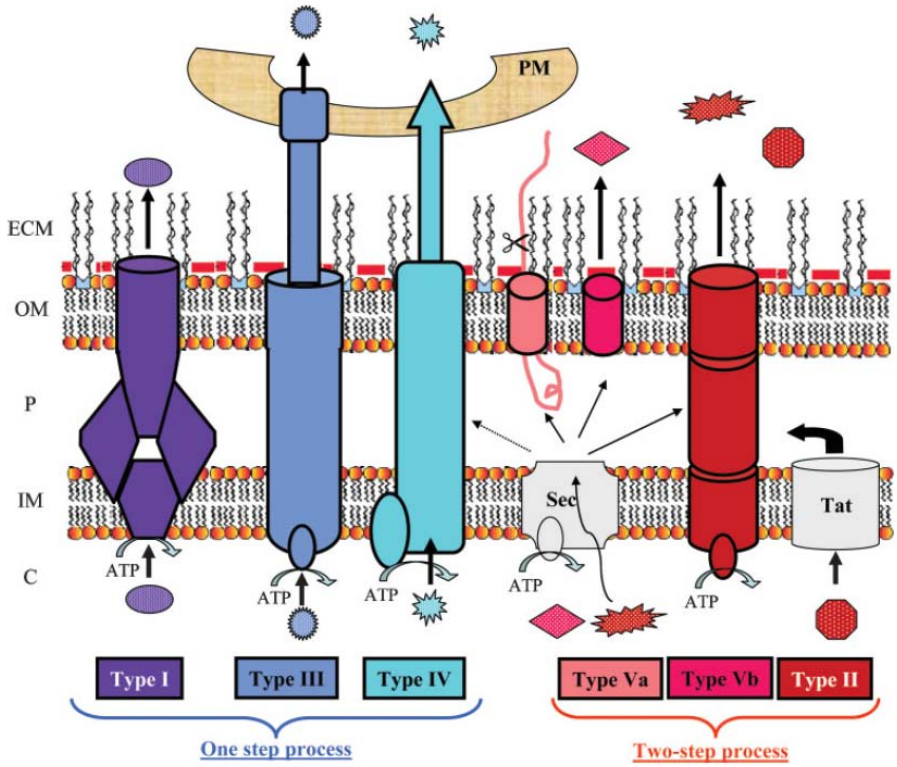

Figure 3. Type I-V secretion systems in Gram-negative bacteria.

T1, T3 and T4SSs (left) are thought to transport proteins in one step from the bacterial cytosol to the bacterial cell surface and external medium. In the case of T3 and T4SSs, the proteins are transported from the bacterial cytoplasm to the target cell cytosol. One exception for T4SS is the

pertussis toxin, which is secreted in two steps and released into the extracellular medium. This exception is represented by the dotted arrow, which connects Sec and the T4SS. T2 and T5SSs transport proteins in two steps. In that case, proteins are first transported to the periplasm via the Sec or Tat system before reaching the cell surface. T5a is a putative autotransporter, indicating that the C-terminus of the protein forms the outer-membrane channel (cylinder) whereas the N-terminus (pink line) is exposed to the surface or released by proteolytic cleavage (scissors). C, bacterial cytoplasm; IM, bacterial inner membrane; P, bacterial periplasm; OM, bacterial outer membrane; ECM, extracellular milieu. PM (brown zone), host cell plasma membrane. When appropriate coupling of ATP hydrolysis to transport is highlighted. Arrows indicate the route followed by transported proteins. Figure taken from Filloux *et al.* 2008.

Presently T6SSs have been identified in approximately 25% of sequenced bacterial genomes, although most are found in the phylum Proteobacteria. However, there are examples within the Planctomycetes and Acidobacteria (27). Although T6SSs are often found in pathogenic bacteria, they perform a variety of tasks, not all of which are related to virulence. For instance, T6SSs have been implicated in biofilm formation as well as the destruction of other bacterial cells (68, 100). Comparative genomic studies have characterized the T6SS loci as a core set of 13 conserved genes. The system has been further divided into five subgroups based upon accessory and regulatory proteins present (29).

Two proteins that are always present in T6SSs, Hcp and VgrG appear to be evolutionarily related to the cell-puncturing apparatus found in bacteriophages. This device is used by the phage to deliver viral DNA into the bacterial cytoplasm. Specifically, Hcp forms a hexameric ring with a 40 angstrom diameter that can stack, forming nanotubes *in vitro* (19, 145). The Hcp protein also shows a high degree of structural similarity to the lambda phage tail protein, gene product V (gp), as well as the T4 phage tail tube protein, gp19 (122, 163). The conserved region of VgrG proteins contains a merger of two T4 bacteriophage proteins, gp27 and gp5, which

together form the phage tail spike complex. (170). Presumably, VgrG pierces the membranes of target eukaryotic or bacterial cells. Interestingly, many VgrG proteins contain accessory C-terminal domains that may function as effectors in the target's cytoplasm. For instance, *V.cholera* VgrG-1 exhibits actin cross-linking activity in target cells dependent upon a C-terminal domain called repeats-in-toxin A (RtxA) (129). The experimental evidence appears to support the hypothesis that T6SSs encode an injection system that is derived from bacteriophage. As a result, T6SSs are not only the most widespread and recently discovered, but also the first that have not been derived from bacterial organelles (34).

The FPI encodes some, but not all, of what are considered to be core T6SS components. This has led to debate in the literature about which components of the FPI are or are not T6SS homologues, as well as whether it encodes a bona fide T6SS at all. There is a consensus that the FPI encoded proteins IglA, IglB, IglD, IglG, PdpB, VgrG and DotU are homologues of T6SSs (21, 22, 27, 146).

1.4 Intracellular lifestyle of *Francisella*

1.4.1 Uptake of *Francisella* by macrophages

When microbes enter sterile sections of the body, professional phagocytes are recruited to the scene whereupon the microbes are engulfed and destroyed. There are, however, some microorganisms, such as *Francisella,* that have developed strategies that allow them not only to avoid destruction, but to flourish within the phagocyte.

Most bacteria, along with inert particles, are taken up by macrophages through a process called conventional phagocytosis. Phagocytic receptors on the surface of the macrophage plasma membrane interact with ligands on the surface of the particle. This process continues resulting in the tight symmetrical engulfment of the particle by pseudopodia in a zipper-like manner (Fig. 4A) (90). Unconventional phagocytosis includes coiling phagocytosis and macropinocytosis. Uptake by coiling phagocytosis is exemplified by the intracellular pathogen *Legionella pneumophila*, in which the bacteria are tightly surrounded by several coils of pseudopodia. This process does not depend upon metabolically active *L. pneumophila* but rather upon a surface component, since treatment of the bacteria with anti-*L. pneumophila* antibodies results in uptake by conventional phagocytosis (Fig.4B) (102). *Salmonella typhimurium* enter host cells via macropinocytosis triggered by host membrane ruffling. This mechanism is directed by bacterial effector proteins that alter host cytoskeleton, causing a ruffling of the host cell surface followed by uptake by macropinocytosis (77). This mode of cell entry reportedly resembles a "splash pattern", in which short pseudopodia symmetrically envelop the bacteria (Fig. 4C) (44).

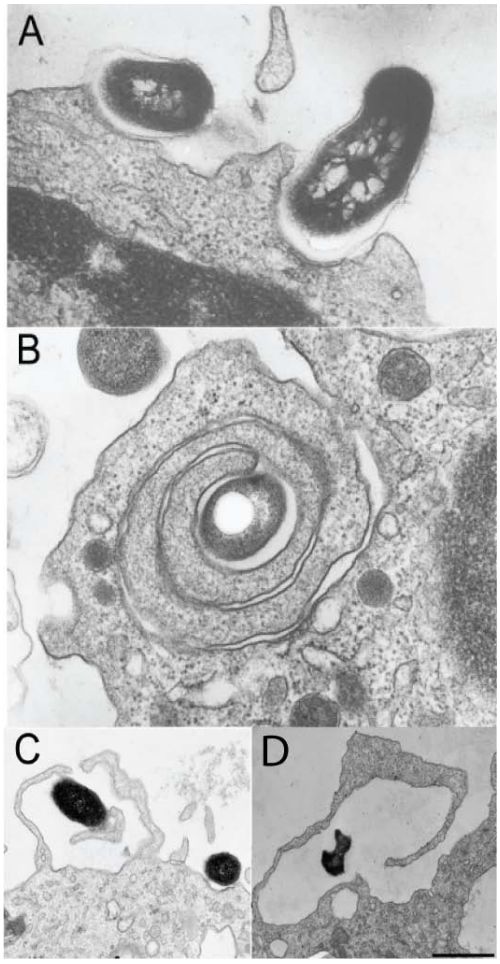

Figure 4. Morphology of uptake of various bacterial intracellular pathogens by human macrophages.

(A) The uptake of *M. tuberculosis* via conventional phagocytosis, (B) *L. pneumophila* via coiling phagocytosis, (C) *S. typhimurium* via macropinocytosis, and (D) *F. tularensis* via looping phagocytosis. Scale bar in panel D indicates 1 µm. Adapted from Clemens, D. and M. Horwitz 2007, and Clemens *et al*., 2005.

The uptake of *Francisella* by macrophages takes place by a unique mechanism that has been termed looping phagocytosis (45). The ultrastructure morphology of looping phagocytosis is characterized by asymmetric spacious pseudopod extensions that surround the bacteria (Fig 4 D). Uptake by this novel mechanism is dependent upon preformed molecules situated on the surface of the bacteria, the rearrangement of the actin cytoskeleton and phosphatidyl inositol-3-

phosphokinase (PI3K) signalling. This finding was demonstrated by the observation that formalin-killed bacteria are taken up by the same morphological process. Additionally, treatment of macrophages with either wortmannin (a PI3K inhibitor) or cytochalasin D (a fungal compound that interferes with actin polymerization) prohibited uptake (45). *Francisella* can also enter monocytes via the complement factor C3 receptor pathway (198). Clements and Horwitz speculate that the looping phagocytosis morphology may arise from a scarcity of complement fixed to the bacteria combined with a strong stimulus for pseudopod extension initiated by the bacteria. The former is proposed to account for the large gap between bacteria and pseudopodia and the latter for the exaggerated extension of the pseudopodia (44).

Once a particle or non-pathogenic bacterium has been taken up by a macrophage, it is contained within a vacuole called a phagosome. The phagosome follows distinct steps along the endocytic pathway, ultimately fusing with a lysosome to form a phagolysosome. Lysosomes contain a variety of hydrolytic enzymes, resulting in an extremely harsh environment within the phagolysosome that quickly degrades ingested material (85). However, in *Francisella* infections, the phagosome fails to fuse with the lysosome and the bacteria escape into the macrophage cytosol and begin multiplying. Although the exact mechanism is unclear and changes between hosts, the following outlines the timeline and characteristics of early *Francisella* infections.

As mentioned, in certain situations *Francisella* uptake is mediated via the complement receptor. This mode of entry prevents the phagocyte from initiating an oxidative burst and thus likely contributes to the success of the pathogen (185). The mannose receptor and class A scavenger receptors have both been shown to contribute to uptake (18, 168).

1.4.2 Escape from the phagosome

Francisella initially resides in a phagosome that stains positive for the early endosome antigen 1 (EEA1). The vacuole subsequently matures along the endocytic pathway to acquire the following late endosomal markers: lysosome associated membrane protein (LAMPs), LAMP1 and LAMP2, and the small GTPase, Rab7 (39, 47, 188, 189). The late endosome fails to fuse with lysosomes based upon the absence of the acid hydrolase, cathepsin D (47). In infected human macrophages, phagosomes do not acidify, which is contrary to the finding that in mouse macrophages, acidification of the phagosome is essential for bacterial multiplication (46, 74). Presumably these differences can be explained by the difference in host macrophages employed.

In both hosts, the phagosomal membrane is degraded, and following escape into the cytosol, bacterial replication occurs. Ultrastructure studies examining human macrophages reveal the presence of a dense fibrillar coat that surround the phagosome shortly before they fragment (47). Escape from the phagosome occurs between 1-4 hours after uptake and varies depending upon which strain and host cell are used (39, 86, 186). An explanation for the variance of time-to-escape among strains is not clear. The replicative phase of the bacterium occurring in the cytosol lasts from 4-20 hours post-infection (186). After 24 hours an increase of 1.5-2.5 $\log_{10}$ bacteria per cell has been reported (86).

Following the replication phase in the J774A.1 mouse macrophage model of infection, apoptosis was induced 12 hours post-infection. Lai *et al.* based this finding upon the release of cytochrome *c* from mitochondria coupled with the activation of caspase-9 and the apoptosis

executor, caspase-3. Additionally, the study found that caspase-8, Bcl-2, Bid and caspase-1 were not involved in this case of apoptosis (115). A study by the Monack group found that caspase-1 negative peritoneal mouse macrophages (which are more susceptible to disease) did not induce significant cell death 8 hours post-infection, while wild-type macrophages converted pro-caspase-1 to caspase-1 during the same period. At 24 hours post-infection the caspase-1 negative macrophages underwent apoptosis with the same frequency as wild type (134). In this study it was suggested that caspase-1 mediated apoptosis might be important during the early stages of infection, but that during a later stage of infection, cell death is induced by another mechanism, independent of caspase-1. The importance of caspase-1 is also supported *in vivo* by the increased susceptibility of caspase-1 knockout mice to *Francisella* infection. Although the study by Lai *et al.* did not detect the activation of caspase-1 from 2-18 hours post-infection, it is likely that the differences observed stem from the use of different cell lines as models of infection.

Recently *Francisella* has been observed within large double membrane bounded vacuoles termed *Francisella*-containing vacuoles (FCVs). More than 50% of the FCVs displayed the microtubule associated protein light chain 3 (LC3-II), which is an autophagosome specific marker, 24 hours post-infection (39). Autophagy is a term arising from Greek, meaning "self eating". It is a process by which cellular elements are trafficked from the cytosol to lysosomes, where they are degraded (104). Originally thought of as exclusively a process used to cope with cellular stress, particularly metabolic stress, autophagy has also emerged as an immune defence mechanism against cytosolic invaders (14, 112). The FCVs interacted with lysosomes to become fusogenic mature autolysosomes. Despite this, most FCVs did not show signs of bacterial degradation. In support of these results, *Francisella* LVS contained within double membrane

bounded compartments *in vivo* have been observed in mouse peritoneal cells (74). In this case after the replicative cycle, autophagy, rather than apoptosis, was induced.

1.4.3 Intramacrophage signalling

As a first line of defence, the innate immune system faces the challenge of identifying and taking action against pathogenic organisms. The immune system accomplishes this feat, in part, by making use of pattern recognition receptors (PRRs), which recognise evolutionarily conserved features present on pathogens, termed pathogen associated molecular patterns (PAMPs) (139). Toll-like receptors (TLRs) function as PRRs and are important initiators of innate immunity. Many TLRs, including TLR 2-6 and TLR 9, are activated by microbial components such as flagella, peptidoglycan and lipopolysacharide (2, 208). TLR activation leads to a signal cascade that initiates the transcriptional regulator, nuclear factor kappa beta (NF-κβ), leading to the expression of proinflammatory cytokines such as tumor necrosis factor alpha (TNF-α) and interleukin 1 (IL-1) (17). Under most circumstances bacterial LPS acts as a ligand for TLR 4 (141). *Francisella* LPS is immunologically inert and fails to elicit an inflammatory response. Consequently, it is considered a virulence factor (5, 20, 94, 184, 209, 217). The uncommon structure of the lipid A portion of *Francisella* LPS compared to that of other Gram-negative pathogens has been suggested as the basis of this effect.

Intracellular *Francisella* actively inhibit the inflammatory response by restricting the ability of the host cell to secrete proinflammatory cytokines. Telepnev *et al.* demonstrated that *Francisella*-infected J774A.1 cells do not secrete TNF-α and IL-1β despite being stimulated by *Escherichia coli* LPS, a potent immunogenic element. Infection with a mutant defective for

phagosome escape, Δ*iglC*, reversed this effect (209). In another study, mouse peritoneal cells and J774A.1 cells were infected with wild type *Francisella* and the Δ*iglC* mutant. Both infective strains initially activated NF-κβ, but only the mouse peritoneal cells secreted TNF-α. Within five hours, these factors were down regulated in wild type but not in the Δ*iglC* mutant (210).

Chapter 2: Virulence of *Francisella* spp. in Chicken Embryos

(Infection and Immunity 2006, **74**, 4809-4816)

Eli B. Nix[1], Karen K.. M. Cheung[1], Diana Wang[2], Na Zhang[1], Robert D. Burke[2] and Francis E. Nano[1]
Department of Biochemistry and Microbiology[1] and Department of Biology[2]
University of Victoria, Victoria, BC, Canada

2.1 Introduction

Although all strains of *Francisella* spp. are highly infectious, there is great variety in the morbidity and mortality that each strain is able to induce in different host animals. *F. tularensis* is clearly the most virulent in both humans and laboratory animals, and is found naturally only in North America (69). *F. holarctica* is found throughout the Northern Hemisphere. Although it is highly infectious in all of the animals that it infects and is fatal to mice, this subspecies rarely causes death in humans, although it can cause considerable morbidity (42). The LVS strain of *F. holarctica* and *F. novicida* have been widely used as models of *F. tularensis* infection, primarily because these bacteria have low virulence in humans and can be handled in Biosafety Level 2 facilities (12, 62, 64, 75). In the mouse model of infection the LVS has an intradermal 50% lethal dose (LD_{50}) of about 3×10^5 CFU, and *F. novicida* has an LD_{50} of about 2×10^3 CFU; however, both strains have an intraperitoneal LD_{50} of less than 10 organisms (111). Hence, mouse infections with LVS and *F. novicida* may be approximations of *F. tularensis* infections in humans.

F. tularensis is thought to grow primarily inside cells during infection of animals. *In vitro* studies of intramacrophage growth have shown that initially *F tularensis* resides in a phagosome, from which it largely escapes between two and four hours after cell entry (47, 86). The *F. tularensis*-laden phagosome has a relatively neutral pH and accumulates some markers of late endosomes, such as LAMP1 and cluster of differentiation 63 (CD63), while it excludes

another late endosome marker, cathepsin D (47). Expression of the *F. tularensis* protein IglC is required for escape of *F. tularensis* from the phagosome, but its role is unknown (124). The LVS strain has been shown to induce apoptosis in the J774A.1 mouse macrophage cell line and to inhibit secretion of TNF-α and IL-1 (114, 209). Although the suppression of cytokines probably represents an *F. tularensis* virulence strategy, the induction of apoptosis likely reflects a defensive response of the host, as caspase-1 knockout mice are more susceptible to *F. tularensis* infection (134). A number of virulence factors have been identified in *F. tularensis*, and most of these factors affect intramacrophage growth. Inactivation of the *mglAB* global regulatory genes results in strains whose growth is severely hampered in macrophages (24). Presumably, MglA and MglB are required for transcription of genes encoding effector proteins, especially genes found in the FPI (120). There is genetic evidence that the FPI associated genes *iglA, iglC,* and *pdpA* are required for intramacrophage growth (87, 89, 147). There is biochemical and genetic evidence that a capsule exists and is needed for infectivity and virulence (99, 183). Defects in the production of LPS can affect intracellular growth (49, 138). The observed *in vitro* intracellular growth and the requirement for cell-mediated immunity for clearance of an *F. tularensis* infection suggest that intracellular growth is required for virulence in animals (4, 13, 48, 62). The observation that mutants defective for growth in macrophages are also less virulent in animals supports this notion (138, 147).

F. tularensis infects a wide variety of animals, and several animals, including rabbits, guinea pigs, primates, hamsters, rats, and mice, have been used as models of infection (10, 62-64, 142, 151, 197). Chicken embryos have also been used to test *F. tularensis* virulence and pathology (32, 174). Recently, researchers have begun to use simple biological systems, such as the nematode *Caenorhabditis elegans*, flies, and insect larvae, to examine the virulence

properties of bacterial pathogens (50, 218). Such systems permit large-scale testing that is humane and relatively inexpensive. Our objective in this work was to develop an assay system that allowed us to evaluate the virulence of *F. tularensis* strains without having to infect animals that have fully developed nervous systems.

2.2 Materials and methods

Microscopy was performed by D. Wang and R. Burke
Remaining experiments were performed by E. Nix, K. Cheung and N. Zhang

2.2.1 Bacterial strains and growth conditions

The *F. tularensis* strains used in this study are listed in Table 1. All of the *F. novicida* strains were derived from the prototype strain U112 (ATCC 15482), which had been passaged through a mouse and aliquoted for subsequent experiments. The LVS (ATCC 29684) was obtained from the American Type Culture Collection. Strains were grown aerobically at 37ºC in either tryptic soy broth (TSB) or on tryptic soy agar (TSA) supplemented with 0.1% L-cysteine.

2.2.2 Chicken embryo infections

F. tularensis strains were grown to the late log phase (optical density at 600 nm, 0.9 to 1.0) and diluted in phosphate buffered saline (PBS) (Gibco) for injection. The inoculating dose was calculated retrospectively by determining the colony forming units (CFU) following dilution and plating on TSA. Fertilized White Leghorn eggs were obtained from the University of Alberta Poultry Research Station. Chicken embryos were incubated at 37ºC with high humidity for seven days prior to infection, and throughout the experiment, were mechanically tilted to a

45º angle every 40 min. After the initial seven day incubation the eggs were examined in order to discard those that lacked a viable embryo, a phenomenon that occurred in between 5 and 10% of the fertilized eggs. For inoculation the tops of the egg shells were disinfected with 70% ethanol. A 1-cm-diameter window was made in the air sac end of an egg, and the egg shell membrane was reflected. With a tuberculin syringe, 100 µl of inoculum was injected under the chorioallantoic membrane. After injection the shells were sealed with clear packing tape. Eggs were candled to detect signs of death every 24 hours for 6 days. This process consisted of shining a focused bright light at one end of an egg to determine if the network of blood capillaries was intact. Embryos that died within 24 hours of inoculation were assumed to have suffered lethal trauma during the inoculation and were removed from the experiment. For the study of the time course of *F. tularensis* growth, the chicken embryos were killed by incubating the eggs in a -20ºC freezer for 1 hour, followed by blending of the eggs and plating dilutions of the homogenized egg contents on TSA to determine the bacterial load. All experiments were terminated by the time the embryos were 14 days old. Chicken embryos that were less than 17 days old are not subject to regulatory control in many countries, including Canada.

2.2.3 Microscopy

Embryos were removed from shells and rinsed with PBS, and organs of interest were removed by dissection and fixed overnight with PBS containing 4% paraformaldehyde. The organs were rinsed with PBS, infiltrated with OCT compound (Tissue-Tek 4583), and snap frozen with liquid nitrogen, and then they were transferred to -80ºC for storage. Ten-micrometer cryostatic sections were cut and mounted on gelatine-coated slides. The tissue sections were blocked with 5% lamb serum-PBS containing 0.05% Tween 20 at room temperature for 45 minutes. Primary antibodies (anti-*F. novicida* rabbit serum, anti-*F. tularensis* LVS mouse

monoclonal antibody reactive with O-antigen and anti-*F. tularensis* LVS rabbit serum) were diluted 1:1,000 in 5% lamb serum-PBS and incubated overnight at 4ºC with the sections. After several washes in PBS, sections were incubated with Alexa 488 or 568-conjugated (Molecular Probes) goat anti-rabbit or goat anti-mouse secondary antibodies for 2 hours at room temperature, rinsed with PBS, and counterstained with 4',6-diamidino-2-phenylindole (DAPI) (Molecular Probes) After mounting with a coverslip, specimens were examined with a Leica DM-6000 compound microscope.

Digital images were collected, and colour was added with OpenLab (version 4.04) or Scion Image (version 4.03). Figures were prepared with Photoshop (Adobe 6.0) by cropping and adjusting the brightness and contrast.

2.3 Results and discussion

2.3.1 Growth of *F. tularensis* in 7-day-old chicken embryos

When a small inoculum of LVS or *F. novicida* was introduced into chicken embryos, exponential growth occurred for 4 to 5 days, and the concentration reached about 5×10^8 bacteria per gram of egg mass (Fig. 5). *F. novicida* and LVS appeared to grow at approximately the same rate, and the concentrations levelled off at similar total numbers of bacteria by day 5 post-infection.

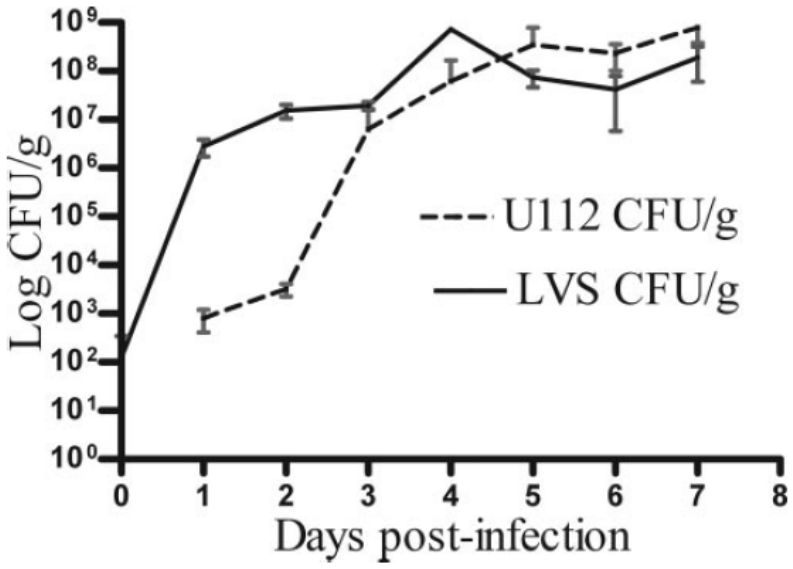

Figure 5. Growth of LVS and *F. novicida* in chicken embryos.

Twenty-one chicken embryos were infected with 168 CFU of LVS or 159 CFU of *F. novicida* U112. Immediately after infection and every 24 hours after infection the bacterial burden of three embryos was determined. At zero time for the U112 strain there were too few bacteria to count. Error bars represent standard error.

2.3.2 Virulence of *F. novicida*

The wild type strain of *F. novicida* is highly virulent in mice and also appears to be highly virulent in chicken embryos, and 100% lethality was observed with 30 to 200 CFU (Fig. 6). Infections with different doses and repetitions of experiments with different lots of eggs demonstrated that the time to death due to infection generally correlated with the infectious dose and was consistent for different experiments. Some aberrations were seen, like the results obtained with the intermediate dose given in experiment 2, and these aberrations may have been due to the natural variation in embryos or to the inexact nature of the inoculation. All of the

embryos inoculated with PBS lived until the termination of the experiment on day 6 post-infection (data not shown).

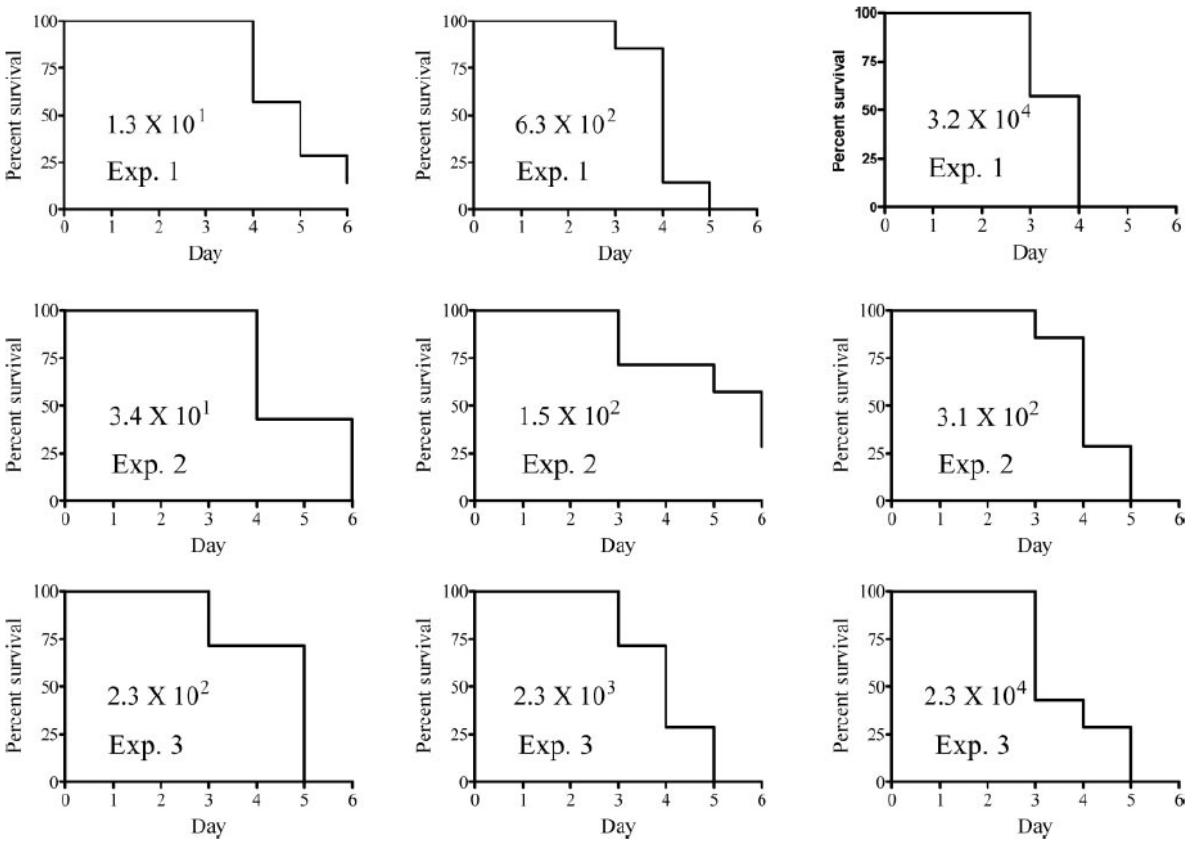

Figure 6. Reproducibility of the time to death induced by *F. novicida* U112.

Three inocula that were different sizes were each used for infection of seven fertilized eggs. The inoculum used for infection (in CFU) is indicated on each graph. In each experiment eggs were infected on separate days and different lots of fertilized eggs were used.

2.3.3 Virulence of LVS

In the mouse, *F. novicida* is about 100-fold more virulent than LVS when both organisms are delivered via intradermal injection. Infection of chicken embryos revealed an even larger

difference in virulence between the two organisms, and *F. novicida* was at least 10,000-fold more lethal than LVS (Fig. 6 and 7).

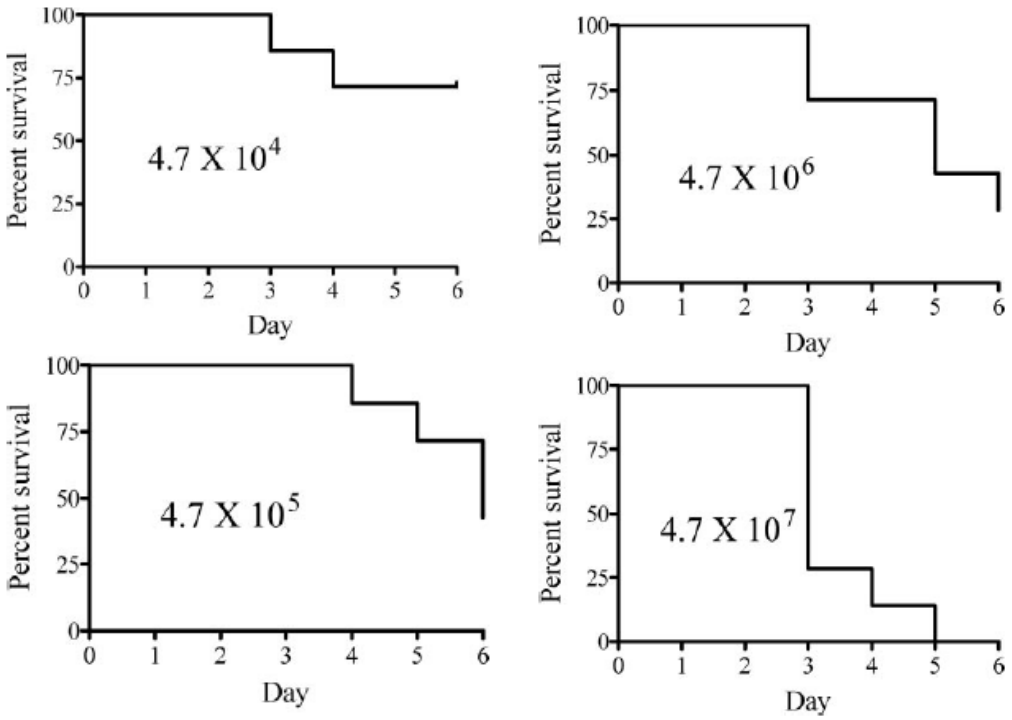

Figure 7. Virulence of LVS in chicken embryos.

Seven fertilized eggs were infected using each inoculation dose, and the doses (in CFU) are indicated on the graphs. The infection series was repeated two times, and similar results were obtained.

2.3.4 Virulence of mutants of *F. novicida*

The virulence of the strains listed in Table 1 was evaluated by performing a series of infection experiments using different numbers of bacteria as inocula and determining the time to death of the chicken embryos. First, a pilot experiment was performed for each mutant to determine the approximate lethal dose, and then at least two repetitions of experiments were

carried out using inoculums concentrations in the sublethal to lethal range. For each inoculating dose seven eggs were infected. Mutants of *F. novicida* U112 which had previously been shown to have defects in virulence or growth in macrophages displayed a range of virulence levels in chicken embryos. In total, the mutant strains were about 100-fold less virulent to more than 100,000-fold less virulent (Fig. 8) than wild-type *F. novicida* U112 strain. Mutant GB2, which has a defect in the global regulator MglA, and mutant NZ9, which has a substitution in the FPI gene *pdpA,* are both avirulent in mice and were found to be unable to kill any of the six chicken embryos that were infected with inocula larger than 10^6 CFU. The previously described mutants SC66, CG57 and CG69 exhibited intermediate levels of virulence. Strain SC66, which has a defect in O-antigen production, required an inoculums that was about 100 times that of its parent strain, strain U112, to induce 100% lethality. A *purA* mutant, CG57, was shown to be attenuated about 10,000-fold compared to wild-type *F. novicida*. Finally, mutant CG69, which has an insert in the gene encoding the heat shock-induced protease ClpB, was shown to be attenuated about 10^6-fold compared to the wild-type strain.

Table 1. *Francisella* sp. strains used in the development of a chicken embryo model of infection.

Strain	Genotype or phenotype	Reference
LVS	Live vaccine strain of *F. tularensis* subsp. *holarctica*	(60)
U112	Wild-type F. novicida	(117)
SC66	U112 derivative; lacks complete O-antigen; delayed growth in thioglycolate-induced C57BL/6 peritoneal macrophages	(49)
CG57	U112 derivative with insertion in *purA* gene affecting purine biosynthesis; suppressed growth in thioglycolate-induced C57BL/6 peritoneal macrophages	(89)
CG69	U112 derivative with insertion in *clpB* gene which encodes a heat shock response protease; suppressed growth in thioglycolate-induced C57BL/6 peritoneal macrophages	(89)
NZ9	U112 derivative in which the *pdpA* gene is replaced with an erythromycin resistance cassette; unable to grow in macrophages	(147)
GB2	U112 derivative; point mutation in *mglA* which encodes a global regulator of virulence; unable to grow in macrophages and aviurlent in mice	(24)

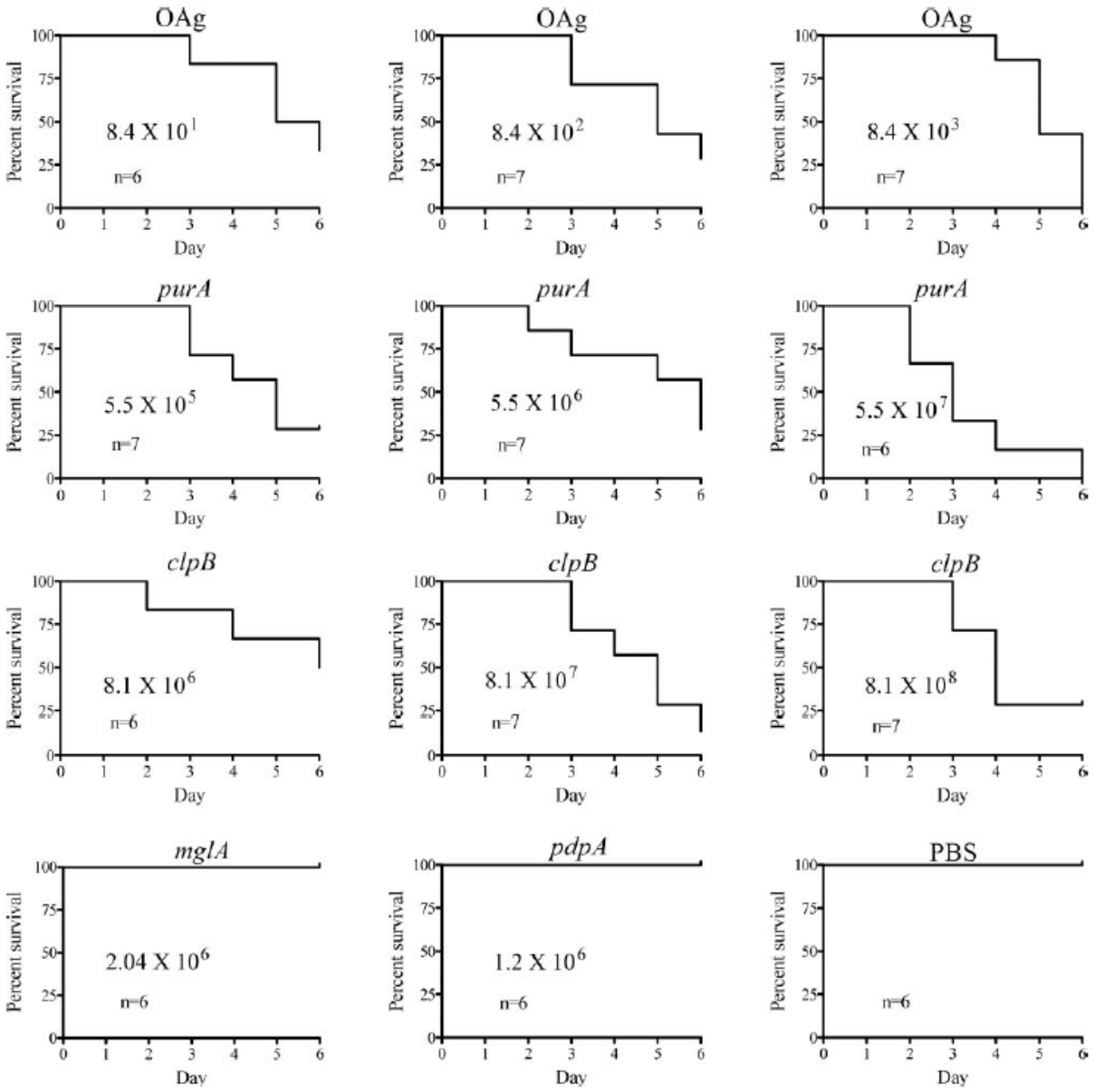

Figure 8. Levels of virulence of *F. novicida* strains in chicken embryos.

A dilution series was prepared for each *F. novicida* strain, and seven embryos were infected with each inoculating dose. The death of the embryos was monitored each day. In some instances the embryos died within 24 hours of inoculation (indicated by $n = 6$), and such deaths were attributed to injury induced during the inoculation and thus were discounted. The number in each graph indicates the inoculating dose (in CFU). The graphs labelled OAg, *purA*, *clpB*, *mglA*, and *pdpA* indicate the results for infections with strains SC66, CG57, CG69, GB2, and NZ9,

respectively. The virulence of each strain was tested at least twice, and similar results were obtained in all trials.

2.3.5 *F. tularensis* in chicken embryonic tissue

Infected chicken embryos were surveyed by microscopy to localize tissues that support *F. tularensis* growth. Embryos that had been infected with the U112 strain or LVS were sectioned, and bacteria were visualized with strain-specific antisera or monoclonal antibodies (Fig 9 and 10). Two days after infection of the embryos, the immunoreactive foci were small and widely dispersed (Fig. 10A-C). Immunoreactive material was found in all of the tissues examined, including the heart, liver, kidney, and bone marrow. For both the U112 strain and LVS immunoreactivity was found inside individual chicken cells in which distinctive granular DAPI staining dominated the cytoplasm. Four days after infection, immuoreactive foci were abundant and were present throughout embryonic tissues. Bacterial cells appeared to be contained within chicken cells, and the infected cells were typically in clusters (Fig. 9A-F and 10D-I). Often, lesions had necrotic tissue at the center that was surrounded by a ring of infected cells. In some instances the host cell nucleus was pyknotic, which is typical of an apoptotic response (Fig. 9G).

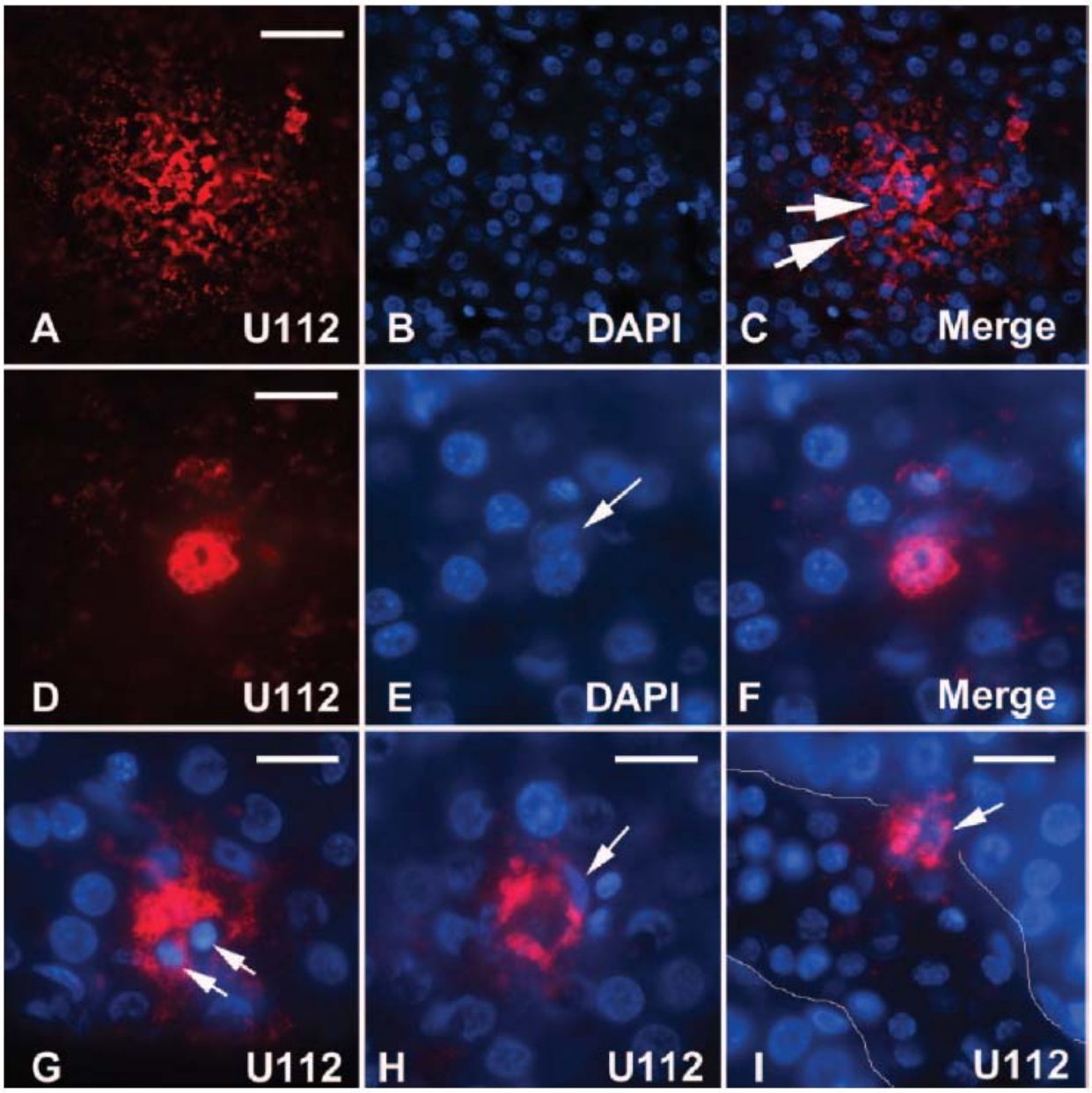

Figure 9. Immunofluorescence of *F. novicida* U112 in chicken embryonic tissues.

(A-C) Focal infections in livers resulted in intense immunoreactivity in the cytoplasm of the central cells and a gradation of immunoreactive material in surrounding cells. The arrows indicate individual nuclei that were surrounded by immunoreactive cytoplasm. (D-F) Higher magnification, showing that the immunoreactive material in the cytoplasm also stained with DAPI in a granular pattern consistent with intracellular accumulation of bacterial cells (arrow). (G) In some liver cells the nuclei of infected cells were pyknotic and fragmented (arrows), which

was indicative of an apoptotic response. (H) In some instances cells associated with sites of infection had the flattened nuclear morphology of liver macrophage cells. (I) Infected cells (arrow) were also associated with the walls of blood vessels (indicated by a thin white line). Nucleated erythrocytes were present in the blood vessels. All images are images of tissue from embryos at 3 days post-infection, and all tissues were reacted with anti-*F. novicida* rabbit serum. (A-C) Bar = 25 µm. (D-I) Bars = 15 µm.

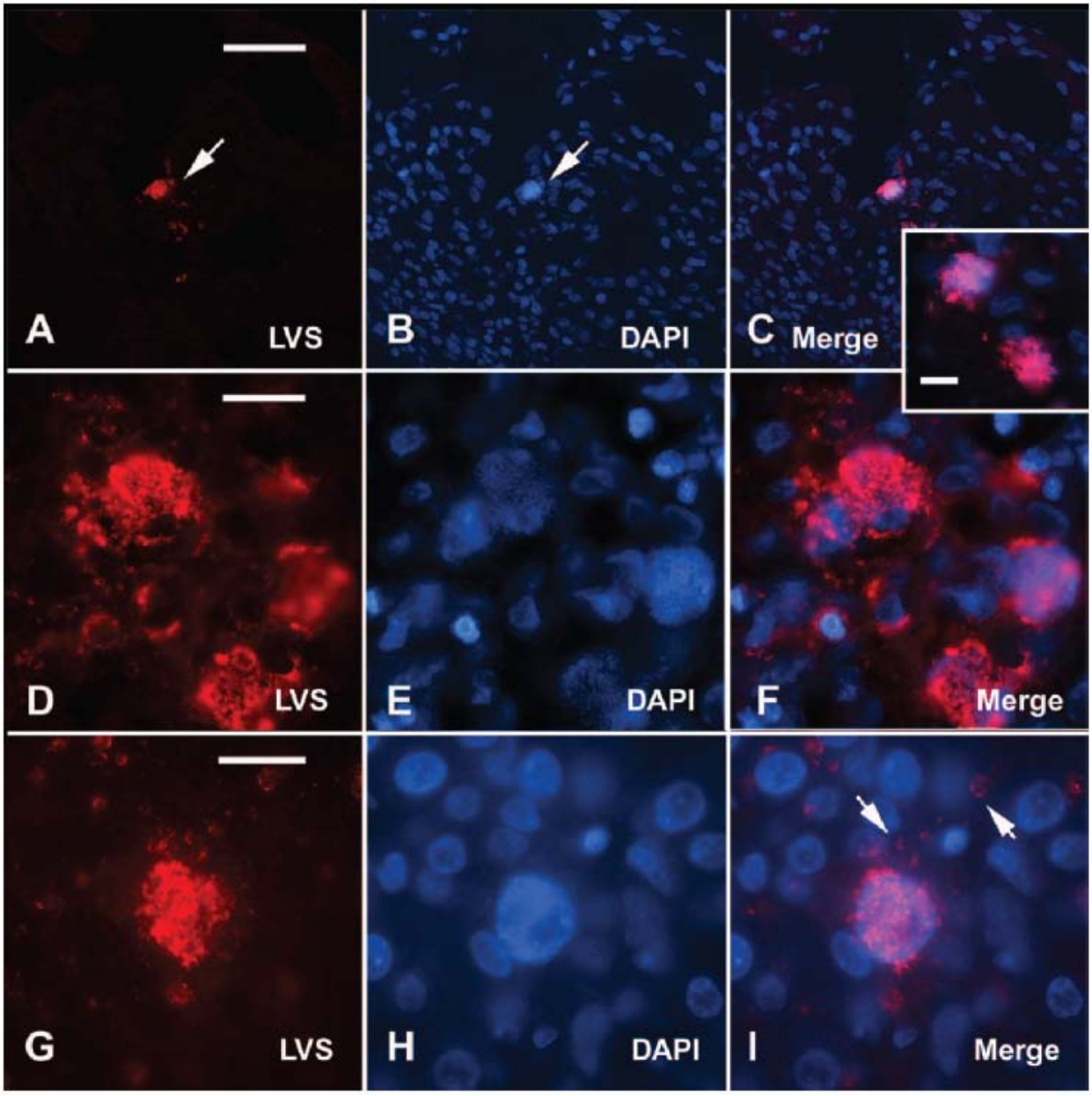

Figure 10. Immunofluorescence localization of LVS in chicken embryonic tissues.

(A-C) In embryos 2 days after inoculation, immunoreactive cells were scattered throughout embryonic tissues. In sections through the heart immunoreactivity and characteristic granular DAPI staining were tightly clustered around individual heart nuclei (arrows and inset). (D-F) In embryos 4 days after inoculation, large foci of immunoreactive material were present in most tissues. Details of infected cells suggested that bacterial cells were in individual heart cells. (G-I) Focal infections also occurred in the liver 6 days after infection, and in individual cells there

was granular immunoreactive material in the cytoplasm that also stained with DAPI. There was scattered immunoreactive material in the surrounding cells (arrows). Panels A to F show tissues that were reacted with anti-LVS monoclonal antibody that is reactive with O-antigen. Panels G to I show tissues that were reactive with anti-LVS rabbit serum. (A-C) Bar = 25 µm. (D-I) Bars = 15 µm. (Inset) Bar = 5 µm.

These studies indicate that the chicken embryo system is a useful system for evaluating the virulence of *F. tularensis* strains. *F. tularensis* grew vigorously in chicken embryos and induced death within 1 week after inoculation. The bacteria were intracellular, and the structure of the lesions suggested that the initial infections spread by localized infection of adjacent cells. The use of chicken embryo infection is not intended to replace mammalian models of tularemia, which involve complex immune responses and approximate human tularemia. However, despite its flaws, *F. tularensis* infection of chicken embryos provides a rapid, inexpensive test to determine differences in levels of bacterial strain virulence that does not induce pain in animals. This procedure could be combined with *in vitro* intracellular assays to screen mutants, allowing researchers to plan subsequent animal experiments so that the minimal number of animals is used.

Chapter 3: Genetic elements for deletion mutagenesis and complementation in *Francisella* spp.

(This chapter represents part of a manuscript published in FEMS Microbiology Letters 2008, **278**, 86-93)

Jagit S. Ludu[1], Eli B. Nix[1], Barry N. Duplantis[1], Olle M. de Bruin[1], Larry Gallagher[2], Laura M. Hawley[1], and [1]Francis E. Nano
[1]Department of Biochemistry and Microbiology, University of Victoria, BC, Canada, and [2]Department of Genome Sciences, University of Washington, Seattle, WA, USA

3.1 Introduction

The biology of *Francisella* lends itself to genetic analysis, and most virulence factors have been indentified using genetic approaches. For example, a variety of random transposon mutagenesis approaches have been applied to the analysis of *Francisella* strains (89, 110, 131, 173). Recently, a comprehensive transposon mutant bank consisting of 16, 508 unique insertions has been made in *F. novicida*, allowing the identification of putative essential genes (84). In addition, insertional allelic replacement and deletion mutagenesis have been used to identify or analyze genes needed for virulence (8, 87, 119, 138, 147, 213). Despite recent advances, there are still gaps in the molecular tools needed for the genetic analysis of *Francisella* spp. This chapter describes methods for antibiotic selection, deletion mutagenesis and complementation in *Francisella* strains.

3.2 Materials and methods

All work presented in this chapter was performed by E. Nix

3.2.1 Bacterial strains and growth conditions

Strains and plasmids used in this study are listed in Table 2. *F. novicida* and LVS were grown using trypticase soy broth or agar supplemented with 0.1% cysteine (TSB, TSA). When

needed, kanamycin (Km) was added to a final concentration of 15 μg ml^{-1}; hygromycin (Hyg) was used at 200 μg ml^{-1}. *Escherichia coli* strains were grown using Luria-Bertani broth or agar supplemented with Km (30 μg ml^{-1}), or ampicillin (Ap) (100 μg ml^{-1}) as needed.

3.2.2 Transformation and conjugation

DNA was introduced into *F. novicida* U112 and mutant strains exclusively by chemical transformation as described previously, with the following modification (9). Efficient chemical transformation of *F. novicida* normally requires the use of a complex synthetic medium, Chamberlain's broth (35). In this work it was found that the simple addition of 0.4% glucose rendered fresh TSB equally suitable as a transformation medium. The high experiment-to-experiment variation in transformation was also reduced using disposable plastic tubes and plate spreaders. DNA was introduced into LVS by electroporation as described previously (130). Conjugation was performed essentially as described by Golovliov, except that plasmid transfer functions were supplied by pRK2013 via tri-parental mating (56, 86).

Table 2. Bacterial strains and plasmids used to develop mutagenesis and complementation strategies in *Francisella*.

Strain or plasmid	Genotype or phenotype	Source or reference
Bacterial strains		
E. coli DH5α	*E. coli* F^- ϕ80d*lac*ZΔM15Δ (*lac*ZYA-*arg*F)U169 *rec*A1 *end*A1 *hsd*R17(r^-_k, m_k^+) *pho*A *sup*E44 *thi*-1 *gyr*A96 *rel*A1λ^-	Invitrogen
F. novicida U112	Prototype *F. novicida* strain	Laboratory strain
Plasmids		
pWSK29	Low copy cloning vector, Ap^R	(220)
pRK2013	Narrow-range plasmid carrying the transfer functions that operate *in trans* for broad- host-range plasmids, Km^R	(56)
pMMB207	Broad-host-range plasmid, Cm^R	(144)
pMP527	*Francisella* shuttle plasmid that is stable in the absence of selection, Km^R	(125)
pMP633	*Francisella* shuttle plasmid that is stable in the absence of selection, Hyg^R	(125)
pEN1	pMMB207 with Cm^R gene disrupted and Km^R gene inserted into the Pst I site in the MCS region.	This work
pEN2	pMMB207 with Cm^R gene disrupted and Km^R gene inserted into the Pst I site in the MCS region.	This Work

3.3 Results

3.3.1 Deletion mutagenesis via co-transformation with plasmid DNA

F. novicida is unusual in that it readily takes up and integrates linear DNA. This property of *F. novicida* makes it amenable to deletion mutagenesis by combining the transformation of unmarked DNA along with a selectable marker (Fig. 11).

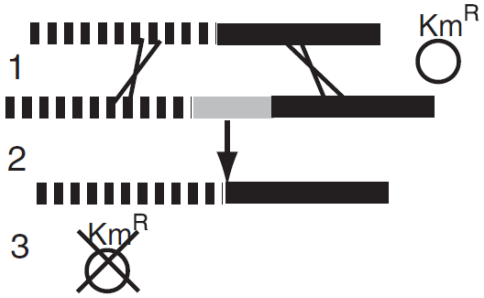

Figure 11. Deletion mutagenesis in *F. novicida* via co-transformation.

Step 1. A linear recombinant deletion clone is transformed along with a plasmid. Step 2. The recombinant deletion integrates into 1-5% of the Km^R transformants. Step 3. The unstable plasmid is allowed to be lost by growth of the strain in non-selective medium.

To test this approach, *F. novicida* was transformed with linear DNA containing a chromosomal deletion along with the stable, hygromycin-resistant (Hyg^R) plasmid pMP633, or the unstable, kanamycin-resistant (Km^R) plasmid pMP527 as selectable markers (125). In all experiments an approximate 10-fold excess of the chromosomal fragment to the plasmid DNA was used. First it was demonstrated that transformation and selection for pMP633 (Hyg^R) along with a chromosomal fragment carrying a Km^R cassette in the FTN_*1758* gene resulted in 3% (14/500) of the Hyg^R colonies also being Km^R, thus demonstrating co-transformation. When an unmarked deletion of the FTN_*1758* gene was co-transformed with pMP633, about 4% (2/48) of the Hyg^R colonies had a deletion of the FTN_*1758* gene as detected by PCR. Co-transformation was also performed using small deletions (120 and 156 base pair) in the *pdpC* gene. Using the stable pMP633 plasmid (Hyg^R) as the selectable marker in two experiments, integration of the co-transformed DNA was found in 66% (8/12) or 5% (6/122) of the Hyg^R colonies. When the unstable plasmid pMP527 (Km^R) was used as the selectable marker in three experiments, it was found that the co-transformed DNA integrated in < 0.4% (0/270), 1% (6/600) and 1% (2/200) of

the Km^R colonies. In one of the deletion mutants created by co-transformation with pMP527, the plasmid was lost during the replica-plating of colonies, verifying its instability during the series of genetic manipulations.

3.3.2 Engineered broad-host-range plasmids

Previously the Nano laboratory had introduced derivatives of the broad-host-range plasmid RSF1010 into *F. novicida* (147). It was noted that while it was possible to introduce a recombinant plasmid carrying *F. novicida* DNA, it was not possible to introduce the parent-cloning vector. One possible reason for this phenomenon is that the parent vector lacked a promoter strong enough to drive sufficient expression of the selectable antibiotic cassette. To test this idea a Km^R cassette carrying the strong P_{FT} promoter was inserted into the broad host range, Chloramphenicol resistant (Cm^R) plasmid, pMMB207 and used it to transform LVS (144). From one Km^R colony plasmid DNA was recovered and used to transform *E. coli* DH5α. The plasmid pMMB207::Km^R recombinant was isolated from *E. coli* and partially digested with Dra I and religated so as to destroy the Cm^R marker. Chloramphenicol can be used as a therapeutic agent to treat tularemia and hence Cm^R markers may be considered inappropriate to use with virulent *Francisella* strains. The resulting plasmid (Fig. 12), designated pEN1, and a derivative with the Km^R cassette oriented in the opposite direction, pEN2, were tested for their efficiency to transform *F. novicida* and electroporate into LVS. As expected, the plasmids, isolated from *E. coli*. transformed more efficiently into LVS (2-9 × 10^6 transformants per μg of plasmid DNA) than into *F. novicida* because the former apparently lacks a restriction-modification system. Transformation of pEN1 into *F. novicida* was three to four orders of magnitude less efficient

than electroporation into LVS, and it was difficult to obtain even a single *F. novicida* transformant in some experiments. In contrast, conjugation via tri-parental matings of pEN1 to *F. novicida* and LVS generated approximately the same number of exconjugants (10^{-5} per recipient cell). However, in some experiments, no exconjugants were obtained for the LVS strain, and this was attributed to its fragility in the co-culture conditions. Hence, with the appropriate use of electroporation or conjugation for a particular strain, one can recover several hundred transformants or exconjugants in a typical experiment.

Plasmid pEN1 was unstable in *F. novicida* when grown in the absence of antibiotic selection; after 20 hours of broth cultivation of *F. novicida* (pEN1) up to 99.9% of the cells lacked the plasmid. When the pFNL10-based plasmid pMP633 (Hyg^R) was transformed into *F. novicida* harbouring pEN1, the number of Km^R colonies approximately equalled the number of Km^R-Hyg^R transformants, indicating that the two plasmids are compatible.

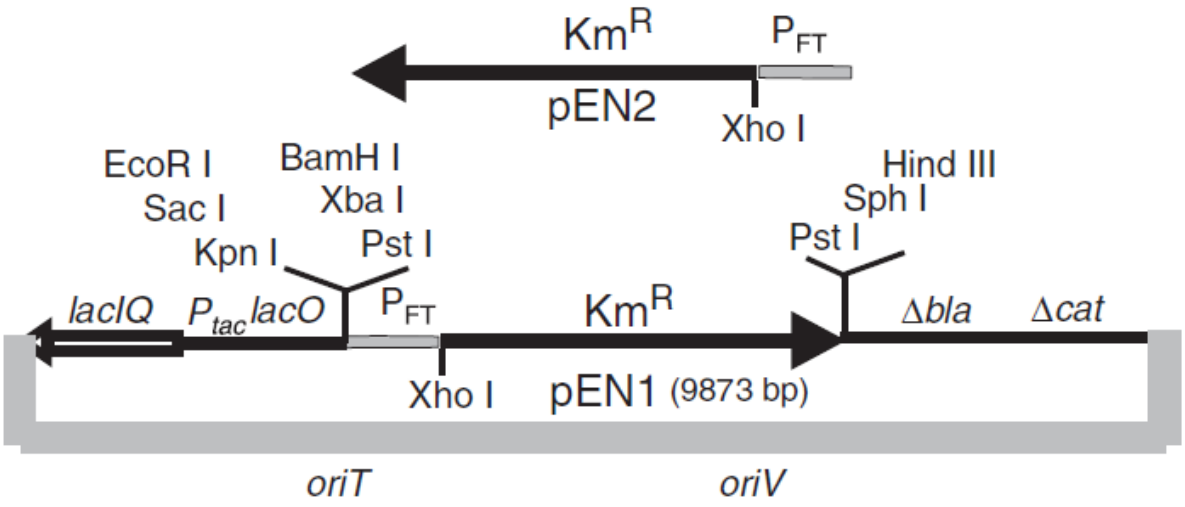

Figure 12. Organization of plasmids pEN1 and pEN2.

Diagram shows the relative position of unique cloning sites on pEN1 and pEN2. Ap^R and Cm^R are not encoded by these plasmids. The sites for BamH I, Kpn I, Sac I, Sph I and EcoR I are

appropriate for cloning *Francisella* genes because these sites are relatively rare in *Francisella* genomic DNA. The thick, gray line indicates the backbone of the plasmid and the relative positions of *oriT* and *oriV*. The elements of the plasmid are not drawn to scale.

3.4 Discussion

In this work, approaches for making unmarked deletion mutants in *F. novicida* and tools to genetically complement mutants were described. In many cases it is essential to make deletion mutations rather than antibiotic-resistant allelic replacements, because the latter often lead to disruption of expression of genes downstream of the inserted antibiotic resistance marker. Of course, the approaches for making deletion mutants can also be used for making gene substitution, for example, with site-directed mutant gene alleles.

The importance of inserting a *Francisella* promoter in front of the selective markers can only be understood in the context of the biology of exogenous gene expression in *Francisella* species. It is well established that exogenous gene expression in *Francisella* is dependent on a *Francisella* promoter or on very high gene dosages of the exogenous gene (84, 125, 173). Antibiotic markers that lack an appropriate promoter will preferentially generate strains with insertions downstream of endogenous *Francisella* promoters, thus creating a bias in many experiments.

The pEN1/pEN2 plasmids represent a different plasmid incompatibility group than the plasmids commonly used in *Francisella*, and thus allow an expansion of the types of complementation experiments that can be performed. In addition, the use of conjugation eliminates the need for electroporation equipment and the generation of aerosols, which

facilitates gene transfer experiments to highly virulent *F. tularensis* strains in a biological safety level 3 environment. Finally, the success in using tri-parental matings to *F. novicida* and LVS potentially enhances cloning experiments by allowing the use of any *E. coli* strain to serve as the cloning vehicle before mating to *Francisella*. The use of tri-parental mating obviates the need to construct clones in potentially unstable and poorly transformable *E. coli* strains carrying integrated broad-host-range plasmids.

Chapter 4: PdpC, a *Francisella* T6SS protein, is required for full virulence but not for intracellular growth.

Eli B. Nix[1,3], Karen K. M. Cheung[1], Crystal L. Schmerk[1], Alicia Y. Chou[2], Rebekah F. Hare-Sanford[3], Karen L. Elkins[2], Francis E. Nano[1] and Karsten Hueffer[3]
Department of Biochemistry and Microbiology, University of Victoria, Victoria, BC, Canada[1]. Center for Biologics Evaluation and Research, Food and Drug Administration, Rockville, MD[2], and The Institute of Arctic Biology and Department of Biology and Wildlife, University of Alaska, Fairbanks, AK, USA[3]

4.1 Introduction

Intracellular bacteria, especially those surviving and replicating within macrophages, have to evade cellular defence mechanisms. They often interfere with the biology of infected cells by secreting proteins into the host cell, altering host cell functions. Intracellular pathogens have evolved intricate secretion systems that can translocate so called effector proteins into the host cell. Well studied examples of such secretion systems include the Type III secretion system of *Salmonella* and *Shigella*, as well as the Type IV secretion system in *Legionella* (83, 149). The presence of such secretion systems often distinguishes virulent strains from closely related avirulent bacteria. A Type VI secretion system (T6SS) has recently been proposed in *Francisella tularensis* based on bioinformatics and experimental evidence (21, 146).

Francisella tularensis is a facultative intracellular Gram-negative bacterial pathogen that causes the acute febrile disease tularemia (66). There are two major pathogenic *F. tularensis* subspecies, *F. tularensis* ssp. *tularensis*, which is found almost exclusively in North America and *F. tularensis* ssp. *holarctica*, which is found throughout the Northern hemisphere. Although there are conflicting data about the relative human virulence of the different *Francisella* strains, they are all highly infectious (203). *F. novicida* is often used as a research surrogate for *F. tularensis* since it is very similar at the genomic level to *F. tularensis*, but is not infectious for immunocompetent humans (176). For studies of the FPI *F. novicida* has an additional advantage

in having a single copy of this genetic element in its genome, compared to two copies in other *Francisella* subspecies.

Despite recent advances, relatively little is known about the biology of *F. tularensis* intracellular growth and the bacterial factors that allow it to parasitize host cells and cause disease. *F. tularensis* uptake into macrophages is promoted by complement and to a lesser extent by types I and II class A scavenger receptors (18, 45, 168). After entering macrophages *F. tularensis* initially resides inside of a phagosome, but after one to four hours it escapes to the cytoplasm where the bulk of the bacterial replication occurs (47, 86). There is evidence that *F. tularensis* associates with autophagy vesicles at later time points of intracellular replication (39). Although some *Francisella* genes are required for phagosome escape and intramacrophage growth, there has been no description of the mechanism of action of the gene products (86, 147, 186, 210). Thus, we do not know if any of the proteins required for virulence have a direct or indirect effect on host cell functions.

Recently a pathogenicity island (FPI) was discovered in *Francisella* (147). The FPI contains 16 to 19 genes, depending on the strain, and is duplicated in the chromosome of all strains except *F. novicida*. The larger of the two presumed operons of the FPI is 17 kb long and has a G+C content of 26.6% which is 6% lower than the rest of the genome (Fig. 2). Although FPI genes are essentially identical among all strains, *F. tularensis* and *F. novicida* contain two genes *anmk* and *pdpD*, that are not present in the FPIs of *F. holarctica*.

Despite the fact the FPI was only recently discovered there are already multiple lines of evidence that FPI-encoded proteins play essential roles in virulence and are co-ordinately regulated with other virulence factors. Disruption of many FPI genes including *iglA*, *iglC*, *iglD*,

pdpA or *pdpB*, leads to loss of intracellular growth and virulence of *F. tularensis* (52, 87, 89, 124, 175, 186, 187). The gene *pdpD* was shown to be required for full virulence but was not necessary for intracellular growth (128). However, very little is known about the precise roles of these FPI encoded proteins during the infection process. Microarray data have shown that all of the FPI genes are regulated by the global virulence regulator protein MglA (30). More recent data shows that MglA and SspA interact with RNA polymerase in regulating numerous virulence genes (38). In addition, low iron conditions up regulate a number of virulence associated genes including FPI genes (53). Bioinformatic analyses suggest that several FPI genes encode proteins involved in a T6SS (21, 52). T6SSs have been demonstrated in other pathogens such as *Vibrio cholera* and *Pseudomonas aeruginosa* (51, 145, 171)

Pathogenicity islands in other bacterial pathogens often encode secretion systems, and at least a subset of secreted effector proteins. These effector proteins interact with host cells and can change host cell biology to favour survival and replication of both extracellular and intracellular pathogens. For *Francisella* no effector proteins of the T6SS have been described to date, although IglG and VgrG have both been shown to be secreted (21).

In contrast to other FPI gene products, the product of the *pdpC* gene is not required for growth in a mosquito derived cell line (175). In this work we examine the role of *pdpC* in intramacrophage growth and virulence in vertebrate hosts.

4.2 Materials and methods

Microscopy was performed by E. Nix, R. Hare-Sanford, and K. Hueffer
Mutants were created (unless stated otherwise) by E. Nix

Mouse experiments were performed by A. Chou, and K. Elkins
FLAG-tagged plasmid constructs were created by R. Hare-Sanford, and K. Hueffer
Macrophage growth experiments were conducted by E. Nix and C. Schmerk
Chicken Embryo experiments were performed by E. Nix

4.2.1 Bacterial strains and plasmids

Bacterial strains and plasmids are listed in Table 3. *F. novicida* strains were grown aerobically at 37ºC in tryptic soy broth supplemented with 0.1% cysteine (TSB) or on trypticase soy agar supplemented with 0.1% cysteine (TSA). The *F. novicida* U112 or JLO strain were used as the wild type strain in all experiments, the JLO strain has a phenotype indistinguishable from the parental type strain, U112 (128). Erythromycin (Em) 30 µg ml^{-1}, hygromycin (Hyg) 200 µg ml^{-1}, or kanamycin (Km) 15 µg ml^{-1} was added as needed. *Escherichia coli* DH5α or DH10B was used for all molecular cloning and was cultured in Luria Bertani (LB) broth with 250 µg mL^{-1} ampicillin (Ap) as needed. The pCR2.1-TOPO vector (Invitrogen), pSMART (Happy Corp) or pFNLTP6-GroE-GFP was used to clone polymerase chain reaction (PCR) products (130).

4.2.2 PCR and primer design

Routine PCR reactions used for screening or analysis of mutants were carried out using Taq polymerase. For the creation of deletion mutants and chromosomal integration of the 3xFLAG epitope tag, overlap extension PCR was used to join two PCR amplicons. For these reactions or any amplification that required proof-reading or highly processive enzyme reactions, Phusion DNA Polymerase (New England Biolabs) was used in a reaction containing nuclease-free water, 1X Phusion HF buffer, 200 µM dNTPs, 0.5 µM each of the forward and reverse

primers (Integrated DNA Technologies), 0.1 ng of template DNA, and 1 unit of Phusion DNA polymerase. PCR reactions were as follows: Initial denaturation at 98ºC for 30 seconds (s); 35 cycles of 98ºC for 30 s, 55ºC for 30 s, 72ºC for 2 minutes (min) and 30 s; final extension at 72ºC for 10 min. All primers were designed based on the *F. novicida* U112 genome sequence (GenBank accession no. NC 008601) and are listed in Appendix Table 1.

4.2.3 Recombinant DNA techniques

The blunt ended PCR products generated with Phusion DNA Polymerase were cloned into the pCR2.1-TOPO vector after an initial purification with QIAquick PCR Purification Kit (Qiagen) followed by the addition of 3' A-overhangs with Taq DNA Polymerase at 72ºC for 15 min in a reaction containing nuclease-free water, 1X PCR ThermoPol buffer, and 0.1 mM dATP. Alternatively, blunt end PCR amplicons were ligated to pSMART. For construction of epitope tagged version of PdpC and PdpE restriction sites were added to primer sequences and the resulting PCR product was cut and ligated into the pFNLTP6-GroE-GFP vector in which the GFP gene was replaced by three repeats of the FLAG sequence. Ligation mixtures were electroporated into the *E. coli* DH5α or DH10B using the Gene Pulser (Bio-Rad) apparatus. Unless otherwise stated, all other recombinant cloning procedures were performed according to the protocols described in *Molecular Cloning* (181).

Table 3. Bacterial strains and plasmids used to characterize PdpC.

Strain or plasmid	Genotype or phenotype	Reference or source
Bacterial strains		
E. coli DH5α	*E. coli* F^- ϕ80d*lac*ZΔM15Δ (*lac*ZYA-*arg*F)U169 *rec*A1 *end*A1 *hsd*R17(r^-_k, m^+_k) *pho*A *sup*E44 *thi*-1 *gyr*A96 *rel*A1λ^-	Invitrogen
LVS	*F. holarctica* Live Vaccine Strain	ATTC
F. novicida U112	Prototype *F. novicida* strain	Laboratory strain

JLO	U112 with deletion in FTN_*1390*	(128)
mglA	U112 with point mutation in *mglA* gene	(24)
Δ*pdpC*	JLO with a complete deletion of *pdpC*	This work
pdpE-1	Tn*5* insertion in *pdpE* at nucleotide 210	(84)
pdpE-2	Tn*5* insertion in *pdpE* at nucleotide 382	(84)
Δ*pdpB*	JLO with a complete deletion of Δ*pdpB*	de Bruin
*Δ*pdpC-E*	JLO with a complete deletion of *pdpC* and *pdpE*	This work
pdpC-3xFLAG	U112 with 3xFLAG tag integrated at the C-terminus of PdpC	This work
Plasmids		
pWSK29	Low-copy-number, Ap^R, *lacZα*	(220)
pSMART	Low-copy-number, Ap^R, *lacZα*	Happy Corp.
pCR2.1-TOPO	*E.coli* cloning vector, high-copy, Ap^R, *lacZα*	Invitrogen
pMP527	*Francisella* shuttle vector, Km^R	(125)
pFNLTP6-GroE	*Francisella* shuttle vector, Km^R	(130)
pKH5	*pdpC-3xFLAG* in pFNLTP6-GroE	This work
pKH16	*pdpE-3xFLAG* in pFNLTP6-GroE	This work

4.2.4 Targeted integration of 3xFLAG tag into the *F. novicida* chromosome

Using pKH5 as template a 0.8 kb PCR product was amplified from the 3-prime end of *pdpC* including the 3xFLAG tag. Next a 0.8 kb product immediately downstream of *pdpC* was amplified from *F. novicida*, using a forward primer in which a portion of the 5-prime end was complementary to part of the 3xFLAG tag. The two amplicons were purified using the Wizard DNA purification system (Promega). Purified products were diluted 100x in water and overlap extension PCR was subsequently employed to fuse the two amplicons together. The resulting PCR product was purified and integrated into the chromosome via co-transformation (128). pMP527 isolated from *E.coli* was transformed and purified from *F. novicida* prior to use in order to increase transformation efficiency. pMP527 (870 ng) was mixed with 8 µg of purified PCR product and then transformed into *F. novicida*. Transformants were picked onto new plates and

successful integration screened for by colony PCR using forward and reverse primers within *pdpC* and the 3xFLAG tag respectively. 3xFLAG tag integrates were screened for the loss of pMP527 by growing isolates in antibiotic-free media and replica plating the resulting colonies onto TSA plates with and without kanamycin. A Western blot of whole cell lysates from kanamycin sensitive integrates was probed with mouse anti-FLAG M2 monoclonal antibody (Sigma) to confirm that a reactive product of the predicted mass of PdpC was present.

4.2.5 Chemical transformation of *F. novicida*

F. novicida strains were grown in fresh TSB supplemented with 0.4% glucose until the exponential phase of growth. Cells were pelleted at 5,000 RPM in a Beckman JA-20 rotor and resuspended in *Francisella* transformation buffer (FTB) at room temperature (9). Plasmid DNA, PCR product, or a ligation mixture, in a volume up to 100 µl, was added to 200 µl of resuspended cells. The mixture was incubated at 37ºC with shaking at 95 revolutions per minute (RPM) for 1 hour. One ml of TSB supplemented with 0.4% glucose was added and the mixture was further incubated at 37ºC for 4 hours with vigorous shaking (200 RPM). Transformants were selected on TSA with antibiotics as needed for 24-48 hours.

4.2.6 SDS-PAGE and immunoblotting

The protein concentrations of samples were determined by the BCA assay (Pierce) and the amount of protein loaded was normalized to 5 µg per lane. Samples of whole cell lysates were mixed with SDS sample buffer containing 62.5 mM Tris (pH 6.8), 1% SDS, 5% β-mercaptoethanol, 0.05% bromophenol blue, and 10% glycerol; and boiled for 10 min prior to electrophoresis. SDS-PAGE was carried out according to the method of Laemmli and samples were electrophoresed through 8% SDS-PAGE gels and transferred to Immobilon-FL membrane

(Millipore) or Pure Nitrocellulose membrane (0.45 µm) (Bio-Rad) (113). Membranes were blocked with 5% skim milk (Difco) in PBS (0.2M NaCl, 4.2 mM KCl, 12.7 mM Na_2HPO_4). Native PdpC was detected using rabbit polyclonal immune serum raised against a PdpC peptide (DDINVDRENRRELVAK) found at amino acids 168-183. After incubation overnight, blots were washed with PBS containing 0.1% Tween-20 for 15 min three times and subsequently probed with IRDye800DX-conjugated goat anti-rabbit Immunoglobulin G (Rockland Immunochemicals). The immunoblots were visualized using the LiCor Odyssey imaging system. The anti-PdpC polyclonal antibody, the anti-IglB, the anti-PdpB monoclonal antibodies, and source hybridomas have been deposited with the Biodefence and Emerging Infections Research Resources Repository program of the American Type Culture Collection. Epitope tagged PdpC, IglA or PdpE was detected using the M2 anti-FLAG monoclonal antibody (Sigma) followed by anti-mouse horse radish peroxidase (HRP) conjugate and SuperSignal West Pico Chemiluminescent Substrate (Thermo Scientific).

4.2.7 Macrophage growth assay

Bone marrow cells were isolated from femurs of healthy BALB/c male mice and cultivated in 96-well cell culture plates at 4×10^5 cells per well (Costar) for one week in complete Dulbecco's Modified Eagle Medium (cDMEM) containing 10% fetal bovine serum (FBS), 1% L-glutamine, 1% MEM non-essential amino acids, 1% 4-(2-hydroxylethyl)-1-piperazineethanesulfonic acid (HEPES) buffer solution, and 10% conditioned L929 supernatant. The resultant bone marrow-derived macrophages (BMDMs) were infected with *F. novicida* strains at a multiplicity of infection (MOI) of 20:1 (bacterium-to-macrophage). Infected monolayers were incubated for 1 hour in cDMEM to allow for phagocytosis to occur, washed five times in Dulbecco's Phosphate Buffered Saline (DPBS), and incubated at 37ºC in 5% CO_2.

Mouse macrophage-like J774A.1 cells were seeded into 96-well cell culture plates at 2×10^5 cells per well and allowed to adhere overnight. Similarly, J774A.1 monolayers were infected at an MOI of 20:1 and incubated for 1 hour in Dulbecco's Modified Eagle Medium (DMEM) containing 10% FBS and 4 mM L-glutamine. To determine bacterial replication, infected macrophages were lysed in 0.1% deoxycholate at 0, 24, and 48 hours post-infection. The lysates were serially diluted in PBS (Gibco) containing 0.1% gelatine and plated on TSA. It has been previously demonstrated that *F. tularensis* extracellular growth in standard DMEM is not supported which makes the macrophage infection assay an appropriate determination of intracellular growth (Nano unpublished results). As a negative control, the *F. novicida mglA* mutant GB2, which does not grow in macrophages, was incorporated into all macrophage growth experiments.

4.2.8 Chicken embryo and mouse infections

Fertilized White Leghorn chicken eggs were obtained from the University of Alberta Poultry Research Station. Seven-day old chicken embryos were injected with various doses of 100 µl of *F. novicida* strains diluted in PBS just beneath the chorioallantoic as previously described (150). The chicken embryos were monitored for death for 6 days. Six-to-eight week-old male specific-pathogen-free BALB/cByJ mice were purchased from the Jackson Laboratory. Animals were housed in sterile micro-isolator cages in a barrier environment at the Center for Biologics Evaluation and Research. Mice were fed autoclaved food and water *ad libitum,* and all experiments were performed under Institutional Animal Care and Use Committee guidelines. Mice were given 0.1 ml of appropriately diluted bacteria intradermally at the base of the tail, and actual doses of inoculated bacteria were simultaneously determined by plate count. All materials

used in animals, including bacteria, were diluted in PBS (BioWhittaker) containing <0.01 ng ml^{-1} endotoxin.

4.2.9 Organ burden assays

Thirteen-day old chicken embryos (n=4) were injected with approximately 1×10^3 bacteria and sacrificed three days later. The liver was removed from the embryo, rinsed with sterile PBS, resuspended in 1 ml PBS containing 0.1% gelatine and homogenized. Embryos minus the liver were suspended in 15 ml of PBS containing 0.1% gelatine and liquefied using a Dounce homogenizer. The resulting homogenate was serially diluted, plated onto TSA, and colony forming units were determined the following day.

4.2.10 Immunofluorescence microscopy

J774A.1 murine macrophage-like cells were grown on coverslips and infected with strains of *F. novicida* as indicated. Cells were infected for 1 hour at an MOI of 50, washed with PBS, and incubated until the desired time point in DMEM containing 10% normal calf serum. At the desired time points post-infection cells were fixed in 4% paraformaldehyde for 15 min at room temperature. 3xFLAG tagged proteins and *Francisella* were detected with anti-FLAG M2 monoclonal antibodies and rabbit anti-*Francisella* serum respectively. The antibodies were diluted in PBS containing 0.5% BSA and 0.1% saponin was added when there was a need to permeabilize host cells. Primary antibodies were detected with goat anti-mouse and goat anti-rabbit serum conjugated to Alexa Fluor 488 and 594 respectively. DNA was detected with DAPI after antibody staining. Coverslips were mounted using Prolong Gold antifade reagent and examined using an Olympus TE81 inverted fluorescent microscope with spinning disc

capabilities. Images were collected as Z-stacks and a projection images was generated using the Intelligent Imaging Slidebook software package.

4.3 Results

4.3.1 PdpC is expressed in *F. novicida* and LVS

Previous bioinformatic and microarray data predicted that the 156 kDa PdpC protein would be produced; however proteomics studies have failed to detect this protein in *Francisella* (30, 53, 160, 214). In order to detect expression of PdpC, two different immunoreactive rabbit sera directed against peptide sequences found in PdpC were developed. Both of the different anti-peptide antisera reacted with the same apparent band on Western immunoblots that were absent from the Δ*pdpC* mutant strain (Fig 13A and data not shown).

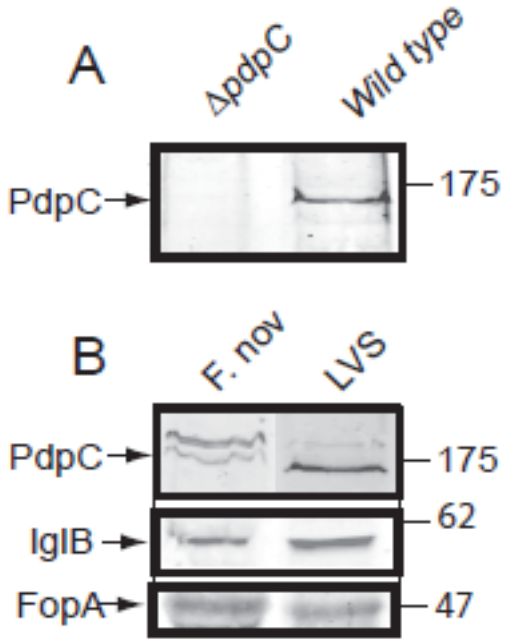

Figure 13. Identification of PdpC with anti-peptide antibody.

(A) Antibody raised against a peptide corresponding to amino acids 168-183 reacted with a band of ca. 160 relative molecular mass in wild type *F. novicida* but not in the Δ*pdpC* mutant. (B) Expression of PdpC in *F. novicida* and LVS. Immunoblotting of 5 µg of *F. novicida* and LVS cell lysates that were grown in the macrophage cell line J774A.1. Top: Rabbit polyclonal anti-PdpC peptide antiserum was used to detect PdpC. The anti-PdpC peptide antiserum used in Panel B was a separate preparation (same antigen) from that used in Panel A, and it consistently reacted with a ca. 180 relative molecular mass band in addition to the PdpC band. The PdpC band in *F. novicida* is often distorted by O-antigen. This effect is seen with other high molecular weight protein bands and the effect is absent in O-antigen mutants of *F. novicida* (data not shown). Middle: Another FPI-encoded protein, IglB, showed slightly higher expression in LVS as compared to *F. novicida*. Bottom: The outer membrane protein FopA was used to give an approximate normalization for the other protein bands.

Once we were confident that we could use our antisersa to detect PdpC we examined expression of PdpC in LVS. In contrast to *F. novicida* all other *Francisella* strains have two copies of the FPI, and thus we wanted to determine if the duplication of the FPI affected expression levels of

PdpC. We quantified the intensity level of PdpC relative to the fluorescence signal generated by antibody directed against the outer membrane protein FopA. We found that the fluorescence signal generated by PdpC relative to FopA was about 1.5-fold stronger in LVS than in *F. novicida* (Fig. 13B). Also in several immunoblots the level of PdpC appeared to be greater in the LVS strain relative to the amount in *F. novicida* when normalized against the total amount of protein analyzed. Another FPI-encoded protein, IglB also showed about 1.5-fold higher levels of expression in LVS as compared to *F. novicida* (Fig. 13B). These expression levels are reasonable, given that LVS has two copies of the FPI, and *F. novicida* has one copy.

4.3.2 *pdpC* is required for virulence in embryonated chicken eggs

As other FPI-encoded proteins are required for virulence we tested *pdpC* for its requirement for full virulence in vertebrate animals. In order to reduce animal suffering we used a chicken embryo model of infection, which is able to discriminate differences in virulence among mutant *Francisella* strains (150). The Δ*pdpC* mutant was found to be less virulent in chicken embryos (Fig. 14). Infection with 10^3 or greater wild type of *F. novicida* results in 75-100% death by day 4 (Fig. 14A), while embryos infected with similar amounts of Δ*pdpC* survived significantly longer (Fig. 14C) (p-value: 0.0182). Infections with the Δ*pdpC* strain required about 7×10^5 CFU in order to generate the time to death pattern seen with the wild type *F. novicida* strain (Fig. 14D).

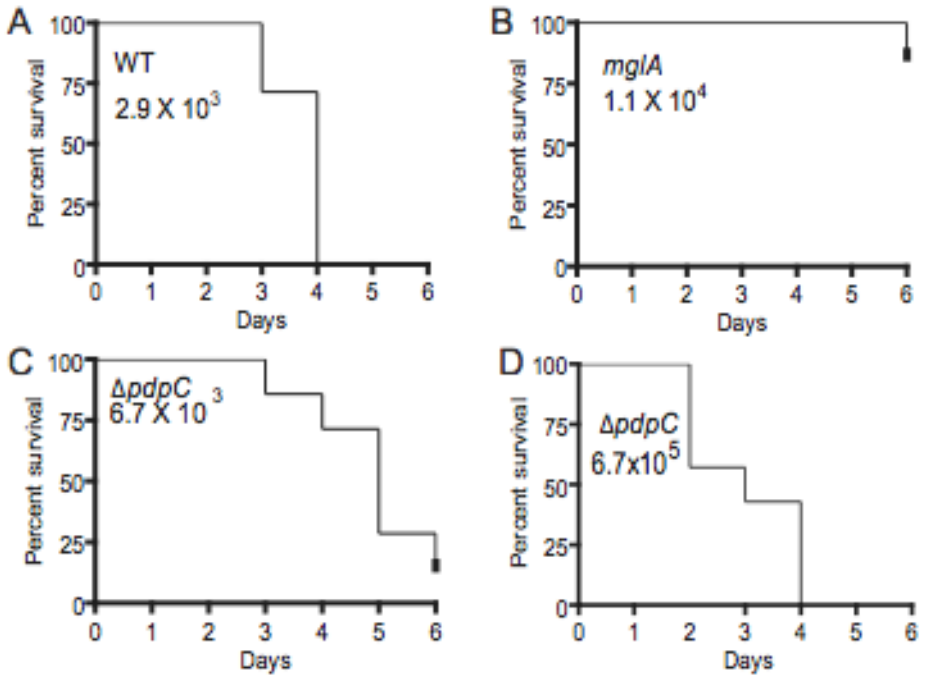

Figure 14. Virulence of *F. novicida* Δ*pdpC* mutant during the infection of chicken embryos. For each indicated strain a series of inocula were used to infected different groups of embryos, but only one dilution is shown, except for Δ*pdpC* (C and D). Panel D illustrates the approximate inoculum of Δ*pdpC* that is required to match the mortality induced by the wild type strain at the dilution represented in the panel. The experiments were performed at least three times, and gave similar results every time. Each experimental run included a positive, wild type control (A), and a negative, GB2 (*mglA*) control (B). All chicken embryo infection experiments used at least 7 embryos per dilution. The inoculum for each chicken embryo infection is indicated by the number inside of each graph. The difference between Wild type and Δ*pdpC* is statistically significant (p-value: 0.0182)

4.3.3 *pdpC* is required for full virulence in mice.

To test if this defect in virulence held true in a mammalian animal model we also tested the Δ*pdpC* mutant for virulence in mice following an intradermal infection. The Δ*pdpC* mutant was found to be at least 100-fold less virulent than the parental strain (Table 4). These results confirm the data obtained in the embryonated chicken eggs that *pdpC* is required for full virulence of *Francisella* in animal models.

Table 4. Virulence of *F. novicida* strains following intradermal infection of BALB/c mice.

F. novicida Strain	Infectious Dose*	Deaths per Total
Experiment 1		
Wild type	7.3×10^4	5/5
Wild type	7.3×10^1	0/5
Δ*pdpC*	9.9×10^6	0/5
Δ*pdpC*	9.9×10^5	0/5
mglA	9.1×10^6	0/5
Experiment 2		
Wild type	6.4×10^2	4/5
Wild type	3.2×10^1	2/7
Δ*pdpC*	9.0×10^6	0/7
pdpE-1	2.5×10^2	5/5
pdpE-2	3.2×10^2	5/5
mglA	1.2×10^6	0/7
PBS	NA	0/7

* Numbers indicated actual inoculating dose, determined at the time of infection.

4.3.4 *pdpC* is not required for intramacrophage growth

The results showing a clear role for *pdpC* in virulence in animals could indicate that the gene plays a role in allowing *Francisella* growth within macrophages, an important host cell type for *Francisella*. Macrophages not only serve as a potential host cell but also play an important

role in the immune defences of the host against *Francisella*. Therefore, the phenotype of a Δ*pdpC* was evaluated for growth within macrophages to assess if the reduced virulence of the Δ*pdpC* strain is due to reduced intramacrophage growth, as seen for most other FPI-encoded proteins. The Δ*pdpC* mutant grew like wild type *F. novicida* inside J774A.1, a mouse macrophage-like cell line (data not shown). To test if this ability of the Δ*pdpC* strain to grow in this permanent cell line held true in primary cells, we also tested the growth of this strain in bone marrow-derived murine macrophages (BMDM). The Δ*pdpC* strain was able to replicate well as wild type *F. novicida*, while a *mglA* mutant did not replicate, as was expected (Fig. 15).

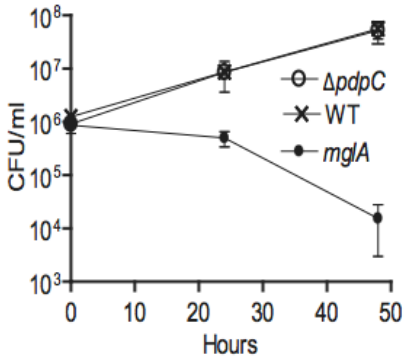

Figure 15. Intramacrophage growth of Δ*pdpC*.

The Δ*pdpC* mutant, with a deletion of the complete *pdpC* structural gene, grew like wild type in BMDMs. All data points represent at least three replicates, and each experiment was done at least three times. Standard errors are indicated by bars.

4.3.5 Reduced virulence of the Δ*pdpC* is not due to effects on *pdpE*

Conceivably, the deletion in the *pdpC* could affect the expression of the downstream gene, *pdpE*, and we wanted to test if disruption of *pdpE* expression was contributing to the phenotype of Δ*pdpC* in animal models. As there are no genes downstream of *pdpE* in the operon there is little concern that its disruption would affect other genes in the FPI. A *pdpE* insertion mutant was obtained from a study by Gallagher *et al.* and tested for virulence in chicken embryos and found to be as virulent as the parental wild type strain (Fig. 16C) (84). No difference in virulence between the *pdpE* mutants and wild type were found even when very low inoculating doses were used (data not shown).

Two *pdpE* insertion mutants were also tested for their virulence in mice (Fig. 16A) All mice inoculated with *pdpE* insertion mutants died (Table 4), demonstrating similar virulence of this mutant strain compared to wild type *F. novicida*. We also tested *pdpE* mutants for intramacrophage growth and found that mutant strains grew like the wild type strain (Fig. 16B). When a double Δ*pdpC-pdpE* mutant was made, it too was able to grow in macrophages (data not shown).

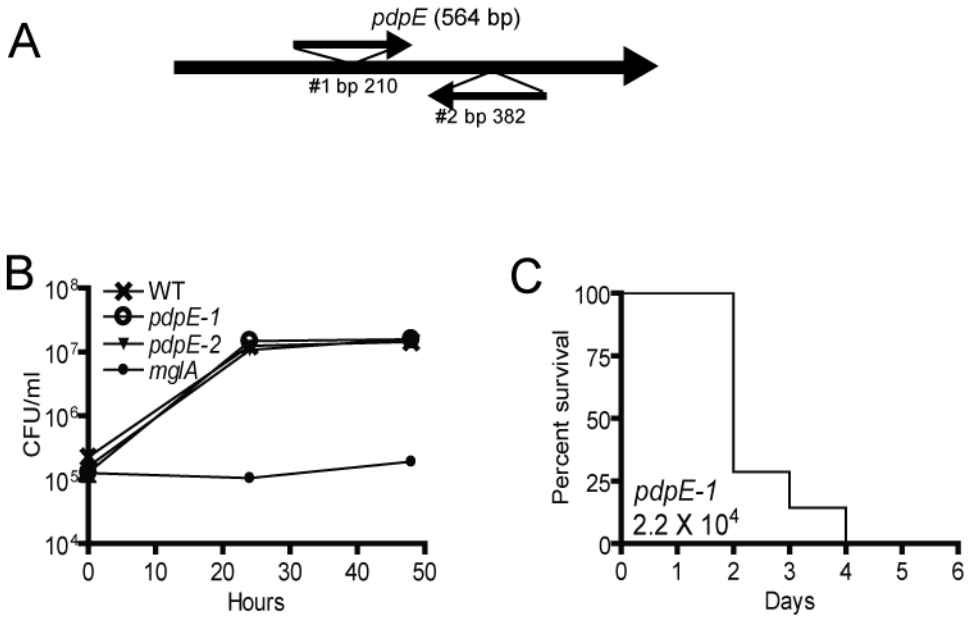

Figure 16. Mutants with insertions in the *pdpE* gene.

(A) Diagrammatic representation of the insertion location of two different *pdpE* mutations. (B) Both *pdpE* mutants grew similarly to wild type *F. novicida* in J774A.1 macrophages. These experiments were done in triplicate and repeated two times. Error bars, indicating standard error, are included but not visible. (C) A mutant with an insertion in *pdpE* was as virulent as wild type *F. novicida* in chicken embryos. This experiment was performed twice with two different innocula (only one shown) with seven embryos.

4.3.6 Reduced accumulation of *pdpC* mutants in the liver of chicken embryos

To help discern the nature of the attenuation of the Δ*pdpC* mutant, the number of bacteria that accumulated in the liver was measured. Infection of 13-day-old chicken embryos with wild type *F. novicida* resulted in about 6-fold more bacteria in the whole embryo (minus the liver) as compared to the number in the liver three days after infection (Fig. 17). The same type of

infection with the Δ*pdpC* strain resulted in about 200-fold more bacteria in the whole embryo relative to the number in the liver (Fig. 17).

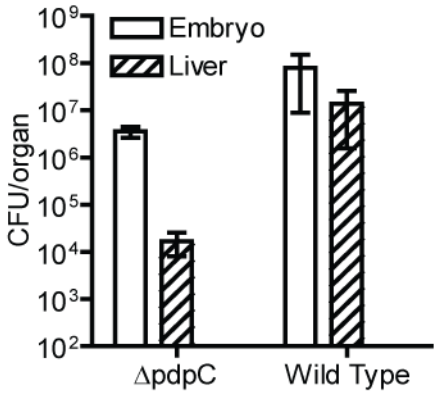

Figure 17. Poor accumulation of Δ*pdpC* mutant strain in the liver of chicken embryos. The levels of the wild type *F. novicida* and the Δ*pdpC* mutant were assayed by homogenizing the liver and the remainder of the embryo and determining CFU on agar plates. The experiment was repeated two times with similar results and four embryos were used for each assay. The standard error is indicated by the error bars. The older embryos (as compared to time-to-death experiments) were used in order to allow for the development of livers that could be easily manipulated.

4.3.7 PdpC is localized to the host cells during infection

To test if PdpC can be detected as a secreted protein within infected cells we cloned the triple FLAG tag at the C-terminus of *pdpC* to increase signal and reduce background in immunofluorescent microscopy experiments. Plasmids expressing this epitope tagged version of

PdpC were transformed into *F. novicida* and these bacteria were used to infect J774A.1 macrophage like cells. In fluorescent microscopy experiments we detected PdpC-3xFLAG in punctuate structures in close proximity, but not colocalizing with the bacteria one hour post-infection (Fig. 18). This finding indicates that PdpC-3xFLAG expressed from a plasmid can be detected as a secreted protein inside infected cells. In addition some bacteria cells were also labelled with the antibody.

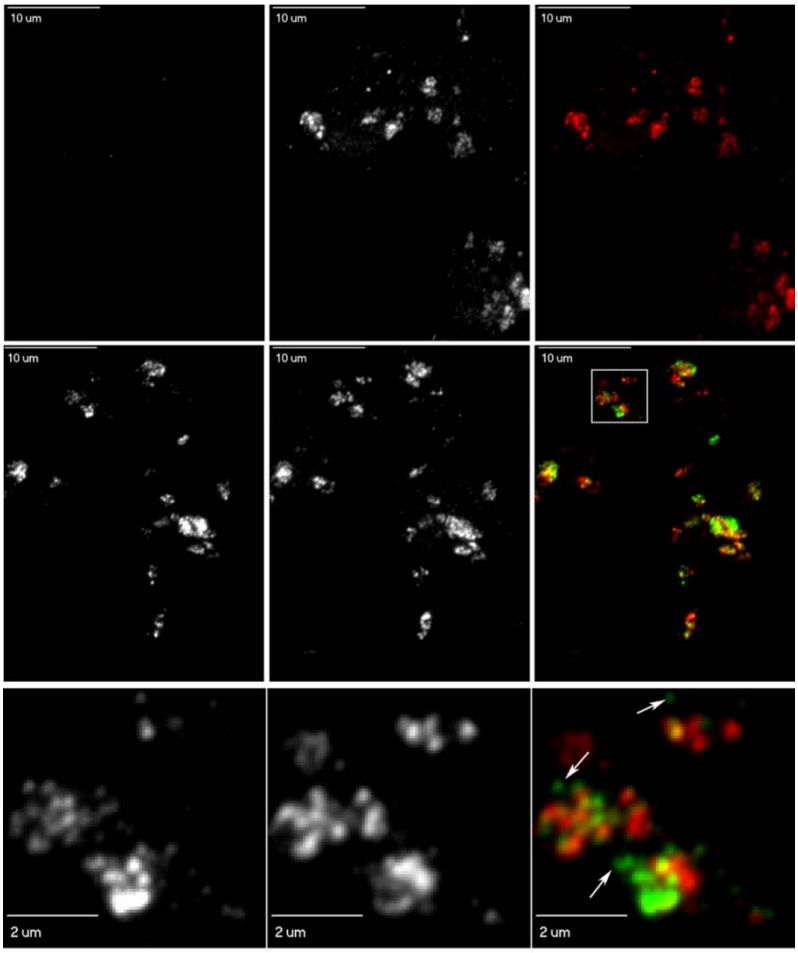

Figure 18. *In trans* PdpC-3xFLAG tag expression during infection of J774A.1 cells. J77A.1 macrophage-like cells infected with wild type (top row) or wild type expressing PdpC-3xFLAG from our expression plasmid pKH5 (middle row). After 1 hour cells were fixed and stained for FLAG (left column) and *F. novicida* (middle column). The right column represents a

merged image of the FLAG (green) and bacterial (red) channels. The bottom row represents a magnification of the area indicated in the middle row. Arrows indicate FLAG signal in infected cells not associated with bacterial staining.

As FPI encoded proteins are tightly regulated, results from plasmid expression systems using the GroEL promoter have to be carefully interpreted. To assess if the staining pattern of PdpC-3xFLAG can be explained by different temporal regulation and expression levels we replaced the native *pdpC* in the *F. novicida* chromosome with a gene that leads to the expression of a C-terminal epitope tagged version of PdpC. When J774A.1 macrophage-like cells were infected with this strain and examined by fluorescent microscopy we found that infected cells showed clear signal for PdpC-3xFLAG in a pattern very similar to the plasmid expressing tagged protein (Fig. 19).

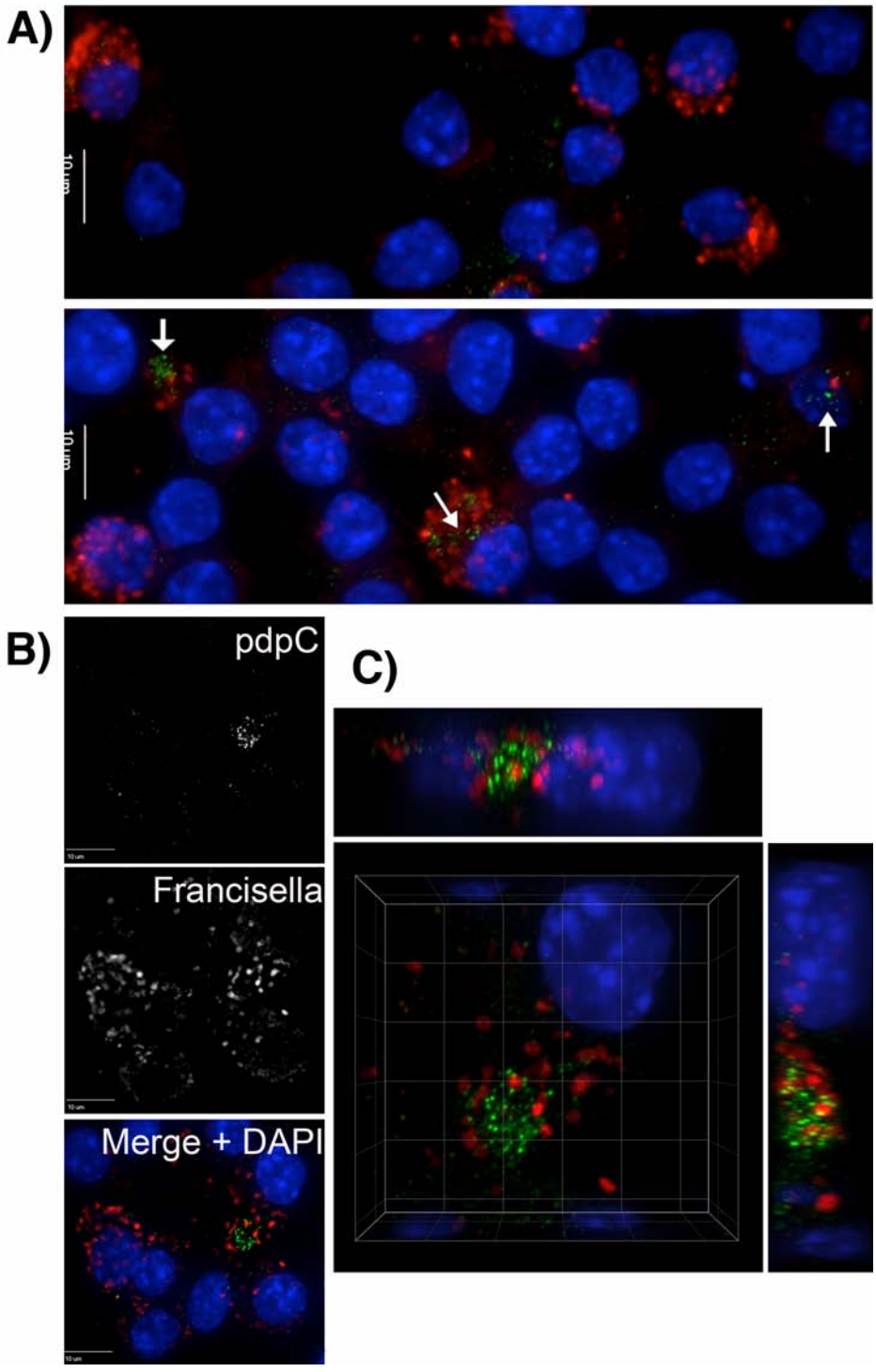

Figure 19. PdpC-3xFLAG expressed from the bacterial chromosome.

(A) Merged images of J774A.1 cells infected with wild type (top) or wild type carrying a gene encoding the PdpC-3xFLAG protein in the chromosome (bottom). (B) A projection image and

(C) three dimensional reconstruction of a cell infected with wild type carrying *pdpC-3xFLAG* integrated into the chromosome 10 hours post-infection.

The integrated form of *pdpC-3xFLAG* also allowed us to assess the temporal regulation of *pdpC* in the infected host cell. During a time course experiment we examined J774A.1 cells for the presence of PdpC in the infected cell (Fig. 20). The first clear signal above background was detected in some infected cells 5 hours post-infection with steadily increasing signal intensity and frequency of infected cells showing signal for PdpC-3xFLAG. By 13 hours strong signal was observed in the majority of cells: signal strength and frequency further increased until 21 hours post-infection. After that time point, large-scale death of the infected host cells prevented further examination. Even at these late time points, some heavily infected cells did not show signal detectable by microscopy, suggesting some heterogeneity in expression or secretion of PdpC.

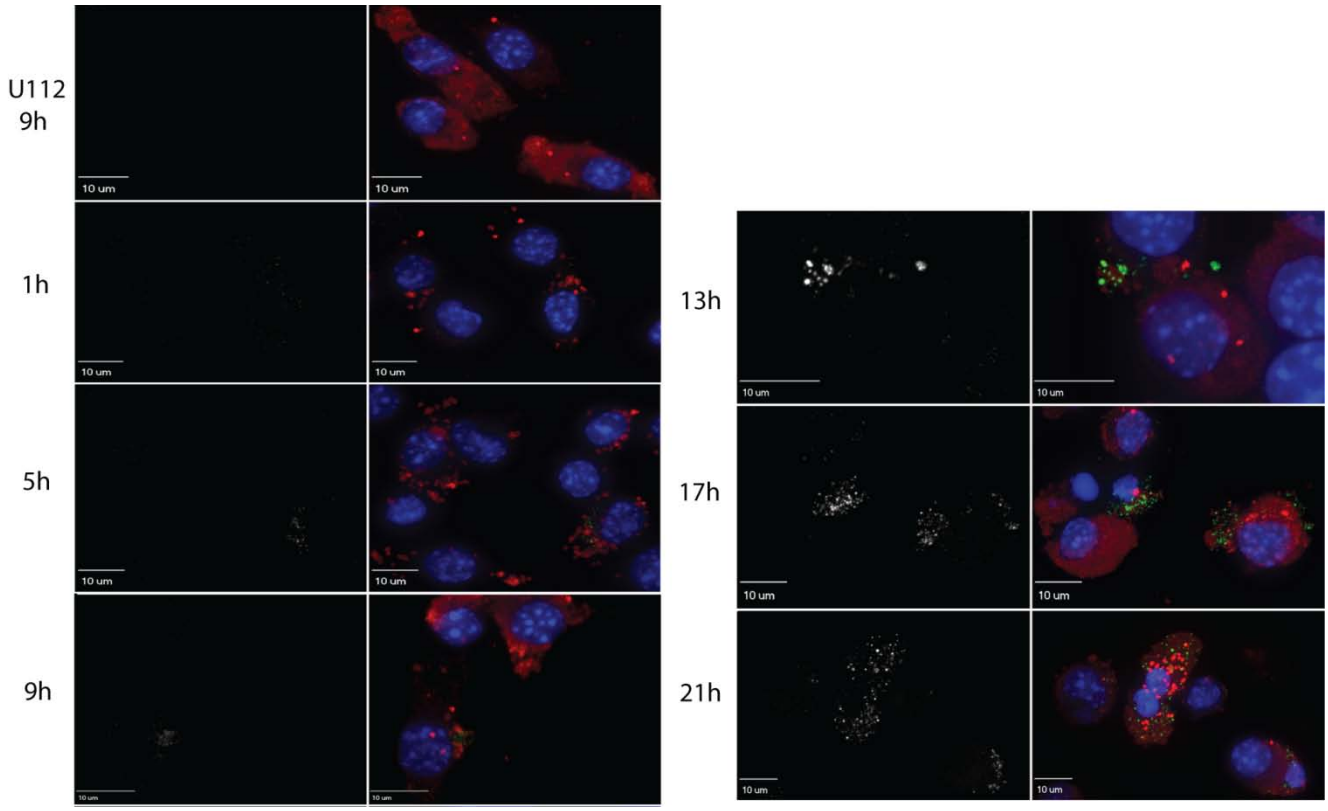

Figure 20. Time course of PdpC detection within infected J774A.1 macrophage-like cells. Cells were infected with *F. novicida* carrying *pdpC-3xFLAG* in the chromosome and fixed at the indicated time points after infection. Cells were permeabilized by Saponin treatment. The channel detecting the epitope tag is shown on the left and a merged image of bacteria (red) PdpC-3xFLAG (green) and DNA (blue) is shown on the right. The top row shows cells infected with wild type lacking the epitope tag 9 hours post-infection.

4.3.8 PdpE is secreted in a *pdpB* dependent manner

Next PdpE was tested to see if it can also be detected by microscopy within infected macrophage-like cells. Infection of J774A.1 cells with wild type *F. novicida* expressing PdpE-3xFLAG from the plasmid pKH16 yielded clear staining for PdpE-3xFLAG associated with a significant proportion of bacteria (Fig. 21). To test if detection was dependent on the T6SS,

pKH16 was also transformed into a Δ*pdpB* strain. The Δ*pdpB*::pKH16 strain expressed PdpE-3xFLAG at levels similar to that of wild type U112::pKH16 (Fig. 21A). However when J774A.1 cells were infected with Δ*pdpB*::pKH16, significantly less anti-FLAG signal was detected compared to wild type U112::pKH16 (Fig. 21B). Using automated computer image analysis in order to eliminate human bias, we determined that this difference was statistically significant over three independent experiments. Our results were unable to confirm that PdpC secretion is dependent upon T6SS because generally less signal was observed for PdpC-3xFLAG than PdpE-3xFLAG during infection resulting in a lower threshold of signal to background fluorescence. The timecourse experiments demonstrate that secretion of PdpC occurs at later time points, when the avirulent escape-defective Δ*pdpB* strain may be degraded. This may release PdpC-3xFLAG that had been sequestered within the bacteria, creating an artefact which obscures the presumed difference in signal between wild type and the T6SS negative strain Δ*pdpB*.

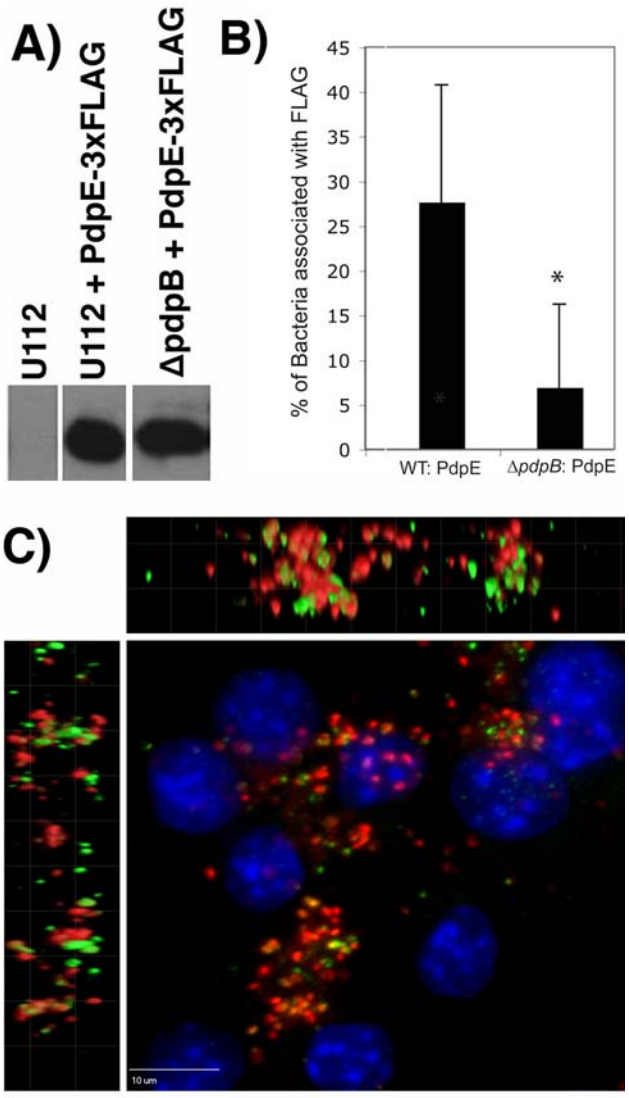

Figure 21. pKH16 in wild type and a Δ*pdpB* background during infection of J774A.1 cells.

(A) Western immunoblot demonstrating expression of PdpE-3xFLAG in whole cell lysates of wild type and the Δ*pdpB* strain that possesses pKH16, but not wild type U112 alone. (B) Automated analysis of bacterial cells associated with FLAG signal in wild type and Δ*pdpB* background during an infection of J774A.1 cells shown in C. Standard deviation is shown by error bars, one-tailed paired t-test (p=0.012); 100-200 bacteria were counted per experiment. The graph represents three independent experiments and * denotes that the means are statistically significantly different. (C) J774A.1 cells infected with wild type U112::pKH16 stained for bacteria and FLAG at 8 hours post-infection. A three dimensional reconstruction is shown

(U112: red, FLAG: green, DAPI: blue) with projection images over the Z-axis and perspective views of the Z-stack from the left and the back.

4.4 Discussion

It remains unclear why such a disparity of virulence exists among different strains of *Francisella*. This variation is surprising, considering the high degree of genetic similarity between strains. The FPI has been recognized as a virulence factor, of which there are two copies present in all strains except *F. novicida* (146). This chapter has presented evidence that a strain possessing two copies of the FPI (LVS) produces about 50% more of the FPI proteins PdpC and IglB than one containing a single copy (*F. novicida*). Increased expression of FPI proteins, which are predicted to encode a T6SS may contribute to the higher pathogenicity observed in these strains.

The fact that *pdpC* was not required for intracellular growth in either J774A.1 macrophage-like cells or BMDMs is interesting since many other FPI genes are required for intracellular growth (52, 192). Despite being dispensable for growth in macrophages, which have been described as a important site of replication for *Francisella* PdpC appears to be required for full virulence in a chicken embryo model and indispensable in a mouse model of infection. The depressed number of Δ*pdpC* bacteria found within the embryo liver could reflect a diminished ability to grow within some liver specific cell type, a defect in dissemination from the site of infection, or perhaps a decreased ability of the mutant to gain entry to cells types other than macrophages.

We were unable to complement the Δ*pdpC* strain despite multiple attempts in different genetic contexts. It has been demonstrated that the FPI is tightly regulated, and it is possible that the ectopic expression of *pdpC* did not fall within wild type expression parameters. As a result it became crucial that we exclude the possibility that the phenotype we had observed was due to a polar effect. *pdpE* is the only gene downstream of *pdpC* as well as the final gene in the operon. Two different insertion mutants in *pdpE* were able to grow in macrophages and were not attenuated in mice and chicken embryos. To exclude the possibility that the observed phenotype was the result of the disruption of both genes, a Δ*pdpC-E* double-knockout mutant was generated. The double knockout mutant was able to grow in macrophages and was no more attenuated than the Δ*pdpC*.

These results suggest that the basis of attenuation is not due to a decreased ability to replicate in macrophages. Such a disconnect between virulence and intramacrophage growth phenotypes is unusual for FPI-encoded proteins and has so far only been described for *pdpD*, a gene also required for full virulence in animal but not required for growth within macrophages. The disruption of other FPI-encoded proteins that have been proposed as structural elements of the secretion system are required for intracellular growth. Therefore it appears unlikely that PdpC is a structural component of the proposed *Francisella*. It is not uncommon for secretion systems encoded within plasmids and pathogenicity islands to also harbour their corresponding secreted effector proteins (82). Given the phenotype exhibited by the Δ*pdpC* strain, it seems plausible that PdpC might indeed function as a secreted effector. While our microscopy experiments suggest that PdpC is secreted during infection, these results are unfortunately only qualitative at this point. Quantitation of the microscopy data would greatly strengthen this notion. There is biochemical evidence that PdpE is secreted during macrophage infection,

supported by both the qualitative and quantitative evidence provided by microscopic investigation.

Chapter 5: Mutagenesis of the FPI gene *pdpC* alters expression of intracellular growth locus genes ABCD.

Eli B. Nix, Karen Cheung, Crystal L. Schmerk, Olle M. de Bruin, and Francis E. Nano
Department of Biochemistry and Microbiology, University of Victoria, Victoria, BC, Canada

5.1 Introduction

The macrophage is one of the most hostile environments that a facultative intracellular bacterium can encounter. Microbes respond to extreme changes in their environment by shifting the expression profile of their genome. In *Francisella*, the first regulator of virulence gene expression was identified by the Nano laboratory in 1998. By investigating a spontaneous mutant that was defective for growth in macrophages, and using an *in cis* complementation strategy, an operon consisting of two genes was identified: *mglAB* for macrophage growth locus (24). MglA and MglB are orthologs of stringent starvation protein A and B (SspA and SspB) in *E.coli*. MglA and SspA share 21% identity and 34% similarity at the primary amino acid level (38). SspA is an RNA polymerase associated protein that regulates a cluster of genes when conditions of stress arise (223). It was subsequently shown that MglA is induced during infection of macrophages and regulates at least 102 genes, mostly positively, including the entire FPI (23, 30, 120). As the complete genome sequence of several *Francisella* strains were published, it became apparent that they encoded an MglA-like protein, annotated as SspA (118). MglA and SspA both associate with the RNA polymerase holoenzyme, and the ability of MglA to control virulence is connected to this association (38). Other bacterial pathogens in which SspA homologs contribute to control of virulence genes, such as *Vibrio cholera* or *Yersinia enterocolitica*, only encode one SspA homolog (16, 140). Charity *et al.* suggest that the use of two SspA homologs might allow for the integration of multiple environmental signals (38).

The genome revealed that, unlike any other bacterium sequenced to date, *Francisella* encodes two rather than one RNA polymerase α subunits. In other bacterial systems the α subunit forms a dimer in the RNA polymerase complex (88). The α subunit of RNA polymerase is a target for transcriptional activators, and aids in promoter recognition by sequence-specific protein-DNA interactions (58, 178). The two α subunits in *Francisella* differ from each other in regions that are critical not only for dimer formation, but also for promoter recognition and activator interaction. Nevertheless there is biochemical evidence that both α subunits are components of the RNA polymerase complex (38). It has been suggested that there could be up to four different species of RNA polymerase in *Francisella*: two composed of either α1 or α2 homodimers and two heterodimers of α1α2 that differ with respect to which α protomer interacts with the β and β' subunits of RNA polymerase (38). It remains to be seen which combinations actually exist, and based on these findings it is unlikely that the mechanisms of *Francisella* gene expression will be prototypical.

One way in which prokaryotes regulate cellular functions in response to environmental stimuli is by signal transduction pathways. These pathways are often composed of a two-component regulatory system that act by way of phosphotransfer between a sensor histidine kinase and a response regulator (97). Commonly, the histidine kinase is membrane-bound with an extracellular input domain that detects an environmental signal, while the response regulator is cytosolic. Upon detection of a signal, the histidine kinase domain is activated, resulting in autophosphorylation. The phosphoryl group is then transferred to a specific aspartate residue of the response regulator, activating its output domain (215). In the majority of characterized systems, this output domain can bind DNA, giving the response regulator control over transcription, and thus, the ability to initiate the appropriate cellular response (206).

Ordinarily, two-component regulatory systems are genetically arranged together in an operon driven from a single promoter (206). Although this is the case in *F. novicida*, the more virulent strains, *F. tularensis holarctica* and *F. tularensis*, contain an orphaned response regulator (25, 143). The response regulator was designated PmrA, owing to its 44% identity over its entire length to the PmrA protein of *Salmonella* (143). The PmrA protein regulates the FPI and as a result, is required for intramacrophage growth and virulence. It is the primary target of the histidine kinase KdpD, and phosphorylation of PmrA enhances its DNA binding activity. Furthermore, PmrA coprecipitates with both MglA and SspA from whole cell lysates and therefore, are part of the same protein complex. It is unknown whether PmrA binds to MglA, SspA, or both proteins (25). In *F. novicida*, phosphorylation of PmrA is likely reduced due to the presence of a secondary target for KdpD, KdpE. The fully virulent strain *F. tularensis* lacks KdpE, which might result in higher expression of the PmrA-regulated genes. This factor could help explain the disparity in virulence between strains.

5.2 Materials and methods

Mutants were created by E. Nix and K. Cheung
Subcellular fractionations were performed by K. Cheung and O. de Bruin
Macrophage experiments were performed by E. Nix and C. Schmerk
Chicken embryo experiments were performed by E. Nix and K. Cheung

5.2.1 Bacterial strains and plasmids

Bacterial strains and plasmids are listed in Table 5. *F. novicida* strains were grown aerobically at 37ºC in trypticase soy broth and supplemented with 0.1% cysteine (TSB) or on trypticase soy agar supplemented with 0.1% cysteine (TSA). The *F. novicida* JLO strain was

used as the wild type strain in all experiments, and has a phenotype indistinguishable from the parental type strain, U112 (128). Erythromycin (Em; 30 μg ml^{-1}) or hygromycin (Hyg; 200 μg ml^{-1}) was added as needed. *Escherichia coli* DH5α was used for all molecular cloning and was cultured in Luria-Bertani broth (LB) with ampicillin (Ap; 250 μg ml^{-1}) as needed. The pCR2.1-TOPO vector (Invitrogen) or pSMART (Happy Corp) was used to clone the polymerase chain reaction (PCR) products. The low copy-number plasmid pWSK29 was used to construct clones for in-frame partial deletions of *pdpC* (220).

Table 5. Bacterial strains and plasmids used to investigate *pdpC* mutant phenotypes.

Strain or plasmid	Genotype or phenotype	Reference or source
Bacterial strains		
E. coli DH5α	*E. coli* F^- ϕ80d*lac*ZΔM15Δ (*lac*ZYA-*arg*F)U169 *rec*A1 *end*A1 *hsd*R17(r^-_k, m_k^+) *pho*A *sup*E44 *thi*-1 *gyr*A96 *rel*A1λ^-	Invitrogen
F. novicida U112	Prototype *F. novicida* strain	Laboratory strain
JLO	U112 with deletion in FTN_*1390*	(128)
mglA	U112 with point mutation in *mglA* gene	(24)
pdpC::Em^R	Allelic replacement of codons 4-1204 of *pdpC* with an erythromycin resistance cassette	This work
Δ*pdpC*	JLO with a complete deletion of *pdpC*	This work
*pdpC*Δ1	JLO missing codons 40-60 of *pdpC*	This work
pdpC#2	JLO with a stop codon introduced at codon 95	This work
*pdpC*Δ3	JLO missing codons 205-244 of *pdpC*	This work
*pdpC*Δ4	JLO missing codons 265-316 of *pdpC*	This work
*pdpC*Δ5	JLO missing codons 385-423 of *pdpC*	This work
*pdpC*Δ9	JLO missing codons 589-625 of *pdpC*	This work
*pdpC*Δ10	JLO missing codons 665-723 of *pdpC*	This work
*pdpC*Δ11	JLO missing codons 880-942 of *pdpC*	This work
*pdpC*Δ12	JLO missing codons 1053-1109 of *pdpC*	This work
C1	U112 with T20 (IS*Fn*2/FRT) insertion in *pdpC* at nucleotide 878	(84)
C2	U112 with T20 (IS*Fn*2/FRT) insertion in *pdpC* at nucleotide	(84)

	1690	
E1	U112 with T18 (IS*Fn*2) insertion in *pdpE* at nucleotide 210	(84)
E2	U112 with T18 (IS*Fn*2) insertion in *pdpE* at nucleotide 382	(84)
*pdpC*Δ4R	*pdpC*Δ4 with wild type DNA integrated in the mutated locus	This work
*pdpC*Δ4mR	*pdpC*Δ4 that failed to integrate the wild type amplicon into the mutated locus	This work
*pdpC*Δ*4b-3xFLAG*	recreation of *pdpC*Δ4 by integrating mutant DNA into a chromosomal C-terminal 3xFLAG tagged version of *pdpC*	This work
pdpC-3xFLAG	U112 with 3xFLAG tag integrated at the C-terminus of PdpC	Chapter 4
*pdpC*Δ4c	recreation of *pdpC*Δ4 by integrating the mutated DNA into wild type strain	This work
C1::*pdpC*Δ4	an allelic exchange of C-1 with *pdpC*Δ4 DNA	This work
C2-1*pdpC*Δ4	*pdpC*Δ4 transformed with C-2 DNA that acquired Km^R	This work
E1-1*pdpC*Δ4	*pdpC*Δ4 transformed with E-1 DNA that acquired Km^R	This work
E1-1-31	E1-1*pdpC*Δ4 integrated into *pdpC*Δ4b-*3xFLAG*	This work
C2-1-1	C2-1*pdpC*Δ4 integrated into *pdpC*Δ4b-*3xFLAG*	This work
Δ*iglD*	JLO with a complete deletion of *iglD*	deBruin *et al.* unpublished
Δ*pdpC-E*	JLO with a complete deletion of *pdpC* and *pdpE*	Chapter 4
Plasmids		
pWSK29	Low-copy-number, Ap^R, *lacZα*	(220)
pSMART	Low-copy-number, Ap^R, *lacZα*	Happy Corp.
pCR2.1-TOPO	*E.coli* cloning vector, high-copy, Ap^R, *lacZα*	Invitrogen
pMP633	*Francisella* shuttle vector, Hyg^R, stable	(125)
pMP823	*Francisella* shuttle vector, Hyg^R, unstable	(125)
SKX	pWSK29 containing a *Francisella* integration cassette	(128)
pFNLTP6-GroE	*Francisella* shuttle vector, Km^R	(130)
pKH5	*pdpC-3xFLAG* in pFNLTP6-GroE	This work
pKHiglD	*iglD-3xFLAG* in pFNLTP6-GroE	This work

5.2.2 Polymerase chain reaction and primer design

Routine PCR reactions that were used for screening or analysis of mutants were carried out using Taq polymerase (Invitrogen). For the creation of deletion mutants, "fusion PCR" was used to join two PCR amplicons. For these reactions or any amplification that required proof-reading or highly processive enzyme reactions, Phusion DNA Polymerase (New England Biolabs) was used in a reaction containing nuclease-free water, 1X Phusion HF buffer, 200 µM dNTPs, 0.5 µM each of the forward and reverse primers (Integrated DNA Technologies), 0.1 ng of template DNA, and 1.0 U of Phusion DNA Polymerase. PCR reactions were essentially as follows: Initial denaturation at 98ºC for 30 s; 35 cycles of 98ºC for 30 s, 55ºC for 30 s, 72ºC for 2 minutes 30 s; final extension at 72ºC for 10 minutes. All primers were designed based on the *F. novicida* U112 genome sequence (GenBank accession no. NC 008601) and are listed in Table 5.

5.2.3 Recombinant DNA techniques

The blunt ended PCR products generated with Phusion DNA Polymerase were TA cloned into the pCR2.1-TOPO vector by an initial purification with QIAquick PCR Purification Kit (Qiagen) followed by the addition of 3' A-overhangs with Taq DNA Polymerase at 72ºC for 15 minutes in a reaction containing nuclease-free water, 1X PCR ThermoPol buffer, and 0.1 mM dATP. Alternatively, blunt end PCR amplicons were ligated to pSMART. Ligation mixtures were electroporated into the *E. coli* DH5α using a Gene Pulser apparatus (Bio-Rad). Unless otherwise noted, all other recombinant cloning techniques were performed according to the protocols described in *Molecular Cloning* (181).

5.2.4 Chemical transformation of *F. novicida*

F. novicida strains were grown in fresh TSB supplemented with 0.4% glucose until the exponential phase of growth. Cells were gently pelleted at 4,000 RPM in a Beckman JA-20 rotor and resuspended in *Francisella* transformation buffer (FTB) at room temperature as previously described (11). Plasmid DNA, PCR product or a ligation mixture, in a volume up to 100 µl, was added to 200 µl of resuspended cells. The mixture was incubated at 37ºC with shaking at 90 RPM for 1 hour. One ml of TSB supplemented with 0.4% glucose was added and the mixture was further incubated at 37ºC for 4 hour or overnight with vigorous shaking at 200 RPM. Transformants were selected on TSA with antibiotics as needed for 24-48 hours.

5.2.5 Deletion mutagenesis

Deletion mutations in *F. novicida* were made essentially as follows: PCR amplicons of about 1.5 kb were generated that corresponded to the regions that flanked the area to be deleted. One primer in each of the amplicons had overlapping sequence with one primer of the other, thus allowing the amplicons to be joined by a subsequent fusion PCR reaction. The final fusion PCR amplicon, containing the deletion, was amplified using primers that annealed close to the ends of the fusion amplicon and contained Xho I sites. After digestion with Xho I, the final fusion PCR amplicon was ligated to an erythromycin resistant (Em^R) cassette that contained the *sacB* gene. The expression of *sacB* in many bacteria allows for counter-selection in the presence of sucrose, but in *F. novicida sacB* expression creates mucoidal colonies that are viable in the presence of sucrose. The ligation mixture was transformed into *F. novicida* and selection was made for Em^R colonies. Transformants were grown in TSBC without Em, and plated onto agar containing 10% sucrose. Colonies that retained the Em^R-*sacB* cassette appeared mucoidal on agar plates containing sucrose, and non-mucoidal colonies were picked to agar plates with and without Em. Non-mucoidal, Em sensitive colonies were screened by PCR for the presence of the desired

deletion. When a strain was found with a possible deletion, PCR was used to amplify the DNA surrounding the deleted area and the PCR amplicon was analyzed by DNA sequencing.

5.2.6 Restoration of mutant to wild type genotype

To restore the *pdpC*Δ4 mutant to a wild type genotype, 600 µg of pMP633 plasmid DNA was used to co-transform the complementing, unmarked DNA. Colonies that were Hyg resistant by virtue of plasmid uptake were screened by PCR to detect restoration of the deleted region. The affected region of the chromosome was PCR amplified and the amplicon was subjected to DNA sequence analysis.

5.2.7 DNA sequence and analysis

PCR products amplified with primers designed for the regions of the *F. novicida* chromosome containing the partial deletions of *pdpC* were purified using the QIAquick PCR Purification Kit (Qiagen) to remove excess primers, dNTPs, salts, and Phusion DNA Polymerase. Sequencing of these amplicons was performed by the CMMT / CFRI DNA Sequencing Core Facility at the University of British Colombia. The accession numbers for the DNA sequence of the mutated regions in *pdpC*Δ1 is EU144122; *pdpC*#2, EU144123; *pdpC*Δ3, EU144124; *pdpC*Δ4, EU144121; *pdpC*Δ5, EU144125; *pdpC*Δ9, EF533681; *pdpC*Δ10, EF533682; *pdpC*Δ11, EF533683; *pdpC*Δ12, EF533684. The accession number for the sequence of the complemented strain of *pdpC*Δ4R is EU144120.

5.2.8 SDS-PAGE and immunoblotting

The protein concentrations of samples were determined by the BCA assay (Pierce) and the amount of protein loaded was normalized to 5 µg per lane. Samples of whole cell lysates

were mixed with SDS sample buffer containing 62.5 mM Tris (pH 6.8), 1% SDS, 5% β-mercaptoethanol, 0.05% bromophenol blue, and 10% glycerol; and boiled for 10 minutes prior to electrophoresis. SDS-PAGE was carried out according to the method of Laemmli and samples were electrophoresed through 8% SDS-PAGE gels and transferred to Immobilon-FL membrane (Millipore) or Pure Nitrocellulose membrane (0.45 µm) (Bio-Rad). Membranes were blocked with 5% skim milk (Difco) in PBS (0.2M NaCl, 4.2 mM KCL, 12.5 mM Na_2HPO_4 2.3 mM $KHPO_4$). Antibody-reactive proteins were detected using rabbit polyclonal immune serum raised against a PdpC peptide (DDINVDRENRRELVAK) found at amino acids 168-183. After incubation overnight, blots were washed with PBS containing 0.1% Tween-20 for 15 minutes three times and subsequently probed with IRDye800DX-conjugated goat anti-rabbit Immunoglobulin G (Rockland Immunochemicals). The immunoblots were visualized using the LiCor Odyssey imaging system. The anti-PdpC polyclonal antibody and the anti-IglA, IglB, IglC, IglD, and the anti-PdpB monoclonal antibodies, and source hybridomas have been deposited with the BEI program of the American Type Culture Collection.

5.2.9 Macrophage growth assay

Bone marrow cells were isolated from femurs of healthy BALB/c male mice and cultivated in 96-well cell culture plates at 4×10^5 cells per well (Costar) for one week in complete Dulbecco's Modified Eagle Medium (cDMEM) containing 10% fetal bovine serum (FBS), 1% L-glutamine, 1% MEM non-essential amino acids, 1% HEPES buffer solution, and 10% conditioned L929 supernatant. The resultant bone marrow-derived macrophages (BMDMs) were infected with *F. novicida* strains at a multiplicity of infection (MOI) of 20:1 (bacterium-to-macrophage). Infected monolayers were incubated for 1 hour in cDMEM to allow for phagocytosis to occur, washed five times in PBS, and incubated at 37ºC in 5% CO_2. Mouse

macrophage-like J774A.1 cells were seeded into 96-well cell culture plates at 2×10^5 cells per well and allowed to adhere overnight. Similarly, J774A.1 monolayers were infected at an MOI of 20:1 and incubated for 1 hour in Dulbecco's Modified Eagle Medium (DMEM) containing 10% FBS and 4 mM L-glutamine. To determine bacterial replication, infected macrophages were lysed in 0.1% deoxycholate at 0, 24, and 48 hours post-infection. The lysates were serially diluted in PBS containing 0.1% gelatine and plated on TSA. It has been demonstrated that *F. novicida* extracellular growth in standard DMEM is not supported which makes the macrophage infection assay an appropriate determination of intracellular growth. As a negative control, the *F. novicida mglA* mutant GB2, which does not grow in macrophages, was incorporated into all macrophage growth experiments.

5.2.10 Chicken embryo infections

Fertilized White Leghorn chicken eggs were obtained from the University of Alberta Poultry Research Station. Seven-day old chicken embryos were injected with various doses of 100 µl of *F. novicida* strains diluted in PBS just beneath the chorioallantoic membrane as previously described (150).

5.2.11 Subcellular fractionation

For *in vitro* grown cultures, *F. novicida* strains (100 ml) were grown overnight at 37ºC, pelleted, and resuspended in 5 ml of PBS. Cells were lysed by sonication with a Sonicator 3000 (Misonix) for 5 pulses of 30 seconds each at 50% duty cycle. The sonicated cells were centrifuged at 10,000 X g for 15 minutes at 4ºC to remove unbroken cells. A sample of the supernatant was taken as the total protein fraction. The lysate was further separated into the soluble protein fraction and the membrane fraction by ultracentrifugation for 1 hour at 100,000 X

g at 4ºC in a Beckman Type 45 Ti rotor. The membrane pellet was resuspended in 2 ml of 1% N-lauroyl sarcosine (Sigma). The sarkosyl soluble (inner membrane-enriched) and insoluble (outer membrane-enriched) fractions were separated by ultracentrifugation for 1 hour at 100,000 X g at 4ºC in a Beckman TLA-100.3 micro-ultracentrifuge. To generate macrophage-grown cells, the J774A.1 macrophage cell line was grown to 90% confluency in a 175 cm^2 tissue culture flask (Costar) and infected with bacteria at an MOI of 1000 (bacteria-to-macrophage) and incubated for 2 hours in DMEM containing 10% FBS and 4 mM L-glutamine at 37ºC in 5% CO_2. The large MOI was used to allow the recovery of large numbers of bacteria. External bacteria were removed by washing the monolayer three times with PBS and returned to the incubator for 18 hours. The macrophages were lysed by adding deoxycholate to a final concentration of 0.1%. Bacteria were separated from the macrophage lysate by centrifugation for 10 minutes at 10,000 X RPM in a JA-20 rotor (Beckman). The resulting pellet was resuspended in 1 ml PBS and subjected to subcellular fractionation. Sonication was used to disrupt cells because this technique could be applied to both large (broth-grown) and small (macrophage-grown) samples of bacteria. *In vitro* grown cells showed the same fractionation pattern when French pressure cell disruption was used.

5.2.12 NADH oxidase assay

NADH oxidase activity was assayed as described by Osborn *et al*. to evaluate the amount of inner membrane associated with different bacterial cell fractions (153). In a volume of 1 ml, incubation of mixtures contained 50 mM Tris-HCl (pH 7.5), 0.12 mM NADH, 0.2 mM dithiothreitol, and the protein fraction (10 µg of protein). The rate of decrease in absorbance at 340 nm was measured at room temperature. The cross-contamination between the different

cellular compartments from the subcellular fractionation was determined as a measure of the relative enzyme activity per mg of protein in each of the fractions.

5.3 Results

5.3.1 Membrane association of PdpC

To assess the cellular localization of PdpC, we biochemically fractionated *F. novicida* cells that had been grown in culture or had been grown in macrophages (Fig. 22). In the broth-grown cells, PdpC was most heavily concentrated in the sarkosyl-soluble portion of the total membrane fraction, suggesting that it localizes to the inner membrane (Fig. 22A). A similar fractionation was done on a smaller scale with macrophage-grown *F. novicida* (Fig. 22B). In this case, PdpC was found equally distributed between the sarkosyl-soluble and the sarkosyl-insoluble portion of the total membrane fraction, suggesting that in these cells, PdpC partially localized to both the inner and the outer membrane. The separation of bacterial membrane fractions from the intramacrophage-grown cells is technically difficult, and the results have to be cautiously interpreted. However, markers for the inner membrane, PdpB and NADH oxidase activity, were distributed similarly in broth-grown and intramacrophage-grown cells, and the membrane distribution pattern of PdpC was consistently found in three repetitions of the experiment. If these membrane localized results reflect real differences between broth-grown and intramacrophage-grown cells, then the inner membrane localization in the broth-grown cultures may represent a pre-secretion localization and the localization in the outer membrane may represent the destination of PdpC during an active infection.

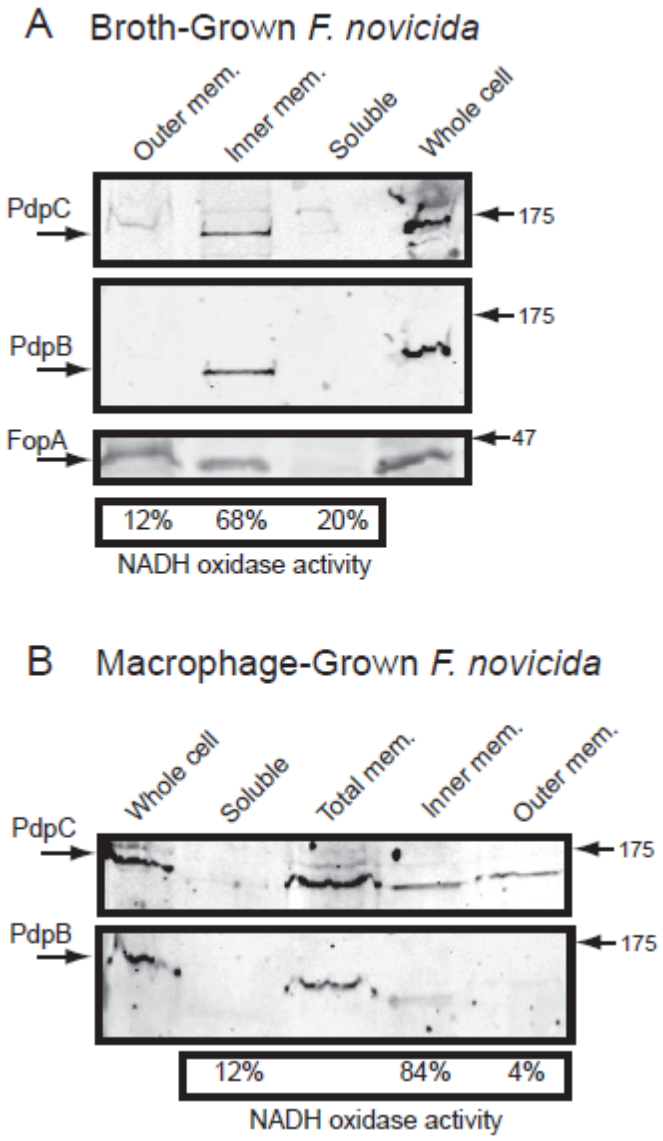

Figure 22. Detection of PdpC in subcellular fractions of *F. novicida* in broth-grown versus macrophage-grown cultures.

(A) Broth-grown *F. novicida* was disrupted by sonication and fractionated by centrifugation and detergent solubilization. PdpC was visualized with rabbit anti-PdpC peptide antisera (same as in Fig. 13A), and PdpB was visualized using anti-PdpB mouse monoclonal antibody. PdpB consistently localized to the sarkosyl soluble fractions in numerous experiments done in this and other studies (de Bruin *et al*. and Nano lab unpublished results). An anti-*F. novicida* serum was diluted 1:50,000 and used to detect FopA, an outer membrane protein. The NADH oxidase activity, which is associated with the inner membrane in *E. coli*, localized predominantly to the

inner membrane of *F. novicida*. (B) Fractionation of *F. novicida* grown in the macrophage-like J774A.1 cell line. An anti-PdpC reactive band was found in all membrane fractions. PdpB bands were found in the total membrane and primarily in the inner membrane fractions. In both panels the migration of pre-stained molecular weight markers (kDa) is shown on the right. Fractionations of broth-grown and J774A.1-grown cells were performed at least three times and gave similar results as those presented. The darkness and contrast in the images were adjusted electronically to achieve the clarity present in the original coloured images.

5.3.2 Intramacrophage growth phenotypes of *pdpC* mutant strains

The first generation of FPI mutants consisted of an allelic exchange between the gene of interest and an erythromycin resistance cassette. The *pdpC*::Em^R mutant strain was compromised in its ability to grow in J774A.1 and BMDM cells (data not shown and Fig. 23D).

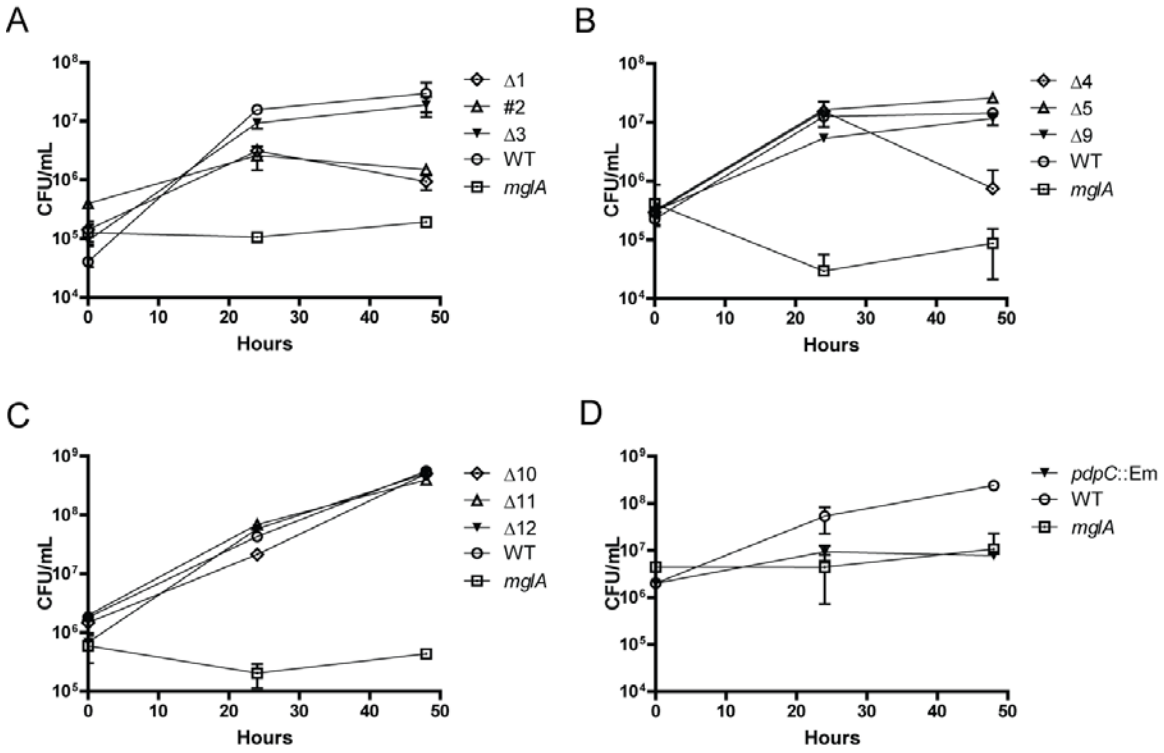

Figure 23. Intramacrophage growth of *F. novicida pdpC* mutants.

Mutant #2 (A) with a translational stop introduced at codon 95 and mutant *pdpC*Δ4 (B) showed poor growth in BMDMs. Mutants *pdpC*Δ3 (A) and *pdpC*Δ5, 9 (B) as well as *pdpC*Δ10, 11, 12 (C) grew like the wild type strain. The parental wild type strain, JLO, and a negative control strain, *mglA*, were included in each experiment. All data points represent at least three replicates and each experiment was done at least three times (with the exception of panel C). Error bars indicate standard deviation.

Gene replacement mutants can sometimes produce aberrant phenotypes, especially by interfering with the translation of downstream genes. As previously mentioned in chapter 4, the complete deletion of *pdpC* as well as the *pdpCE* double knockout, were not impaired for growth inside of both J774A.1 macrophages and BMDMs (Fig. 15). As an approach to assessing the role of *pdpC* in intramacrophage growth and virulence, without disrupting the expression of other genes, we constructed a series of small, in-frame deletions in *pdpC*. This was conducted under the assumption that most of these would generate wild type levels of altered PdpC and thus not interfere with transcription-translational coupling. To accomplish this, eight partial, in-frame deletion mutations of approximately 30-60 codons each were constructed. Inadvertently, we also created one nonsense mutant (*pdpC*#2) at codon 95 (Fig. 24A). We found that 6 of the 8 partial deletion mutants grew like wild type in BMDMs (Fig. 23A-C). Two partial deletion mutants, *pdpC*Δ1, *pdpC*Δ4, and the nonsense mutant, *pdpC*#2, had a defective growth pattern in BMDMs (Fig. 23A, B)

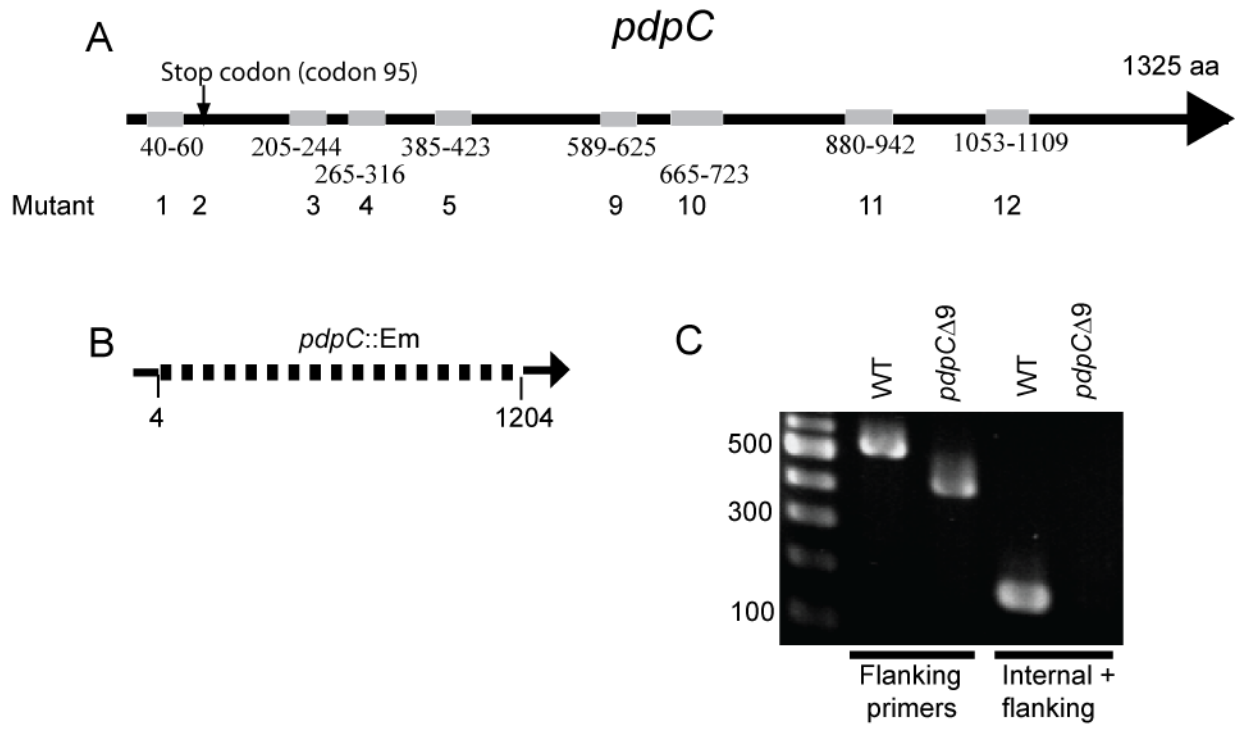

Figure 24. Diagrammatic representation of the *pdpC* deletion mutants.

(A) Grey bars indicated location of each of the partial, in-frame deletion mutations, and the number beneath the bars indicate the deleted codons. Arrow indicates location of stop codon in mutant number 2. At extreme right the number of amino acids in the *F. novicida* strain is indicated. (B) The extent of the Em^R gene replacement is indicated by the codon numbers that were replaced. (C) A representative genotypic analysis of deletion mutations. Each mutant was analyzed by PCR for the presence of the gene (flanking primers) and the absence of the deletion sequence (internal and flanking primers). As well, each mutant region was amplified, sequenced, and then deposited with GenBank.

5.3.3 Correlation of PdpC production with intramacrophage growth

To ascertain if protein stability of the mutant forms of PdpC affected the intramacrophage growth properties of the various strains we examined the level of PdpC in each of the mutants. Western immunoblot detection of PdpC (Fig. 25, and data not shown) showed that PdpC was

found at approximate wild type levels in mutant strains carrying partial deletions 3, 5, and 9-12, all of which grew like wild type in macrophages. However, mutants *pdpC*Δ1, *pdpC*Δ4 and nonsense mutant *pdpC*#2, all of which grew poorly in macrophages, did not produce detectable PdpC. The *pdpC*::Em^R mutant also did not produce detectable levels of PdpC (Fig 25).

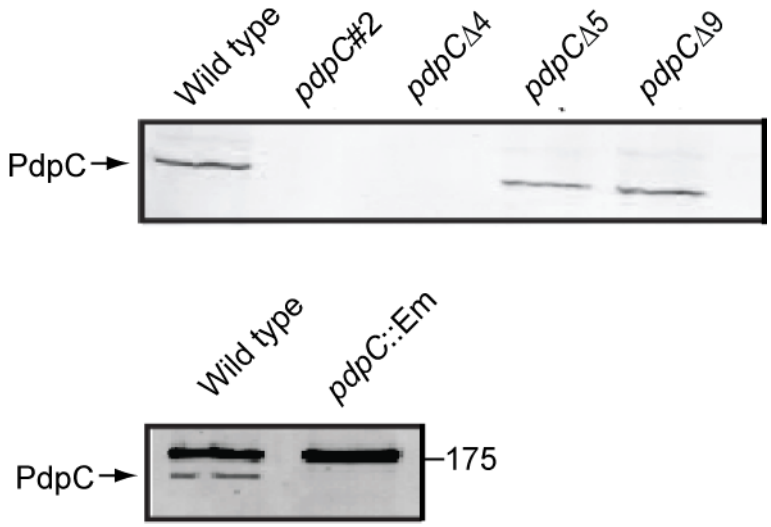

Figure 25. Western immunoblot probed against PdpC in representative mutant strains. *F. novicida* strains were grown in J774A.1 cell line macrophages which optimizes the expression of PdpC. Since some of the *pdpC* mutants grow poorly in macrophages the protein samples were normalized by CFU of *F. novicida* collected from the macrophages.

5.3.4 Virulence of *pdpC* mutants in a chicken embryo model of infection

As a more stringent test than intramacrophage growth for full virulence, we tested the *pdpC* mutants in whole animals. In order to reduce animal suffering, we have used a chicken embryo model of infection, which is able to discriminate large differences in virulence among mutant strains (150). With the exception of mutants carrying the *pdpC*Δ5 deletion, all of the

pdpC mutants were found to be less virulent than wild type in chicken embryos (Fig. 26). Those mutations which resulted in a defect for intracellular growth were the most attenuated in the chicken embryo model (Fig. 26B,D,E,G). The *pdpC*Δ5 mutant appeared to be equally virulent as wild type. The region deleted in *pdpC*Δ5 is a hydrophilic region that may be dispensable to the function of PdpC. As previously mentioned in chapter 4 (Fig. 16C), insertion mutants located in the sole downstream gene, *pdpE*, were as virulent as the wild type strain. Therefore, the attenuation of the partial deletions in chicken embryos cannot be attributed to downstream polarity.

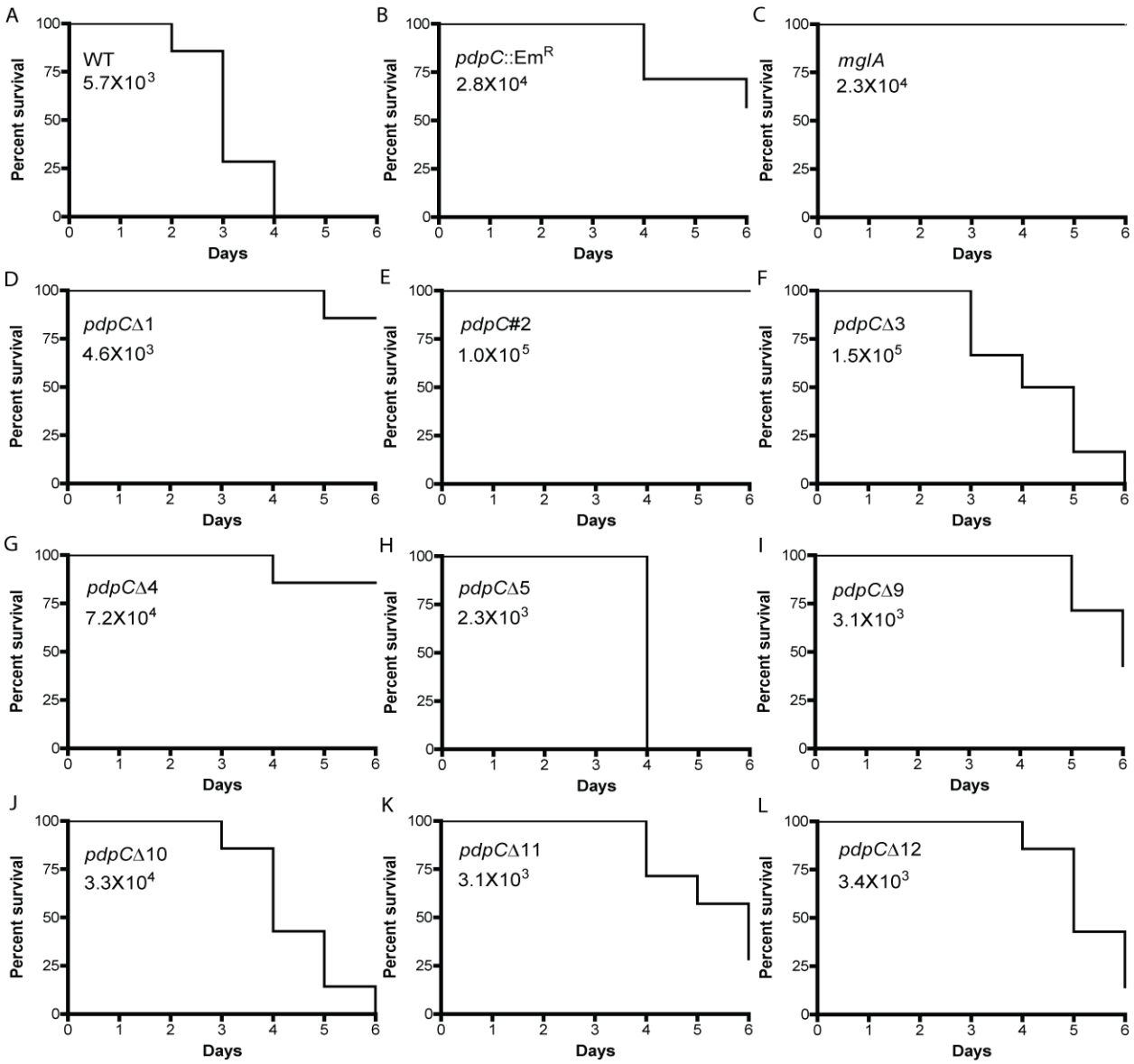

Figure 26. Virulence of *F. novicida pdpC* mutants during infection of chicken embryos.

In each panel the time-to-death of 7-day-old chicken embryos is shown. For each strain, a series of inocula was used to infect different groups of embryos, but only one group is shown. All experiments were performed at least three times and gave similar results. Each experimental run included a positive, wild type control and a negative *mglA* control. All chicken embryo infection experiments used 7 embryos. The inoculums for each infection are indicated by the number inside of each graph.

5.3.5 In a *pdpC*Δ4 background IglABCD are undetectable

A concurrent study was working to identify structural components of the *Francisella* T6SS required for secretion. This study demonstrated that if putative structural components of the T6SS were disrupted then IglA failed to localize to the outer membrane fraction. Mutants in which IglA did not reach the outer membrane were also defective for intracellular growth. We hypothesized that perhaps the *pdpC* mutants defective for growth in macrophages were somehow interfering with secretion. Initially we tested *pdpC*Δ5 and *pdpC*Δ4 to see if we could detect IglA in the outer membrane fraction. The *pdpC*Δ5 mutant had detectable IglA in the outer membrane fraction as expected, while *pdpC*Δ4 did not (Fig. 27). Surprisingly, in the *pdpC*Δ4 mutant, IglA was not detectable even in whole cell lysates, nor were IglB, IglC, and IglD (Fig. 28A, B). The remaining mutants defective for intramacrophage growth produced IglABCD in whole cell lysates (Fig. 28A, B, data not shown). The effect upon protein expression by *pdpC*Δ4 appeared to be limited to the minor operon, since major operon proteins PdpB and VgrG were detectable in whole cell lysates (data not shown).

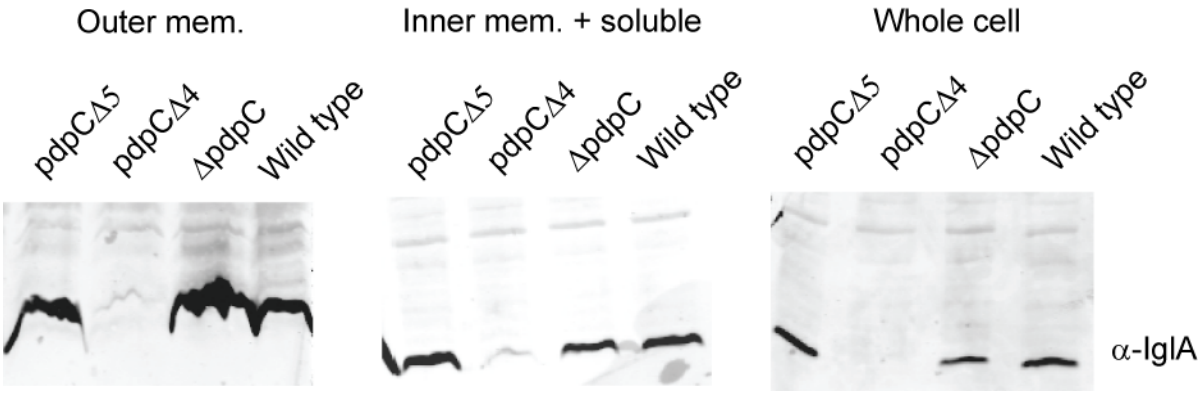

Figure 27. Western immunoblot probed for IglA in subcellular fractions of *pdpC*Δ4. Wild type, Δ*pdpC* and *pdpC*Δ5 function as positive controls. Non specific bands attest to equal loading of sample between lanes.

To determine if the loss of detectable IglA-D was caused by a post translational mechanism, we transformed a plasmid expressing IglD into the *pdpC*Δ4 strain. The plasmid pKHiglD encoded IglD fused to a FLAG tag at the Carboxyl terminus, and was driven by the constitutive *Francisella* promoter of *GroE*. IglD was detectable in this background, probed with either anti-FLAG (data not shown) or anti-IglD antibodies (Fig. 28C). Although these results argue against a post translational effect, it may be that the high copy number of pKHiglD titrated out the defective pdpC, masking a possible interference effect. To account for this possibility we inserted *iglD* into the chromosome of *pdpC*Δ4 using the *Francisella* integration construct SKX (128). The resulting strain *pdpC*Δ4-SKX IglD produced IglD, albeit at lower levels than the wild type strain (Fig. 28C). Although this construct is not driven by the gene's native promoter, nonetheless it produces IglD at levels comparable to that of a successful complement of Δ*iglD* (de Bruin *et al.* unpublished). This indicated that plasmid copy number was not causing an artefact.

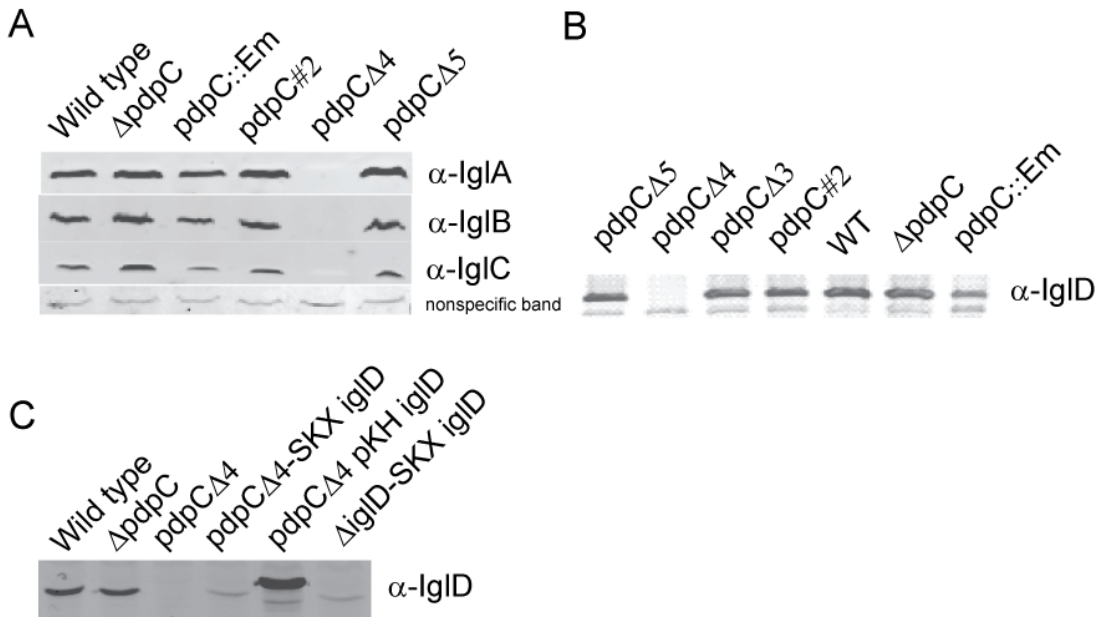

Figure 28. Western Immunoblot probed against IglABCD in select mutant strains.

(A) Western immunoblot probed with antibody against IglA, IglB, and IglC. A nonspecific band attests to equal loading of samples. (B) Various strains examined by Western immunoblot for IglD. (C) Western immunoblot of *pdpC*Δ4 complemented with *iglD* probed with anti-IglD antibody.

5.3.6 Restoration of *pdpC*Δ4 lesion lead to IglB protein production and wild type phenotype

As previously discussed in chapter 4, we were unable to complement the Δ*pdpC* mutant. Therefore, we adopted the strategy of restoring *pdpC*Δ4 to the wild type form by introducing only DNA associated with the mutated region within *pdpC* (Fig. 29A). To accomplish this, we transformed the *pdpC*Δ4 mutant strain with a PCR amplicon encompassing the deletion and the surrounding chromosomal region. Since the PCR amplicon did not carry a selective marker, we co-transformed the plasmid pMP633 and selected for the hygromycin resistance (Hyg^R) marker

on the co-transformed plasmid (125). Among the Hyg^R transformants about 60% had integrated the PCR amplicon as demonstrated by PCR analysis and by DNA sequencing of the region. One of these was chosen for further study, designated "*pdpC*Δ4Revertant" (*pdpC*Δ4R), and was found to be able to grow in macrophages like wild type (Fig. 29E). As a negative control we chose an antibiotic resistant transformant that retained the mutant gene form, and this isolate was designated " *pdpC*Δ4mockRevertant" (*pdpC*Δ4mR). This strain was found to have the mutant defect for intramacrophage growth (Fig. 29E). The virulence in chicken embryos of the restored mutant strain was identical to the wild type strain (Fig. 29D), but the mock-restored strain was still severely attenuated (Fig. 29C). A Western immunoblot probed against PdpC and IglB reveals wild type levels of both proteins in the revertant, but not in the mock-restored strain (Fig. 29D). Hence, a true restoration of *pdpC* in the *pdpC*Δ4R strain, but not a mock restoration of *pdpC*, returned the mutant to the wild type virulence and intramacrophage growth phenotypes.

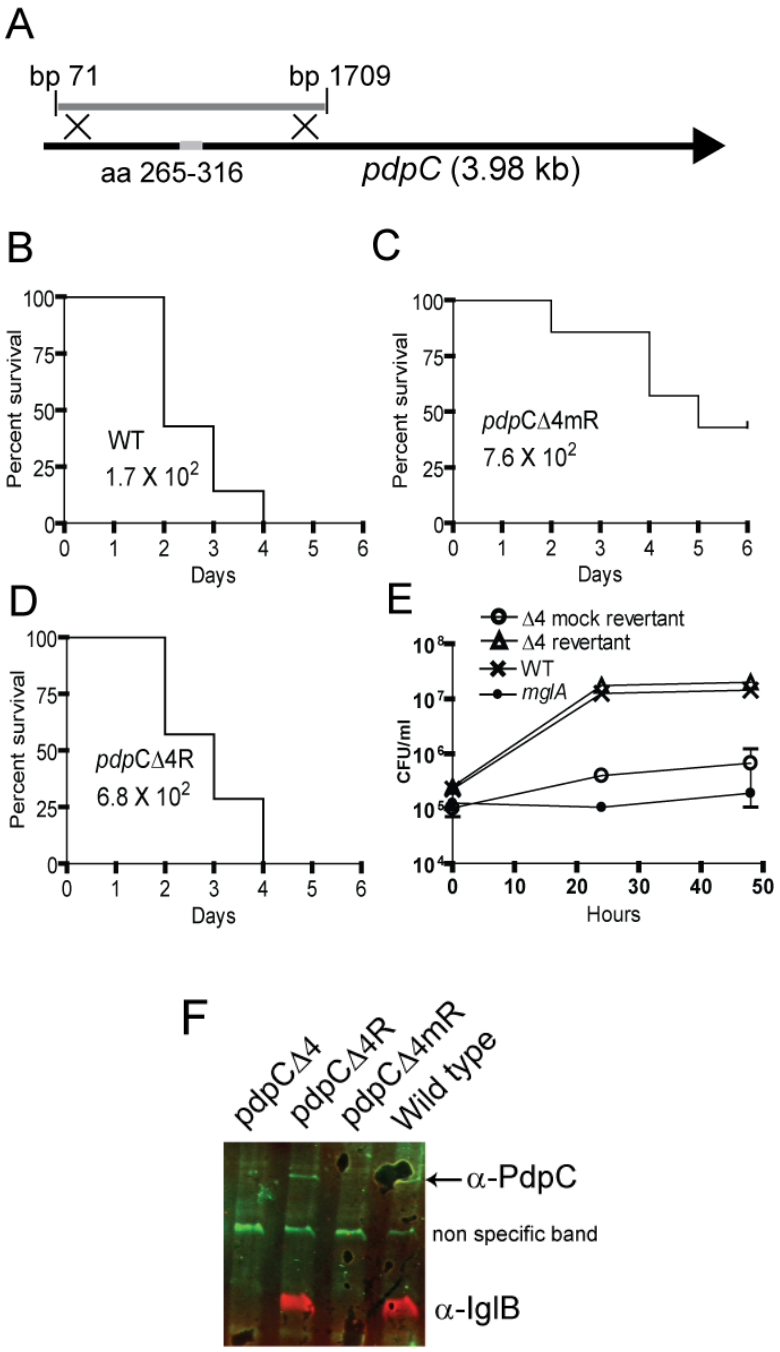

Figure 29. Restoration of *pdpC*Δ4 to the wild type phenotype.

(A) Diagrammatic representation of the transformation and integration of a PCR amplicon from wild type DNA into the mutated locus of *F. novicida pdpC*Δ4. Transformants were detected by virtue of a co-transformed plasmid DNA. (B) Virulence of wild type *F. novicida* in chicken embryos. (C) Virulence as measured by time-to-death, of the strain *pdpC*Δ4mR, that was "mock

restored" by transformation, but failed to integrate the wild type PCR amplicon. (D) Virulence of the *pdpC*Δ4R that had regained the wild type region that was mutated in *F. novicida pdpC*Δ4. (E) Growth of *F. novicida* strains in BMDMs. The revertant of *pdpC*Δ4 grew like the wild type strain, but the mock revertant grew like the *pdpC*Δ4 mutant strain. (F) Western immunoblot demonstrating the production of PdpC and IglB in the revertant, but not the mock revertant strain. Standard errors are indicated by bars. The chicken embryo infections were performed three times and the macrophage growth experiments were repeated two times. All chicken embryo infection experiments used at least 7 embryos. The inoculums for each chicken embryo infection are indicated by the number inside of each graph.

5.3.7 The *pdpC*Δ4 phenotype is not ascribed solely to the genetic deletion 4 lesion

To further characterize the *pdpC*Δ4 strain we introduced its genetic lesion into the *pdpC-3xFLAG* strain. The methodology used to restore *pdpC*Δ4 was employed, except that mutated template DNA was PCR amplified from the *E. coli* clone used to create the original *pdpC*Δ4. To our astonishment, the resulting strain *pdpC*Δ4b-*3xFLAG* did not possess altered levels of IglC, nor was it impaired for growth in the J774.A1 cell line (data not shown). To confirm this result, we recreated the *pdpC*Δ4 strain again by using the original mutant as DNA template and mutating the wild type strain. This mutant termed *pdpC*Δ4c, had the same phenotype as the *pdpC*Δ4b-*3xFLAG* strain. Therefore, it is likely that the *E. coli* clone and the *pdpC*Δ4 lesion are genetically consistent.

The *pdpC* mutant strains differ in sequence within the intergenic region upstream of *pdpC*

In an attempt to reconcile the different phenotypes exhibited by the *pdpC* mutations, we sequenced the 39 base pair intergenic region between *iglJ* and *pdpC* in *pdpC*::Em^R and *pdpC*Δ4.

We found that there were differences between the mutants and wild type, as well as between *F. tularensis* and LVS (Fig. 30). Compared to U112 *F. tularensis* and LVS both possess a G in place of an A at position -7. Additionally, LVS contains a C in place of a T at position -5. Interestingly, *pdpC*Δ4 has the same sequence changes as LVS, while *pdpC*::Em^R possesses a substitution identical to *F. tularensis*. Given that both LVS and *F. tularensis* strains are able to grow in macrophages, it seems unlikely that these changes can account for their defective macrophage growth phenotypes.

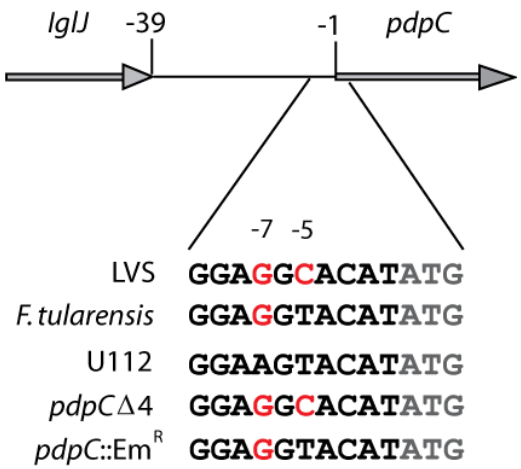

Figure 30. *IglJ-pdpC* intergenic consensus sequence.

The 39 bp *iglJ-pdpC* intergenic region was sequenced from select mutants and the U112 parental strain, then compared to the published sequences of LVS and *F. tularensis*. Grey sequence indicates the start of the reading frame. Differences with respect to parental strain *F. novicida* U112 are indicated in red. Open reading frames are not to scale. Unless otherwise indicated the intergenic region sequence is identical in all strains listed.

5.3.8 Selective marking and transfer of *pdpC*Δ4 DNA into an IglC permissive strain blocks IglC expression

We decided to make use of the transponson mutant library in an effort to uncover the genetic basis of the *pdpC*Δ4 phenotype. First we chose a Km^R insertion mutant (C1) that had been inserted at nt 878 in *pdpC*, relatively close to the *pdpC*Δ4 lesion (Fig. 31A). Using *pdpC*Δ4 as PCR template we amplified a segment of DNA from nucleotide 304 of *iglJ* to 1704 of *pdpC*. Next, we co-transformed the PCR product along with the unstable Hyg^R pMP823 and screened Hyg^R transformants for Km sensitivity. Presumably this would indicate that the *pdpC*Δ4 lesion

had been incorporated into the chromosome via a double cross-over recombination event replacing the Km^R marker, which we confirmed by PCR. However, the resulting strain C1::*pdpC*Δ4 did not alter IglC protein levels (data not shown).

Our theory was that a hereto unknown genetic change, in addition to the *pdpC*Δ4 lesion, was the cause of altered IglA-D protein levels. Because a segment of mutant DNA consisting of the first half of the gene was unable to reproduce the *pdpC*Δ4 phenotype, we decided to focus on the second half of the gene. Again we made use of the transposon library and PCR amplified two separate Km^R transposon mutants, one located at 1690 bp of *pdpC* (C2) and the other at 210 bp of *pdpE* (E1) (Fig. 31A). The respective PCR products were transformed into *pdpC*Δ4, followed by selection for Km^R. All 6 of the C2 and 1-3 of the E1 transformants tested did not produce IglC. E1 transformants 4-6 restored IglC production (Fig. 31B).

Since half of the E1 transformants restored detectable levels of IglC protein, we reasoned that the genetic change we were trying to identify must reside somewhere past nucleotide (nt) 1249 of *pdpC*. Next we isolated chromosomal DNA from E1-1*pdpC*Δ4 transformant 1 (E1-1) and C2-1 *pdpC*Δ4 transformant 1 (C2-1), followed by restriction digestion as indicated (Fig. 31C). We then transformed the digested DNA of both strains with wild type. If our hypothesis was correct, then induction of a *pdpC*Δ4 phenotype would require that both the *pdpC*Δ4 lesion and the change past nt 1249 integrate into the chromosome. To increase the chances of acquiring the desired genotype, we also transformed both sets of digested DNA into the *pdpC*Δ4b-*3xFLAG* strain. Recall this strain contains the *pdpC*Δ4 lesion acquired via co-transformation but still produces detectable IglC protein. Five transformants were tested that arose from the DNA transformation of the wild type strain, and they all produced detectable IglC protein (data not shown). The transformation of C2-1 DNA into *pdpC*Δ4b-*3xFLAG* also produced colonies that

all made detectable IglC protein. In contrast, transformation of E1-1 DNA into *pdpC*Δ4b-*3xFLAG* resulted in transformants that no longer produced detectable IglC protein (Fig. 31D)

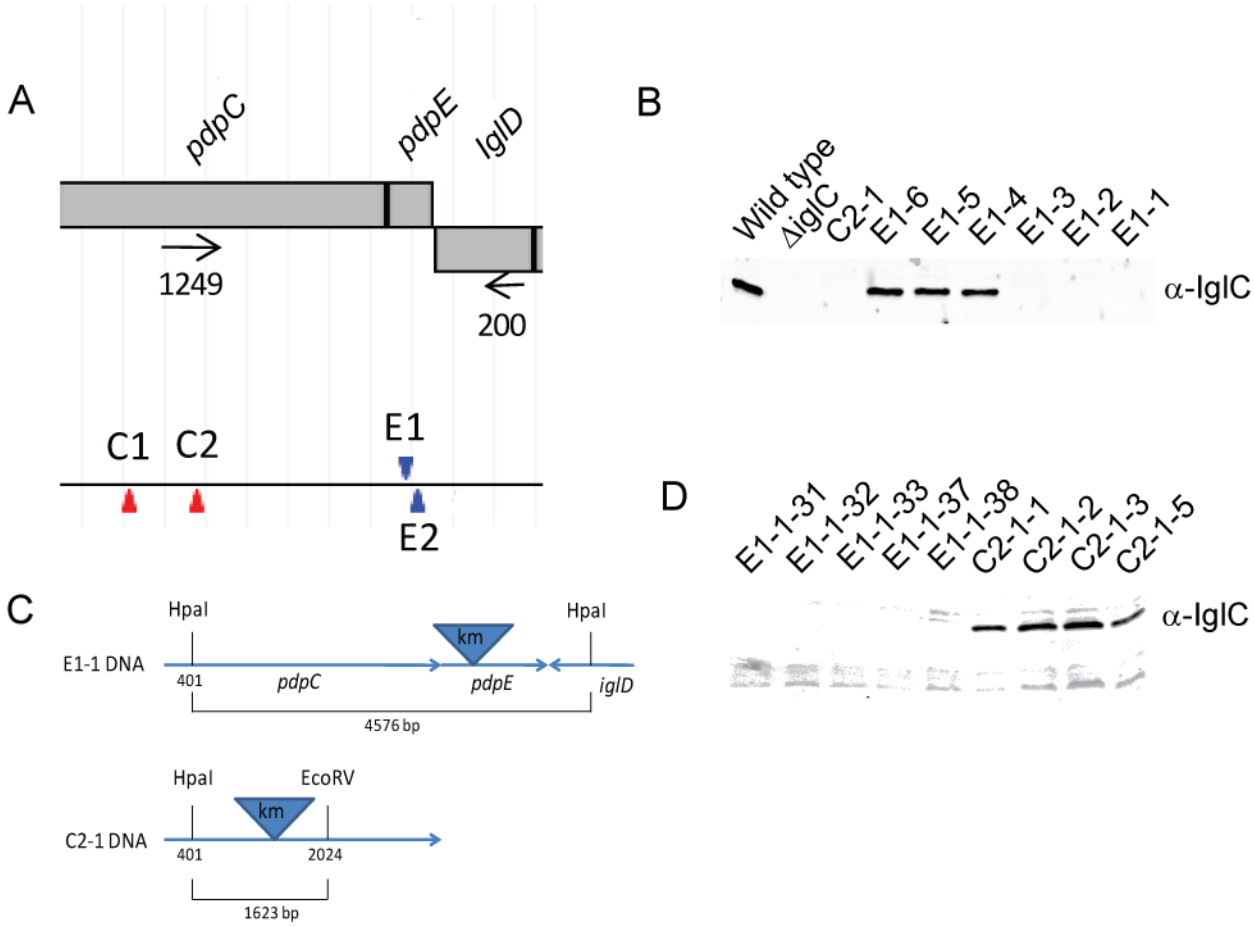

Figure 31. Diagrammatic representation of *pdpC* and *pdpE* transponson mutants accompanied by corresponding Western immunoblots.

(A) Diagram indicating location of Km transposons in *pdpC* and *pdpE*. Arrows under open reading frames indicate primer locations used to amplify transposons. Transposons facing to the left are positioned below the black line, and *vise versa*. (B) *pdpC*Δ4 integrated with a PCR amplicon of either E1 or C2 transposon mutants and analysed by Western immunoblot. (C) Diagram indicating the position, size, and restriction endonuclease employed to digest E1-1*pdpC*Δ4 and C2-1*pdpC*Δ4 DNA. (D) Western immunoblot analysis of transformants resulting from integration of DNA from (C) into *pdpC*Δ4b-*3xFLAG*.

5.4 Discussion

Characterizing PdpC has proven to be exceedingly challenging. The protein does not share significant sequence identity to other known proteins, nor does it possess any predicted functional domains. Therefore, we had to continue without the benefit of any bioinformatic clues to help define the function of PdpC. Further complicating matters are the variety of phenotypes that mutations within *pdpC* have produced. The mutants can be divided into two main categories: first, those who are permissive for growth in macrophages but show some attenuation in the chicken embryo model system (*pdpC*Δ3, and *pdpC* deletion mutants 9-12). This group also includes the complete *pdpC* deletion described in chapter 4. Of mutants in this category, only the complete deletion was tested for virulence in mice. However, if the level of attenuation in the chicken embryo model correlates with virulence in mice, then mutants from this category are likely avirulent in mice as well. PdpC is detectable by Western immunoblot in mutants from this category, with the exception of the complete deletion as expected. Since we demonstrated these mutations have a phenotype identical to that of Δ*pdpC,* for both growth in macrophages and virulence in chicken embryos, it seems likely that they represent a loss of function in the protein.

The second category are those mutants who are unable to grow in macrophages and, as a result, are severely attenuated for virulence in the chicken embryo model. None of the mutants in this category produce detectable PdpC. These characteristics could be explained by a polar effect upon the sole downstream gene in the operon, *pdpE*. We subsequently demonstrated that *pdpE* was completely dispensable for virulence in mice, chicken embryos, and growth in macrophages. Furthermore, a complete Δ*pdpC,* Δ*pdpE* double mutant was able to grow in macrophages and was no more virulent than the single Δ*pdpC* mutant in chicken embryos

(chapter 4). After discounting a polar effect as the basis, it was puzzling that a partial deletion of the protein would be more oppressive to the bacterium than its complete removal. Another plausible explanation is that a misfolded PdpC interacts with its substrate in an interfering manner to cause a dominant-negative effect.

It is difficult to account for the lack of detectable PdpC. Since our antibody was raised against a synthetic peptide, it is highly unlikely it would require a specific conformation to recognize the protein. Additionally, the whole cell lysates are boiled and treated with a detergent and a reducing agent. As a consequence the protein should be linear when it is probed. PdpC is expressed at very low levels during *in vitro* growth and is difficult to detect under these conditions. It may be that this category of mutation produces a less stable protein with a shorter half-life. As a result, there is not a large enough accumulation of PdpC in the cell to reach our detection limit. We have been able to stimulate higher levels of PdpC by growth in macrophages, but because these mutants do not grow well in macrophages, this approach is gainless. Even if we accept these explanations, they do not apply to the *pdpC*::Em^R mutant because the peptide the PdpC antibody was raised against is not present. Regardless, this strain is not likely to produce any PdpC because greater than 90% of the protein has been removed during the allelic exchange.

We wanted to further examine the possibility that defects in macrophage growth were caused by some kind of interference of PdpC with the T6SS machinery. Previous work has demonstrated the requirement of an intact T6SS for intramacrophage growth. When predicted structural components of the T6SS are removed, the FPI protein IglA is unable to localize to the outer membrane fraction, and a phenotype identical to our category 2 mutants occurs. We hypothesized that if the severely deleterious mutants were interfering with the T6SS in either a

direct or indirect manner, IglA localization would also be affected. Initially, we tested *pdpC*Δ4 as it was the most characterized of mutants in this category. Astonishingly, IglA was undetectable in all fractions, as well as the whole cell lysate. Further analysis demonstrated that IglABCD were all undetectable in the whole cell lysates of this mutant. In contrast, IglABCD were detectable at apparent wild type levels in the remaining mutants defective for intracellular growth tested. It is possible that one or more of the aforementioned Igl proteins are altered in a subtle manner undetectable by our assay. One way to explain our findings is to propose there are two mechanisms causing the same phenotype: one resulting from disruption of IglA-D, and the other from a separate unknown mechanism. We knew the effect on IglA-D was not likely to be post-translational considering its ectopic expression was unaffected. When IglA was expressed from a plasmid, as well as an alternate location on the chromosome, alien promoters were employed. Thus, we could not discount an effect upon the promoter region of *iglA* as the cause of the disruption.

We decided to investigate the possibility that these mutations had altered a small non coding regulatory RNA (sRNA). Bacterial sRNAs have been extensively studied in *Salmonella enteric* serovar Typhimurium, and have been indirectly linked to virulence via the RNA chaperon *hfq* (200). Typically they range from 50-250 nt in length, are usually untranslated, and are encoded within the intergenic regions between open reading frames in the chromosome (219). They function as regulators by base pairing with *trans*-encoded mRNAs to either activate or repress genes at the post-transcriptional level(133). The intergenic region immediately upstream of *pdpC* is 39 nt long, and the sequence is highly conserved among *Francisella* strains. In *F. tularensis* and LVS, their respective duplicated intergenic regions are identical. Variation between them consists of a single nucleotide at position -5. *F. novicida* differs from *F.*

tularensis by 1 nt at -7, and from LVS at positions -5 and -7. The high degree of similarity among strains suggests this sequence is not superfluous. The intergenic sequencing of *pdpC*::Em^R and *pdpC*Δ4, revealed what appears to be a bizarre coincidence. The two mutant strains only had variations at positions -5, and -7. The changes mimicked other *Francisella* strains. The *pdpC*Δ4 mutant was identical to LVS, and *pdpC*::Em^R was a complete match for *F. tularensis*. The differences observed exist in other strains permissive for macrophage growth. Accordingly, we have eliminated this mechanism as a basis for the phenotypes in this category of mutants.

We tried to recreate a *pdpC*Δ4 mutant by introducing the *pdpC*Δ4 lesion via co-transformation. The integration was confirmed by PCR, but the mutant had no effect upon IglC. This was confusing since we knew already that by introducing wild type DNA spanning the same region we could restore *pdpC*Δ4 to wild type. We reasoned that there must be another change somewhere in the gene. Our theory is that a *pdpC*Δ4 lesion is required, but not sufficient alone to cause the phenotype. It is possible that an additional unintended error was introduced during the integration/excision events which accompanied our original mutagenesis strategy.

Inexplicably, PCR failed to amplify portions of the C-terminal end of *pdpC*Δ4. Identical primer sets produced robust PCR amplification if wild type DNA was employed. We were, however, able to amplify portions of the N-terminal region as well as *pdpE*. If portions of *pdpC*Δ4 were missing, then we would expect to be able to amplify the truncated sequence. However, despite the use of primers within regions that were PCR permissive, we were unable to amplify the sequence between them.

In the face of these difficulties, we tagged *pdpC*Δ4 by integrating a Km^R transposon and selecting a resistant colony that retained the IglA-D expression defect. Three of the 6 colonies tested that were transformed with E1 were restored to a wild type phenotype. This suggests that the unidentified second mutation is located somewhere after nucleotide 1249 of *pdpC*. In a subsequent experiment we integrated a large segment of E1-1 DNA into both wild type, and the *pdpC*Δ4b-*3xFLAG* strain. None of the wild type transformants acquired a defect for IglC expression. In contrast, 5/5 *pdpC*Δ4b-*3xFLAG* transformants tested did not produce detectable IglC. We also integrated a segment of C2-1 that was smaller than the E1-1 segment into *pdpC*Δ4b-*3xFLAG* (see Fig. 31C). Of the resulting transformants, 4/4 tested produced IglC. This reinforces our theory that both genetic elements are required to induce the IglA-D defect. *pdpC*Δ4b-*3xFLAG* was more likely to acquire the defect since it already possessed one of the two elements. Additionally, the Km^R marker was located in *pdpE*, presumably closer to the undefined element, thus increasing the chances of both requirements being met. Wild type transformants would have required the successful integration of both elements to acquire the defect. It is likely that the relatively large distance between the elements decreases the chances of both elements integrating simultaneously. It is probable that had we screened large numbers of transformants we would have identified wild type transformants that had integrated both elements. Further, the transformation of C2-1 DNA supports our two element theory. This fragment of integrating DNA ends at nucleotide 2024 of *pdpC*. If the second element was located downstream of this position we would not expect these transformants to have the capacity to introduce it. Accordingly, none of the 8 tested were defective for IglC production (4 shown).

The experiments conducted in this chapter suggest that *pdpC* may play a role in the regulation of the FPI minor operon. We did not determine the mechanism by which this occurs, but our experiments suggest it is not post-translational in nature. Despite the difficulties faced in the genetic manipulation of the *pdpC*Δ4 mutant, we were able to make progress towards identifying the underlying genetic cause of its phenotype.

Chapter 6: Conclusions and future studies

The idea that PdpC could potentially function both as a secreted effector and a regulator, will likely be met with some scepticism. As our research study progressed, we have had to adjust our theories about the protein to account for our data. Precedence does exist in bacterial pathogenesis for a regulator protein that is also secreted.

Yersinia pestis is the causative agent of the zoonotic disease plague. The lifecycle of the bacterium mainly revolves around infection of rodents and transmission by infected fleas (166). Humans are considered to be accidental hosts, infected by inhalation of aerosols, ingestion or the bite of infected fleas. Infected cats have been recognized as an effective intermediary of the disease to humans (80). *Y. pestis* uses a T3SS to translocate effector proteins from the bacterial cytoplasm directly into the host cell. This process is tightly regulated, and is initiated upon physical contact with the host cell (196). Different pathogens that make use of the T3SS share some core secretion proteins, and in certain cases they are even interchangeable (148, 177). Despite this, there are many T3SS regulators that are pathogen specific, likely reflecting species specific survival adaptations (226). *Y. pestis* secretes anti-host factors called Yops (*Yersinia* outer proteins) through its type III Yop secretion system (Ysc). The production of Yops is mediated by a transcriptional activator called LcrF and by the Ysc itself (3). A role for Ysc in the regulation of Yops is based on the observation that it must be in an open gate state for Yops to be efficiently transcribed. Deletions in genes encoding inner and outer gate elements cause constitutive Yop expression and secretion (70). It was hypothesized that a repressor protein mediated this effect by linking the gate status of the Ysc to Yop production (167). A protein called Low Calcium Response Q (LcrQ), is unique to *Yersinia* spp., and it negatively regulates

Yop expression when overexpressed. It was originally thought that LcrQ's negative effects were mediated via the transcription factor LcrF, but it could not be demonstrated that they physically interacted. LcrQ and YopH both interact with the chaperon SycH, and this chaperon is required for the secretion of both proteins. It was proposed that SycH mediated secretion of LcrQ promoted expression of Yops (33). Subsequently it was demonstrated that removal of LcrQ from the cytosol alone was not sufficient to signal Yops production (226). Wulff-Strobel *et al.* propose a more complicated model where the Ysc maintains a hierarchy of secretion, partially mediated by LcrQ and its chaperone SycH. They hypothesize that the LcrQ-SycH complex localizes to a secretion substrate acceptor site (SSAS) on the Ysc. This alters the conformation of the Ysc such that the feedback down-regulation of Yop expression is imposed. Environmental stimuli create a secretion-permissive state in the Ysc, allowing LcrQ to be released from SycH and secreted. Either the absence of LcrQ or the presence of free SycH at the SSAS induces a conformational change in the Ysc feedback regulator allowing Yop protein expression. In this model, LcrQ functions to relay the state of Ysc readiness to downstream regulatory proteins.

Although *Francisella* uses a different secretion system to transport proteins to host cell targets, the two pathogens have some similarities. Both pathogens take steps to evade host immune responses. The expression of their secretion system proteins are tightly controlled and highly ordered. It is plausible that PdpC may indirectly play a role in regulating the expression of secretion related genes, as is the case with LcrQ.

Future work should investigate the mechanism of the effect *pdpC*Δ4 has on expression of IglA-D. One of the first experiments that should be conducted is the complementation of *pdpC*Δ4 by introducing wild type DNA limited to the second half of the gene. If successful, this would help to confirm the genetic basis of the mutant. That is, two distinct genetic aberrations

are both required to cause the *pdpC*Δ4 phenotype. Recently, the utility of *lacZ* reporter assay was demonstrated in LVS, where it was used as a readout to screen for positive regulators of *IglA* (37). Constructing transcriptional fusions of *lacZ* to the putative promoters or intergenic regions upstream of *iglA* could tell us if the mechanism altering expression occurs before transcription. Reverse transcription real time PCR would enhance transcriptional fusion studies, and could identify post transcriptional aberrations such as mRNA instability. It would also be very exciting to compare *pdpC*Δ4, Δ*pdpC* and wild type in a microarray study. Global gene expression profiles could provide clues as to which regulators might be directing the effect. Very recently, Bina *et al.* published an article that described the construction and utility of a bioluminescence reporter plasmid in LVS (26). In *Photorhabdus luminescens*, the lux operon contains the genes that are required for the production of both the enzyme luciferase and its substrate luciferin. Co-expression of these genes results in light production. The authors used their reporter to follow the dissemination of LVS in a mouse infection model in real time. Assuming this tool would function in *F. novicida*, it could be used to quickly and easily examine the dissemination of Δ*pdpC* introduced by different routes of infection. The data generated may shed some light on the nature of the defect for this mutant in whole animals.

Recently, one of our collaborators identified a phenotype attributed to PdpC that was measurable during infection of macrophages. The phenomenon was complementable and provides compelling evidence that PdpC is indeed an effector protein. Since these results are currently unpublished, I do not have permission to be any more specific at this time. This thesis has laid the groundwork for future discovery, through the development of tools for the study of PdpC. It has also generated data that will be used to test more specific hypotheses concerning PdpC.

Chapter 7: Bibliography

1. 1970. Health Aspects of Chemical and Biological Weapons. World Health Organization.
2. **Akira, S., K. Takeda, and T. Kaisho.** 2001. Toll-like receptors: critical proteins linking innate and acquired immunity. Nat Immunol **2:**675-80.
3. **Allaoui, A., R. Schulte, and G. R. Cornelis.** 1995. Mutational analysis of the Yersinia enterocolitica virC operon: characterization of yscE, F, G, I, J, K required for Yop secretion and yscH encoding YopR. Mol Microbiol **18:**343-55.
4. **Allen, W. P.** 1962. Immunity against tularemia: passive protection of mice by transfer of immune tissues. J. Exp. Med. **115:**411-420.
5. **Ancuta, P., R. Pedron, R. Girard, G. Sandström, and Chaby.** 1996. Inability of the *Francisella tularensis* lipopolysaccharide to mimic or to antagonize the induction of cell activation by endotoxins. Infect. Immun. **64:**2041-2046.
6. **Anon.** 1947. Deposition of Naito Ryoichi, 24 January 1947. Record Group 153, Records of the Office of the Judge Advocate General (Army), The National Archives.
7. **Anthony, L. D., R. D. Burke, and F. E. Nano.** 1991. Growth of Francisella spp. in rodent macrophages. Infect Immun **59:**3291-6.
8. **Anthony, L. S., S. C. Cowley, K. E. Mdluli, and F. E. Nano.** 1994. Isolation of a Francisella tularensis mutant that is sensitive to serum and oxidative killing and is avirulent in mice: correlation with the loss of MinD homologue expression. FEMS Microbiol Lett **124:**157-65.
9. **Anthony, L. S., M. Z. Gu, S. C. Cowley, W. W. Leung, and F. E. Nano.** 1991. Transformation and allelic replacement in Francisella spp. J Gen Microbiol **137:**2697-703.
10. **Anthony, L. S. D., R. D. Burke, and F. E. Nano.** 1991. Growth of *Francisella* spp. in rodent macrophages. Infection and Immunity **59:**3291-3296.
11. **Anthony, L. S. D., M. Z. Gu, S. C. Cowley, W. Leung, and F. E. Nano.** 1991. Transformation and allelic replacement in Francisella spp. J. Gen. Microbiol. **137:**2697-703.
12. **Anthony, L. S. D., and P. A. L. Kongshavn.** 1987. Experimental murine tularemia caused by *Francisella tularensis*, live vaccine strain: a model of acquired cellular resistance. Microb. Path. **2:**3-14.
13. **Anthony, L. S. D., and P. A. L. Kongshavn.** 1988. H-2 restriction in acquired cell-mediated immunity to infection with *Francisella tularensis* LVS. Infect. Immun. **56:**452-456.
14. **Ashford, T. P., and K. R. Porter.** 1962. Cytoplasmic components in hepatic cell lysosomes. J Cell Biol **12:**198-202.
15. **Backhed, F., R. E. Ley, J. L. Sonnenburg, D. A. Peterson, and J. I. Gordon.** 2005. Host-bacterial mutualism in the human intestine. Science **307:**1915-20.
16. **Badger, J. L., and V. L. Miller.** 1998. Expression of invasin and motility are coordinately regulated in Yersinia enterocolitica. J Bacteriol **180:**793-800.
17. **Baeuerle, P. A., and T. Henkel.** 1994. Function and activation of NF-kappa B in the immune system. Annu Rev Immunol **12:**141-79.
18. **Balagopal, A., A. S. MacFarlane, N. Mohapatra, S. Soni, J. S. Gunn, and L. S. Schlesinger.** 2006. Characterization of the receptor-ligand pathways important for entry and survival of Francisella tularensis in human macrophages. Infect Immun **74:**5114-25.

19. **Ballister, E. R., A. H. Lai, R. N. Zuckermann, Y. Cheng, and J. D. Mougous.** 2008. In vitro self-assembly of tailorable nanotubes from a simple protein building block. Proc Natl Acad Sci U S A **105:**3733-8.
20. **Barker, J. H., J. Weiss, M. A. Apicella, and W. M. Nauseef.** 2006. Basis for the failure of Francisella tularensis lipopolysaccharide to prime human polymorphonuclear leukocytes. Infect Immun **74:**3277-84.
21. **Barker, J. R., A. Chong, T. D. Wehrly, J. J. Yu, S. A. Rodriguez, J. Liu, J. Celli, B. P. Arulanandam, and K. E. Klose.** 2009. The Francisella tularensis pathogenicity island encodes a secretion system that is required for phagosome escape and virulence. Mol Microbiol **74:**1459-70.
22. **Barker, J. R., and K. E. Klose.** 2007. Molecular and genetic basis of pathogenesis in Francisella tularensis. Ann N Y Acad Sci **1105:**138-59.
23. **Baron, G. S., and F. E. Nano.** 1999. An erythromycin resistance cassette and mini-transposon for constructing transcriptional fusions to cat. Gene **229:**59-65.
24. **Baron, G. S., and F. E. Nano.** 1998. MglA and MglB are required for the intramacrophage growth of *Francisella novicida*. Molecular Microbiology **29:**247-259.
25. **Bell, B. L., N. P. Mohapatra, and J. S. Gunn.** 2010. Regulation of virulence gene transcripts by the Francisella novicida orphan response regulator PmrA: role of phosphorylation and evidence of MglA/SspA interaction. Infect Immun **78:**2189-98.
26. **Bina, X. R., M. A. Miller, and J. E. Bina.** 2010. Construction of a bioluminescence reporter plasmid for Francisella tularensis. Plasmid.
27. **Bingle, L. E., C. M. Bailey, and M. J. Pallen.** 2008. Type VI secretion: a beginner's guide. Curr Opin Microbiol **11:**3-8.
28. **Boardman, B. K., and K. J. Satchell.** 2004. Vibrio cholerae strains with mutations in an atypical type I secretion system accumulate RTX toxin intracellularly. J Bacteriol **186:**8137-43.
29. **Boyer, F., G. Fichant, J. Berthod, Y. Vandenbrouck, and I. Attree.** 2009. Dissecting the bacterial type VI secretion system by a genome wide in silico analysis: what can be learned from available microbial genomic resources? BMC Genomics **10:**104.
30. **Brotcke, A., D. S. Weiss, C. C. Kim, P. Chain, S. Malfatti, E. Garcia, and D. M. Monack.** 2006. Identification of MglA-regulated genes reveals novel virulence factors in Francisella tularensis. Infect Immun **74:**6642-55.
31. **Buchrieser, C., M. Prentice, and E. Carniel.** 1998. The 102-kilobase unstable region of Yersinia pestis comprises a high-pathogenicity island linked to a pigmentation segment which undergoes internal rearrangement. J Bacteriol **180:**2321-9.
32. **Buddingh, G. J., and F. C. Womack.** 1941. Observations on the Infection of Chick Embryos with Bacterium Tularense, Brucella, and Pasteurella Pestis. J Exp Med **74:**213-22.
33. **Cambronne, E. D., L. W. Cheng, and O. Schneewind.** 2000. LcrQ/YscM1, regulators of the Yersinia yop virulon, are injected into host cells by a chaperone-dependent mechanism. Mol Microbiol **37:**263-73.
34. **Cascales, E.** 2008. The type VI secretion toolkit. EMBO Rep **9:**735-41.
35. **Chamberlain, R. E.** 1965. Evaluation of live tularemia vaccine prepared in chemically defined medium. Appl. Microbiol. **13:**232-235.
36. **Champion, M. D., Q. Zeng, E. B. Nix, F. E. Nano, P. Keim, C. D. Kodira, M. Borowsky, S. Young, M. Koehrsen, R. Engels, M. Pearson, C. Howarth, L. Larson,**

J. White, L. Alvarado, M. Forsman, S. W. Bearden, A. Sjostedt, R. Titball, S. L. Michell, B. Birren, and J. Galagan. 2009. Comparative genomic characterization of Francisella tularensis strains belonging to low and high virulence subspecies. PLoS Pathog **5:**e1000459.

37. **Charity, J. C., L. T. Blalock, M. M. Costante-Hamm, D. L. Kasper, and S. L. Dove.** 2009. Small molecule control of virulence gene expression in Francisella tularensis. PLoS Pathog **5:**e1000641.
38. **Charity, J. C., M. M. Costante-Hamm, E. L. Balon, D. H. Boyd, E. J. Rubin, and S. L. Dove.** 2007. Twin RNA polymerase-associated proteins control virulence gene expression in Francisella tularensis. PLoS Pathog **3:**e84.
39. **Checroun, C., T. D. Wehrly, E. R. Fischer, S. F. Hayes, and J. Celli.** 2006. Autophagy-mediated reentry of Francisella tularensis into the endocytic compartment after cytoplasmic replication. Proc Natl Acad Sci U S A **103:**14578-83.
40. **Chen, C. R., M. Malik, M. Snyder, and K. Drlica.** 1996. DNA gyrase and topoisomerase IV on the bacterial chromosome: quinolone-induced DNA cleavage. J Mol Biol **258:**627-37.
41. **Chen, I., P. J. Christie, and D. Dubnau.** 2005. The ins and outs of DNA transfer in bacteria. Science **310:**1456-60.
42. **Chen, W., R. KuoLee, H. Shen, and J. W. Conlan.** 2004. Susceptibility of immunodeficient mice to aerosol and systemic infection with virulent strains of Francisella tularensis. Microb Pathog **36:**311-8.
43. **Christopher, G. W., T. J. Cieslak, J. A. Pavlin, and E. M. Eitzen, Jr.** 1997. Biological warfare. A historical perspective. JAMA **278:**412-7.
44. **Clemens, D. L., and M. A. Horwitz.** 2007. Uptake and intracellular fate of Francisella tularensis in human macrophages. Ann N Y Acad Sci **1105:**160-86.
45. **Clemens, D. L., B. Y. Lee, and M. A. Horwitz.** 2005. Francisella tularensis enters macrophages via a novel process involving pseudopod loops. Infect Immun **73:**5892-902.
46. **Clemens, D. L., B. Y. Lee, and M. A. Horwitz.** 2009. Francisella tularensis phagosomal escape does not require acidification of the phagosome. Infect Immun **77:**1757-73.
47. **Clemens, D. L., B. Y. Lee, and M. A. Horwitz.** 2004. Virulent and avirulent strains of Francisella tularensis prevent acidification and maturation of their phagosomes and escape into the cytoplasm in human macrophages. Infect Immun **72:**3204-17.
48. **Conlan, J. W., A. Sjostedt, and R. J. North.** 1994. CD4+ and CD8+ T-cell-dependent and -independent host defense mechanisms can operate to control and resolve primary and secondary Francisella tularensis LVS infection in mice. Infect Immun **62:**5603-7.
49. **Cowley, S. C., C. J. Gray, and F. E. Nano.** 2000. Isolation and characterization of Francisella novicida mutants defective in lipopolysaccharide biosynthesis. FEMS Microbiol Lett **182:**63-7.
50. **Darby, C., C. L. Cosma, J. H. Thomas, and C. Manoil.** 1999. Lethal paralysis of Caenorhabditis elegans by Pseudomonas aeruginosa. Proc Natl Acad Sci U S A **96:**15202-7.
51. **Das, S., and K. Chaudhuri.** 2003. Identification of a unique IAHP (IcmF associated homologous proteins) cluster in Vibrio cholerae and other proteobacteria through in silico analysis. In Silico Biol **3:**287-300.

52. **de Bruin, O. M., J. S. Ludu, and F. E. Nano.** 2007. The Francisella pathogenicity island protein IglA localizes to the bacterial cytoplasm and is needed for intracellular growth. BMC Microbiol **7:**1.
53. **Deng, K., R. J. Blick, W. Liu, and E. J. Hansen.** 2006. Identification of Francisella tularensis genes affected by iron limitation. Infect Immun **74:**4224-36.
54. **Dennis, D. T., T. V. Inglesby, D. A. Henderson, J. G. Bartlett, M. S. Ascher, E. Eitzen, A. D. Fine, A. M. Friedlander, J. Hauer, M. Layton, S. R. Lillibridge, J. E. McDade, M. T. Osterholm, T. O'Toole, G. Parker, T. M. Perl, P. K. Russell, and K. Tonat.** 2001. Tularemia as a biological weapon: medical and public health management. JAMA **285:**2763-73.
55. **Dienst, F. T., Jr.** 1963. Tularemia: a perusal of three hundred thirty-nine cases. J La State Med Soc **115:**114-27.
56. **Ditta, G., S. Stanfield, D. Corbin, and D. R. Helinski.** 1980. Broad host range DNA cloning system for gram-negative bacteria: construction of a gene bank of Rhizobium meliloti. Proc Natl Acad Sci U S A **77:**7347-51.
57. **Dorofe'ev, K. A.** 1947. Classification of the causative agent of tularemia. Symp. Res. Works Inst. Epidemiol. Mikrobiol. Chita. **1:**170-180.
58. **Ebright, R. H., and S. Busby.** 1995. The Escherichia coli RNA polymerase alpha subunit: structure and function. Curr Opin Genet Dev **5:**197-203.
59. **Eigelsbach, H. T., W. Braun, and R. D. Herring.** 1951. Studies on the variation on *Bacterium tularensis*. J. Bacteriol. **61:**557-569.
60. **Eigelsbach, H. T., and C. M. Downs.** 1961. Prophylactic effectiveness of live and killed tularemia vaccines. J. Immunol. **87:**415-425.
61. **Eigelsbach, H. T., R. B. Hornick, and J. J. Tulis.** 1967. Recent studies on live tularemia vaccine. Med Ann Dist Columbia **36:**282-6.
62. **Eigelsbach, H. T., D. H. Hunter, W. A. Janssen, H. G. Dangerfield, and S. G. Rabinowitz.** 1975. Murine model for study of cell-mediated immunity: protection against death from fully virulent Francisella tularensis infection. Infect Immun **12:**999-1005.
63. **Eigelsbach, H. T., J. J. Tulis, M. H. McGavran, and J. D. White.** 1962. Live tularemia vaccine. I. Host-parasite relationship in monkeys vaccinated intracutaneously or aerogenically. J. Bacteriol. **84:**1020-1027.
64. **Elkins, K. L., T. R. Rhinehart-Jones, S. J. Culkin, D. Yee, and R. K. Winegar.** 1996. Minimal requirements for murine resistance to infection with *Francisella tularensis* LVS. Infect. Immun. **64:**3288-3293.
65. **Elliott, S. J., L. A. Wainwright, T. K. McDaniel, K. G. Jarvis, Y. K. Deng, L. C. Lai, B. P. McNamara, M. S. Donnenberg, and J. B. Kaper.** 1998. The complete sequence of the locus of enterocyte effacement (LEE) from enteropathogenic Escherichia coli E2348/69. Mol Microbiol **28:**1-4.
66. **Ellis, J., P. C. Oyston, M. Green, and R. W. Titball.** 2002. Tularemia. Clin Microbiol Rev **15:**631-646.
67. **Enderlin, G., L. Morales, R. F. Jacobs, and J. T. Cross.** 1994. Streptomycin and alternative agents for the treatment of tularemia: review of the literature. Clin Infect Dis **19:**42-7.
68. **Enos-Berlage, J. L., Z. T. Guvener, C. E. Keenan, and L. L. McCarter.** 2005. Genetic determinants of biofilm development of opaque and translucent Vibrio parahaemolyticus. Mol Microbiol **55:**1160-82.

69. **Evans, M. E., D. W. Gregory, W. Schaffner, and Z. A. McGee.** 1985. Tularemia: A 30-year experience with 88 cases. Medicine **64:**251-269.
70. **Fields, K. A., M. L. Nilles, C. Cowan, and S. C. Straley.** 1999. Virulence role of V antigen of Yersinia pestis at the bacterial surface. Infect Immun **67:**5395-408.
71. **Filloux, A., A. Hachani, and S. Bleves.** 2008. The bacterial type VI secretion machine: yet another player for protein transport across membranes. Microbiology **154:**1570-83.
72. **Foley, J. E., and N. C. Nieto.** 2010. Tularemia. Vet Microbiol **140:**332-8.
73. **Forsman, M., E. W. Henningson, E. Larsson, T. Johansson, and G. Sandstrom.** 2000. Francisella tularensis does not manifest virulence in viable but non-culturable state. FEMS Microbiol Ecol **31:**217-224.
74. **Fortier, A. H., D. A. Leiby, R. B. Narayanan, E. Asafoadjei, R. M. Crawford, C. A. Nacy, and M. S. Meltzer.** 1995. Growth of *Francisella tularensis* LVS in macrophages: the acidic intracellular compartment provides essential iron required for growth. Infect. Immun. **63:**1478-1483.
75. **Fortier, A. H., M. V. Slayter, R. Ziemba, M. S. Meltzer, and C. A. Nacy.** 1991. Live vaccine strain of *Francisella tularensis*: infection and immunity in mice. Infect. Immun. **59::**2922-2928.
76. **Foshay, L., W. H. Hesselbrock, H. J. Wittenberg, and A. H. Rodenberg.** 1942. Vaccine Prophylaxis against Tularemia in Man. Am J Public Health Nations Health **32:**1131-45.
77. **Francis, C. L., T. A. Ryan, B. D. Jones, S. J. Smith, and S. Falkow.** 1993. Ruffles induced by Salmonella and other stimuli direct macropinocytosis of bacteria. Nature **364:**639-42.
78. **Francis, E.** 1921. Deer-Fly Fever; a Disease of Man of Hitherto Unknown Etiology. Pub. Health Rep. **34:**2061-2062.
79. **Francis, E., Mayne. B.** 1921. Experimental Transmission of Tularemia by Flies of the Species Chrysops Discalis. Pub. Health Rep. **36:**1738-1746.
80. **Gage, K. L., D. T. Dennis, K. A. Orloski, P. Ettestad, T. L. Brown, P. J. Reynolds, W. J. Pape, C. L. Fritz, L. G. Carter, and J. D. Stein.** 2000. Cases of cat-associated human plague in the Western US, 1977-1998. Clin Infect Dis **30:**893-900.
81. **Gaillard, M., T. Vallaeys, F. J. Vorholter, M. Minoia, C. Werlen, V. Sentchilo, A. Puhler, and J. R. van der Meer.** 2006. The clc element of Pseudomonas sp. strain B13, a genomic island with various catabolic properties. J Bacteriol **188:**1999-2013.
82. **Gal-Mor, O., and B. B. Finlay.** 2006. Pathogenicity islands: a molecular toolbox for bacterial virulence. Cell Microbiol **8:**1707-19.
83. **Galan, J. E., and H. Wolf-Watz.** 2006. Protein delivery into eukaryotic cells by type III secretion machines. Nature **444:**567-73.
84. **Gallagher, L. A., E. Ramage, M. A. Jacobs, R. Kaul, M. Brittnacher, and C. Manoil.** 2007. A comprehensive transposon mutant library of Francisella novicida, a bioweapon surrogate. Proc Natl Acad Sci U S A **104:**1009-14.
85. **Goldsby, R. A., Kindt, T.J., Osborne, B.A., Kuby, J. .** 2003. Immunology, 5th ed. W.H. Freeman and Company, New York.
86. **Golovliov, I., V. Baranov, Z. Krocova, H. Kovarova, and A. Sjostedt.** 2003. An attenuated strain of the facultative intracellular bacterium *Francisella tularensis* can escape the phagosome of monocytic cells. Infect Immun **71:**5940-5950.

87. **Golovliov, I., A. Sjostedt, A. Mokrievich, and V. Pavlov.** 2003. A method for allelic replacement in Francisella tularensis. FEMS Microbiol Lett **222:**273-80.
88. **Gourse, R. L., W. Ross, and T. Gaal.** 2000. UPs and downs in bacterial transcription initiation: the role of the alpha subunit of RNA polymerase in promoter recognition. Mol Microbiol **37:**687-95.
89. **Gray, C. G., S. C. Cowley, K. K. Cheung, and F. E. Nano.** 2002. The identification of five genetic loci of Francisella novicida associated with intracellular growth. FEMS Microbiol Lett **215:**53-6.
90. **Griffin, F. M., Jr., J. A. Griffin, J. E. Leider, and S. C. Silverstein.** 1975. Studies on the mechanism of phagocytosis. I. Requirements for circumferential attachment of particle-bound ligands to specific receptors on the macrophage plasma membrane. J Exp Med **142:**1263-82.
91. **Groisman, E. A., and H. Ochman.** 1996. Pathogenicity islands: bacterial evolution in quantum leaps. Cell **87:**791-4.
92. **Hacker, J., L. Bender, M. Ott, J. Wingender, B. Lund, R. Marre, and W. Goebel.** 1990. Deletions of chromosomal regions coding for fimbriae and hemolysins occur in vitro and in vivo in various extraintestinal Escherichia coli isolates. Microb Pathog **8:**213-25.
93. **Hacker, J., and J. B. Kaper.** 2000. Pathogenicity islands and the evolution of microbes. Annu Rev Microbiol **54:**641-79.
94. **Hajjar, A. M., M. D. Harvey, S. A. Shaffer, D. R. Goodlett, A. Sjostedt, H. Edebro, M. Forsman, M. Bystrom, M. Pelletier, C. B. Wilson, S. I. Miller, S. J. Skerrett, and R. K. Ernst.** 2006. Lack of in vitro and in vivo recognition of Francisella tularensis subspecies lipopolysaccharide by Toll-like receptors. Infect Immun **74:**6730-8.
95. **Hakenbeck, R., N. Balmelle, B. Weber, C. Gardes, W. Keck, and A. de Saizieu.** 2001. Mosaic genes and mosaic chromosomes: intra- and interspecies genomic variation of Streptococcus pneumoniae. Infect Immun **69:**2477-86.
96. **Harris, S.** 1992. Japanese biological warfare research on humans: a case study of microbiology and ethics. Ann N Y Acad Sci **666:**21-52.
97. **Hoch, J. A.** 2000. Two-component and phosphorelay signal transduction. Curr Opin Microbiol **3:**165-70.
98. **Hollis, D. G., R. E. Weaver, A. G. Steigerwalt, J. D. Wenger, C. W. Moss, and D. J. Brenner.** 1989. Francisella philomiragia comb. nov. (formerly Yersinia philomiragia) and Francisella tularensis biogroup novicida (formerly Francisella novicida) associated with human disease. J Clin Microbiol **27:**1601-8.
99. **Hood, A. M.** 1977. Virulence factors of *Francisella tularensis*. J. Hyg. **79:**47-60.
100. **Hood, R. D., P. Singh, F. Hsu, T. Guvener, M. A. Carl, R. R. Trinidad, J. M. Silverman, B. B. Ohlson, K. G. Hicks, R. L. Plemel, M. Li, S. Schwarz, W. Y. Wang, A. J. Merz, D. R. Goodlett, and J. D. Mougous.** 2010. A type VI secretion system of Pseudomonas aeruginosa targets a toxin to bacteria. Cell Host Microbe **7:**25-37.
101. **Hopla, C. E.** 1974. The ecology of tularemia. Adv Vet Sci Comp Med **18:**25-53.
102. **Horwitz, M. A.** 1984. Phagocytosis of the Legionnaires' disease bacterium (Legionella pneumophila) occurs by a novel mechanism: engulfment within a pseudopod coil. Cell **36:**27-33.

103. **Hsiao, W. W., K. Ung, D. Aeschliman, J. Bryan, B. B. Finlay, and F. S. Brinkman.** 2005. Evidence of a large novel gene pool associated with prokaryotic genomic islands. PLoS Genet **1:**e62.
104. **Hussey, S., L. H. Travassos, and N. L. Jones.** 2009. Autophagy as an emerging dimension to adaptive and innate immunity. Semin Immunol **21:**233-41.
105. **Johansson, A., M. Forsman, and A. Sjostedt.** 2004. The development of tools for diagnosis of tularemia and typing of Francisella tularensis. APMIS **112:**898-907.
106. **Johnston, S., S. Lin, P. Lee, S. M. Caffrey, J. Wildschut, J. K. Voordouw, S. M. da Silva, I. A. Pereira, and G. Voordouw.** 2009. A genomic island of the sulfate-reducing bacterium Desulfovibrio vulgaris Hildenborough promotes survival under stress conditions while decreasing the efficiency of anaerobic growth. Environ Microbiol **11:**981-91.
107. **Juhas, M., J. R. van der Meer, M. Gaillard, R. M. Harding, D. W. Hood, and D. W. Crook.** 2009. Genomic islands: tools of bacterial horizontal gene transfer and evolution. FEMS Microbiol Rev **33:**376-93.
108. **Kantardjiev, T., P. Padeshki, and I. N. Ivanov.** 2007. Diagnostic approaches for oculoglandular tularemia: advantages of PCR. Br J Ophthalmol **91:**1206-8.
109. **Kaufmann, A. F., M. I. Meltzer, and G. P. Schmid.** 1997. The economic impact of a bioterrorist attack: are prevention and postattack intervention programs justifiable? Emerg Infect Dis **3:**83-94.
110. **Kawula, T. H., J. D. Hall, J. R. Fuller, and R. R. Craven.** 2004. Use of transposon-transposase complexes to create stable insertion mutant strains of Francisella tularensis LVS. Appl Environ Microbiol **70:**6901-4.
111. **Kieffer, T. L., S. Cowley, F. E. Nano, and K. L. Elkins.** 2003. Francisella novicida LPS has greater immunobiological activity in mice than F. tularensis LPS, and contributes to F. novicida murine pathogenesis. Microbes Infect **5:**397-403.
112. **Klein, L., C. Munz, and J. D. Lunemann.** 2010. Autophagy-mediated antigen processing in CD4(+) T cell tolerance and immunity. FEBS Lett **584:**1405-10.
113. **Laemmli, U. K.** 1970. Cleavage of structural proteins during the assembly of the head of bacteriophage T4. Nature **227:**680-685.
114. **Lai, X. H., I. Golovliov, and A. Sjostedt.** 2001. Francisella tularensis induces cytopathogenicity and apoptosis in murine macrophages via a mechanism that requires intracellular bacterial multiplication. Infect Immun **69:**4691-4.
115. **Lai, X. H., and A. Sjostedt.** 2003. Delineation of the molecular mechanisms of Francisella tularensis-induced apoptosis in murine macrophages. Infect Immun **71:**4642-6.
116. **Larbig, K. D., A. Christmann, A. Johann, J. Klockgether, T. Hartsch, R. Merkl, L. Wiehlmann, H. J. Fritz, and B. Tummler.** 2002. Gene islands integrated into tRNA(Gly) genes confer genome diversity on a Pseudomonas aeruginosa clone. J Bacteriol **184:**6665-80.
117. **Larson, C. L., W. Wicht, and W. L. Jellison.** 1955. An organism resembling *P. tularensis* isolated from water. Public Health Rep. **70:**253-258.
118. **Larsson, P., P. C. Oyston, P. Chain, M. C. Chu, M. Duffield, H. H. Fuxelius, E. Garcia, G. Halltorp, D. Johansson, K. E. Isherwood, P. D. Karp, E. Larsson, Y. Liu, S. Michell, J. Prior, R. Prior, S. Malfatti, A. Sjostedt, K. Svensson, N. Thompson, L. Vergez, J. K. Wagg, B. W. Wren, L. E. Lindler, S. G. Andersson, M. Forsman, and**

R. W. Titball. 2005. The complete genome sequence of Francisella tularensis, the causative agent of tularemia. Nat. Genet. **37:**153-159.

119. **Lauriano, C. M., J. R. Barker, F. E. Nano, B. P. Arulanandam, and K. E. Klose.** 2003. Allelic exchange in Francisella tularensis using PCR products. FEMS Microbiol Lett **229:**195-202.
120. **Lauriano, C. M., J. R. Barker, S.-S. Yoon, F. E. Nano, B. P. Arulanandam, D. J. Hassett, and K. E. Klose.** 2004. MglA regulates transcription of virulence factors necessary for *Francisella tularensis* intraamoebae and intramacrophage survival. Proc Natl Acad Sci U S A **101:**4246-4249.
121. **Lawrence, J. G.** 2005. Horizontal and vertical gene transfer: the life history of pathogens. Contrib Microbiol **12:**255-71.
122. **Leiman, P. G., M. Basler, U. A. Ramagopal, J. B. Bonanno, J. M. Sauder, S. Pukatzki, S. K. Burley, S. C. Almo, and J. J. Mekalanos.** 2009. Type VI secretion apparatus and phage tail-associated protein complexes share a common evolutionary origin. Proc Natl Acad Sci U S A **106:**4154-9.
123. **Limaye, A. P., and C. J. Hooper.** 1999. Treatment of tularemia with fluoroquinolones: two cases and review. Clin Infect Dis **29:**922-4.
124. **Lindgren, H., I. Golovliov, V. Baranov, R. K. Ernst, M. Telepnev, and A. Sjostedt.** 2004. Factors affecting the escape of Francisella tularensis from the phagolysosome. J Med Microbiol **53:**953-8.
125. **LoVullo, E. D., L. A. Sherrill, L. L. Perez, and M. S. Pavelka, Jr.** 2006. Genetic tools for highly pathogenic Francisella tularensis subsp. tularensis. Microbiology **152:**3425-35.
126. **Lozupone, C. A., and R. Knight.** 2007. Global patterns in bacterial diversity. Proc Natl Acad Sci U S A **104:**11436-40.
127. **Ludu, J. S., O. M. de Bruin, B. N. Duplantis, C. L. Schmerk, A. Y. Chou, K. L. Elkins, and F. E. Nano.** 2008. The Francisella pathogenicity island protein PdpD is required for full virulence and associates with homologues of the type VI secretion system. J Bacteriol **190:**4584-95.
128. **Ludu, J. S., E. B. Nix, B. N. Duplantis, O. M. de Bruin, L. A. Gallagher, L. M. Hawley, and F. E. Nano.** 2008. Genetic elements for selection, deletion mutagenesis and complementation in Francisella spp. FEMS Microbiol Lett **278:**86-93.
129. **Ma, A. T., S. McAuley, S. Pukatzki, and J. J. Mekalanos.** 2009. Translocation of a Vibrio cholerae type VI secretion effector requires bacterial endocytosis by host cells. Cell Host Microbe **5:**234-43.
130. **Maier, T. M., A. Havig, M. Casey, F. E. Nano, D. W. Frank, and T. C. Zahrt.** 2004. Construction and characterization of a highly efficient Francisella shuttle plasmid. Appl Environ Microbiol **70:**7511-9.
131. **Maier, T. M., R. Pechous, M. Casey, T. C. Zahrt, and D. W. Frank.** 2006. In vivo Himar1-based transposon mutagenesis of Francisella tularensis. Appl Environ Microbiol **72:**1878-85.
132. **Mailman, T. L., and M. H. Schmidt.** 2005. Francisella philomiragia adenitis and pulmonary nodules in a child with chronic granulomatous disease. Can J Infect Dis Med Microbiol **16:**245-8.
133. **Majdalani, N., C. K. Vanderpool, and S. Gottesman.** 2005. Bacterial small RNA regulators. Crit Rev Biochem Mol Biol **40:**93-113.

134. **Mariathasan, S., D. S. Weiss, V. M. Dixit, and D. M. Monack.** 2005. Innate immunity against Francisella tularensis is dependent on the ASC/caspase-1 axis. J Exp Med **202:**1043-9.
135. **McCoy, G. W., and C. W. Chapin.** 1912. Further observations on a plague like disease of rodents with a preliminary note on the causative agent *bacterium tularense*. J. Infect. Dis. **10:**61-72.
136. **McDaniel, T. K., and J. B. Kaper.** 1997. A cloned pathogenicity island from enteropathogenic Escherichia coli confers the attaching and effacing phenotype on E. coli K-12. Mol Microbiol **23:**399-407.
137. **McGavran, M. H., J. D. White, H. T. Eigelsbach, and R. W. Kerpsack.** 1962. Morphologic and Immunohistochemical Studies of the Pathogenesis of Infection and Antibody Formation Subsequent to Vaccination of Macaca irus with an Attenuated Strain of Pasteurella tularensis: I. Intracutaneous Vaccination. Am J Pathol **41:**259-271.
138. **Mdluli, K. E., L. S. Anthony, G. S. Baron, M. K. McDonald, S. V. Myltseva, and F. E. Nano.** 1994. Serum-sensitive mutation of Francisella novicida: association with an ABC transporter gene. Microbiology **140:**3309-18.
139. **Medzhitov, R., P. Preston-Hurlburt, and C. A. Janeway, Jr.** 1997. A human homologue of the Drosophila Toll protein signals activation of adaptive immunity. Nature **388:**394-7.
140. **Merrell, D. S., D. L. Hava, and A. Camilli.** 2002. Identification of novel factors involved in colonization and acid tolerance of Vibrio cholerae. Mol Microbiol **43:**1471-91.
141. **Miller, S. I., R. K. Ernst, and M. W. Bader.** 2005. LPS, TLR4 and infectious disease diversity. Nat Rev Microbiol **3:**36-46.
142. **Moe, J. B., P. G. Canonico, J. L. Stookey, M. C. Powanda, and G. L. Cockerell.** 1975. Pathogenesis of tularemia in immune and nonimmune rats. Am J Vet Res **36:**1505-10.
143. **Mohapatra, N. P., S. Soni, B. L. Bell, R. Warren, R. K. Ernst, A. Muszynski, R. W. Carlson, and J. S. Gunn.** 2007. Identification of an orphan response regulator required for the virulence of Francisella spp. and transcription of pathogenicity island genes. Infect Immun **75:**3305-14.
144. **Morales, V. M., A. Backman, and M. Bagdasarian.** 1991. A series of wide-host-range low-copy-number vectors that allow direct screening for recombinants. Gene **97:**39-47.
145. **Mougous, J. D., M. E. Cuff, S. Raunser, A. Shen, M. Zhou, C. A. Gifford, A. L. Goodman, G. Joachimiak, C. L. Ordonez, S. Lory, T. Walz, A. Joachimiak, and J. J. Mekalanos.** 2006. A virulence locus of Pseudomonas aeruginosa encodes a protein secretion apparatus. Science **312:**1526-30.
146. **Nano, F. E., and C. Schmerk.** 2007. The Francisella pathogenicity island. Ann N Y Acad Sci **1105:**122-37.
147. **Nano, F. E., N. Zhang, S. C. Cowley, K. E. Klose, K. K. M. Cheung, M. J. Roberts, J. S. Ludu, G. W. Letendre, A. I. Meierovics, G. Stephens, and K. L. Elkins.** 2004. A *Francisella tularensis* Pathogenicity Island Required for Intramacrophage Growth. J. Bacteriol. **186:**6430-6436.
148. **Nguyen, L., I. T. Paulsen, J. Tchieu, C. J. Hueck, and M. H. Saier, Jr.** 2000. Phylogenetic analyses of the constituents of Type III protein secretion systems. J Mol Microbiol Biotechnol **2:**125-44.

149. **Ninio, S., and C. R. Roy.** 2007. Effector proteins translocated by Legionella pneumophila: strength in numbers. Trends Microbiol **15:**372-80.
150. **Nix, E. B., K. K. Cheung, D. Wang, N. Zhang, R. D. Burke, and F. E. Nano.** 2006. Virulence of Francisella spp. in chicken embryos. Infect Immun **74:**4809-16.
151. **Nutter, J. E., and H. T. Eigelsbach.** 1967. Response of guinea pig to sublethal x-irradiation and live tularemia vaccine. Proc Soc Exp Biol Med **124:**1227-30.
152. **Olsufjev, J. G., and I. S. Meshcheryakova.** 1983. Subspecific taxonomy of Francisella tularensis McCoy and Chapin 1912. Int. J. Syst. Bacteriol. **33:**872-874.
153. **Osborn, M. J., J. E. Gander, E. Parisi, and J. Carson.** 1972. Mechinism of assembly of the outer membrane of Salmonella typhimurium. Isolation and characterization of cytoplasmic and outer membrane. J Biol Chem **247:**3962-72.
154. **Ottem, K. F., A. Nylund, E. Karlsbakk, A. Friis-Moller, and T. Kamaishi.** 2009. Elevation of Francisella philomiragia subsp. noatunensis Mikalsen et al. (2007) to Francisella noatunensis comb. nov. [syn. Francisella piscicida Ottem et al. (2008) syn. nov.] and characterization of Francisella noatunensis subsp. orientalis subsp. nov., two important fish pathogens. J Appl Microbiol **106:**1231-43.
155. **Owen, C. R.** 1974. Genus *Francisella*. The Williams and Wilkins Co., Baltimore.
156. **Oyston, P. C.** 2009. Francisella tularensis vaccines. Vaccine **27 Suppl 4:**D48-51.
157. **Parker, R. R., E. A. Steinhaus, G. M. Kohls, and W. L. Jellison.** 1951. Contamination of natural waters and mud with Pasteurella tularensis and tularemia in beavers and muskrats in the northwestern United States. Bull Natl Inst Health **193:**1-161.
158. **Parker, R. T., L. M. Lister, R. E. Bauer, H. E. Hall, and T. E. Woodward.** 1950. Use of chloramphenicol (chloromycetin) in experimental and human tularemia. J Am Med Assoc **143:**7-11.
159. **Parsons, D. A., and F. Heffron.** 2005. sciS, an icmF homolog in Salmonella enterica serovar Typhimurium, limits intracellular replication and decreases virulence. Infect Immun **73:**4338-45.
160. **Pavkova, I., M. Reichelova, P. Larsson, M. Hubalek, J. Vackova, A. Forsberg, and J. Stulik.** 2006. Comparative proteome analysis of fractions enriched for membrane-associated proteins from Francisella tularensis subsp. tularensis and F. tularensis subsp. holarctica strains. J Proteome Res **5:**3125-34.
161. **Pearse, R. A.** 1911. Insect Bites. Northwest Med.
162. **Pechous, R. D., T. R. McCarthy, and T. C. Zahrt.** 2009. Working toward the future: insights into Francisella tularensis pathogenesis and vaccine development. Microbiol Mol Biol Rev **73:**684-711.
163. **Pell, L. G., V. Kanelis, L. W. Donaldson, P. L. Howell, and A. R. Davidson.** 2009. The phage lambda major tail protein structure reveals a common evolution for long-tailed phages and the type VI bacterial secretion system. Proc Natl Acad Sci U S A **106:**4160-5.
164. **Perez-Castrillon, J. L., P. Bachiller-Luque, M. Martin-Luquero, F. J. Mena-Martin, and V. Herreros.** 2001. Tularemia epidemic in northwestern Spain: clinical description and therapeutic response. Clin Infect Dis **33:**573-6.
165. **Perna, N. T., G. F. Mayhew, G. Posfai, S. Elliott, M. S. Donnenberg, J. B. Kaper, and F. R. Blattner.** 1998. Molecular evolution of a pathogenicity island from enterohemorrhagic Escherichia coli O157:H7. Infect Immun **66:**3810-7.
166. **Perry, R. D., and J. D. Fetherston.** 1997. Yersinia pestis--etiologic agent of plague. Clin Microbiol Rev **10:**35-66.

167. **Pettersson, J., R. Nordfelth, E. Dubinina, T. Bergman, M. Gustafsson, K. E. Magnusson, and H. Wolf-Watz.** 1996. Modulation of virulence factor expression by pathogen target cell contact. Science **273:**1231-3.
168. **Pierini, L. M.** 2006. Uptake of serum-opsonized Francisella tularensis by macrophages can be mediated by class A scavenger receptors. Cell Microbiol **8:**1361-70.
169. **Prudhomme, M., L. Attaiech, G. Sanchez, B. Martin, and J. P. Claverys.** 2006. Antibiotic stress induces genetic transformability in the human pathogen Streptococcus pneumoniae. Science **313:**89-92.
170. **Pukatzki, S., A. T. Ma, A. T. Revel, D. Sturtevant, and J. J. Mekalanos.** 2007. Type VI secretion system translocates a phage tail spike-like protein into target cells where it cross-links actin. Proc Natl Acad Sci U S A **104:**15508-13.
171. **Pukatzki, S., A. T. Ma, D. Sturtevant, B. Krastins, D. Sarracino, W. C. Nelson, J. F. Heidelberg, and J. J. Mekalanos.** 2006. Identification of a conserved bacterial protein secretion system in Vibrio cholerae using the Dictyostelium host model system. Proc Natl Acad Sci U S A **103:**1528-33.
172. **Pullen RL, S. B.** 1945. Tularemia: analysis of 225 cases. JAMA. **129:**495-500.
173. **Qin, A., and B. J. Mann.** 2006. Identification of transposon insertion mutants of Francisella tularensis tularensis strain Schu S4 deficient in intracellular replication in the hepatic cell line HepG2. BMC Microbiol **6:**69.
174. **Ransmeier, J. C.** 1943. The reaction of the chicken embryo to virulent and nonvirulent strains of *Bact. tularense.* J Infect Dis **72:**86-90.
175. **Read, A., S. J. Vogl, K. Hueffer, L. A. Gallagher, and G. M. Happ.** 2008. Francisella genes required for replication in mosquito cells. J Med Entomol **45:**1108-16.
176. **Rohmer, L., C. Fong, S. Abmayr, M. Wasnick, T. J. Larson Freeman, M. Radey, T. Guina, K. Svensson, H. S. Hayden, M. Jacobs, L. A. Gallagher, C. Manoil, R. K. Ernst, B. Drees, D. Buckley, E. Haugen, D. Bovee, Y. Zhou, J. Chang, R. Levy, R. Lim, W. Gillett, D. Guenthener, A. Kang, S. A. Shaffer, G. Taylor, J. Chen, B. Gallis, D. A. D'Argenio, M. Forsman, M. V. Olson, D. R. Goodlett, R. Kaul, S. I. Miller, and M. J. Brittnacher.** 2007. Comparison of Francisella tularensis genomes reveals evolutionary events associated with the emergence of human pathogenic strains. Genome Biol **8:**R102.
177. **Rosqvist, R., S. Hakansson, A. Forsberg, and H. Wolf-Watz.** 1995. Functional conservation of the secretion and translocation machinery for virulence proteins of yersiniae, salmonellae and shigellae. EMBO J **14:**4187-95.
178. **Ross, W., K. K. Gosink, J. Salomon, K. Igarashi, C. Zou, A. Ishihama, K. Severinov, and R. L. Gourse.** 1993. A third recognition element in bacterial promoters: DNA binding by the alpha subunit of RNA polymerase. Science **262:**1407-13.
179. **Roussel, E. G., M. A. Bonavita, J. Querellou, B. A. Cragg, G. Webster, D. Prieur, and R. J. Parkes.** 2008. Extending the sub-sea-floor biosphere. Science **320:**1046.
180. **Salomonsson, E., K. Kuoppa, A. L. Forslund, C. Zingmark, I. Golovliov, A. Sjostedt, L. Noppa, and A. Forsberg.** 2009. Reintroduction of two deleted virulence loci restores full virulence to the live vaccine strain of Francisella tularensis. Infect Immun **77:**3424-31.
181. **Sambrook, J., E. F. Fritsch, and T. Maniatis.** 1989. Molecular Cloning, 2nd ed. Cold Spring Harbor Laboratory Press, Cold Spring Harbor.
182. **Sandstrom, G.** 1994. The tularaemia vaccine. J Chem Technol Biotechnol **59:**315-20.

183. **Sandström, G., S. Löfgren, and A. Tärnvik.** 1988. A capsule-deficient mutant of *Francisella tularensis* LVS exhibits enhanced sensitivity to killing by serum but diminished sensitivity to killing by polymorphonuclear leukocytes. Infect. Immun. **56:**1194-1202.
184. **Sandström, G., A. Sjöstedt, T. Johansson, K. Kuoppa, and J. C. Williams.** 1992. Immunogenicity and toxicity of lipopolysaccharide from *Francisella tularensis* LVS. FEMS Microbiol. Immunol. **105:**201-210.
185. **Santic, M., S. A. Khodor, and Y. A. Kwaik.** 2009. Cell biology and molecular ecology of Francisella tularensis. Cell Microbiol.
186. **Santic, M., M. Molmeret, and Y. Abu Kwaik.** 2005. Modulation of biogenesis of the Francisella tularensis subsp. novicida-containing phagosome in quiescent human macrophages and its maturation into a phagolysosome upon activation by IFN-gamma. Cell Microbiol **7:**957-67.
187. **Santic, M., M. Molmeret, J. R. Barker, K. E. Klose, A. Dekanic, M. Doric, and Y. Abu Kwaik.** 2007. A Francisella tularensis pathogenicity island protein essential for bacterial proliferation within the host cell cytosol. Cell Microbiol **9:**2391-403.
188. **Santic, M., M. Molmeret, K. E. Klose, and Y. Abu Kwaik.** 2006. Francisella tularensis travels a novel, twisted road within macrophages. Trends Microbiol **14:**37-44.
189. **Santic, M., M. Molmeret, K. E. Klose, S. Jones, and Y. A. Kwaik.** 2005. The Francisella tularensis pathogenicity island protein IglC and its regulator MglA are essential for modulating phagosome biogenesis and subsequent bacterial escape into the cytoplasm. Cell Microbiol **7:**969-79.
190. **Saslaw, S., H. T. Eigelsbach, J. A. Prior, H. E. Wilson, and S. Carhart.** 1961. Tularemia vaccine study. II. Respiratory challenge. Archives of Internal Medicine **107:**134-146.
191. **Saslaw, S., H. T. Eigelsbach, H. E. Wilson, J. A. Prior, and S. Carhart.** 1961. Tularemia vaccine study. I. Intracutaneous challenge. Archives of Internal Medicine **107:**121-133.
192. **Schmerk, C. L., B. N. Duplantis, P. L. Howard, and F. E. Nano.** 2009. A Francisella novicida pdpA mutant exhibits limited intracellular replication and remains associated with the lysosomal marker LAMP-1. Microbiology **155:**1498-504.
193. **Schmerk, C. L., B. N. Duplantis, D. Wang, R. D. Burke, A. Y. Chou, K. L. Elkins, J. S. Ludu, and F. E. Nano.** 2009. Characterization of the pathogenicity island protein PdpA and its role in the virulence of Francisella novicida. Microbiology **155:**1489-97.
194. **Schmidt, H., and M. Hensel.** 2004. Pathogenicity islands in bacterial pathogenesis. Clin Microbiol Rev **17:**14-56.
195. **Schopf, J. W., A. B. Kudryavtsev, D. G. Agresti, T. J. Wdowiak, and A. D. Czaja.** 2002. Laser--Raman imagery of Earth's earliest fossils. Nature **416:**73-6.
196. **Schotte, P., G. Denecker, A. Van Den Broeke, P. Vandenabeele, G. R. Cornelis, and R. Beyaert.** 2004. Targeting Rac1 by the Yersinia effector protein YopE inhibits caspase-1-mediated maturation and release of interleukin-1beta. J Biol Chem **279:**25134-42.
197. **Schricker, R. L., H. T. Eigelsbach, J. Q. Mitten, and W. C. Hall.** 1972. Pathogenesis of tularemia in monkeys aerogenically exposed to Francisella tularensis 425. Infect Immun **5:**734-44.

198. **Schulert, G. S., and L. A. Allen.** 2006. Differential infection of mononuclear phagocytes by Francisella tularensis: role of the macrophage mannose receptor. J Leukoc Biol **80:**563-71.
199. **Simpson, W. M.** 1928. Tularemia (Francis' Disease). Annals of Internal Medicine **1:**1007-1059.
200. **Sittka, A., S. Lucchini, K. Papenfort, C. M. Sharma, K. Rolle, T. T. Binnewies, J. C. Hinton, and J. Vogel.** 2008. Deep sequencing analysis of small noncoding RNA and mRNA targets of the global post-transcriptional regulator, Hfq. PLoS Genet **4:**e1000163.
201. **Sjostedt, A., A. Tarnvik, and G. Sandstrom.** 1996. Francisella tularensis: host-parasite interaction. FEMS Immunol Med Microbiol **13:**181-4.
202. **Smith, H. O., J. F. Tomb, B. A. Dougherty, R. D. Fleischmann, and J. C. Venter.** 1995. Frequency and distribution of DNA uptake signal sequences in the Haemophilus influenzae Rd genome. Science **269:**538-40.
203. **Staples, J. E., K. A. Kubota, L. G. Chalcraft, P. S. Mead, and J. M. Petersen.** 2006. Epidemiologic and molecular analysis of human tularemia, United States, 1964-2004. Emerg Infect Dis **12:**1113-8.
204. **Stepkowski, T., and A. B. Legocki.** 2001. Reduction of bacterial genome size and expansion resulting from obligate intracellular lifestyle and adaptation to soil habitat. Acta Biochim Pol **48:**367-81.
205. **Stewart, S. J.** 1996. Tularemia: association with hunting and farming. FEMS Immunol Med Microbiol **13:**197-99.
206. **Stock, A. M., V. L. Robinson, and P. N. Goudreau.** 2000. Two-component signal transduction. Annu Rev Biochem **69:**183-215.
207. **Sullivan, J. T., J. R. Trzebiatowski, R. W. Cruickshank, J. Gouzy, S. D. Brown, R. M. Elliot, D. J. Fleetwood, N. G. McCallum, U. Rossbach, G. S. Stuart, J. E. Weaver, R. J. Webby, F. J. De Bruijn, and C. W. Ronson.** 2002. Comparative sequence analysis of the symbiosis island of Mesorhizobium loti strain R7A. J Bacteriol **184:**3086-95.
208. **Takeuchi, O., K. Hoshino, T. Kawai, H. Sanjo, H. Takada, T. Ogawa, K. Takeda, and S. Akira.** 1999. Differential roles of TLR2 and TLR4 in recognition of gram-negative and gram-positive bacterial cell wall components. Immunity **11:**443-51.
209. **Telepnev, M., I. Golovliov, T. Grundstrom, A. Tarnvik, and A. Sjostedt.** 2003. Francisella tularensis inhibits Toll-like receptor-mediated activation of intracellular signalling and secretion of TNF-alpha and IL-1 from murine macrophages. Cell Microbiol **5:**41-51.
210. **Telepnev, M., I. Golovliov, and A. Sjostedt.** 2005. Francisella tularensis LVS initially activates but subsequently down-regulates intracellular signaling and cytokine secretion in mouse monocytic and human peripheral blood mononuclear cells. Microb Pathog **38:**239-47.
211. **Thompson, L. C. A. T.** 1946. Report on Japanese Biological Warfare, 31 May 1946. Record Group 330, the National Archives.
212. **Tigertt, W. D.** 1962. Soviet viable Pasteurella tularensis vaccines. A review of selected articles. Bacteriol Rev **26:**354-73.
213. **Twine, S., M. Bystrom, W. Chen, M. Forsman, I. Golovliov, A. Johansson, J. Kelly, H. Lindgren, K. Svensson, C. Zingmark, W. Conlan, and A. Sjostedt.** 2005. A mutant of Francisella tularensis strain SCHU S4 lacking the ability to express a 58-kilodalton

protein is attenuated for virulence and is an effective live vaccine. Infect Immun **73:**8345-52.

214. **Twine, S. M., N. C. Mykytczuk, M. D. Petit, H. Shen, A. Sjostedt, J. Wayne Conlan, and J. F. Kelly.** 2006. In vivo proteomic analysis of the intracellular bacterial pathogen, Francisella tularensis, isolated from mouse spleen. Biochem Biophys Res Commun **345:**1621-33.
215. **Ulrich, L. E., E. V. Koonin, and I. B. Zhulin.** 2005. One-component systems dominate signal transduction in prokaryotes. Trends Microbiol **13:**52-6.
216. **VanRheenen, S. M., G. Dumenil, and R. R. Isberg.** 2004. IcmF and DotU are required for optimal effector translocation and trafficking of the Legionella pneumophila vacuole. Infect Immun **72:**5972-82.
217. **Vinogradov, E., M. B. Perry, and J. W. Conlan.** 2002. Structural analysis of Francisella tularensis lipopolysaccharide. Eur J Biochem **269:**6112-8.
218. **Vodovar, N., M. Vinals, P. Liehl, A. Basset, J. Degrouard, P. Spellman, F. Boccard, and B. Lemaitre.** 2005. Drosophila host defense after oral infection by an entomopathogenic Pseudomonas species. Proc Natl Acad Sci U S A **102:**11414-9.
219. **Vogel, J., and C. M. Sharma.** 2005. How to find small non-coding RNAs in bacteria. Biol Chem **386:**1219-38.
220. **Wang, R. F., and S. R. Kushner.** 1991. Construction of versatile low-copy-number vectors for cloning, sequencing and gene expression in Escherichia coli. Gene **100:**195-9.
221. **Whipp, M. J., J. M. Davis, G. Lum, J. de Boer, Y. Zhou, S. W. Bearden, J. M. Petersen, M. C. Chu, and G. Hogg.** 2003. Characterization of a novicida-like subspecies of Francisella tularensis isolated in Australia. J Med Microbiol **52:**839-42.
222. **White, J. D., M. H. McGavran, P. A. Prickett, J. J. Tulis, and H. T. Eigelsbach.** 1962. Morphologic and Immunohistochemical Studies of the Pathogenesis of Infection and Antibody Formation Subsequent to Vaccination of Macaca irus With an Attenuated Strain of Pasteurella tularensis: II. Aerogenic Vaccination. Am J Pathol **41:**405-413.
223. **Williams, M. D., T. X. Ouyang, and M. C. Flickinger.** 1994. Starvation-induced expression of SspA and SspB: the effects of a null mutation in sspA on Escherichia coli protein synthesis and survival during growth and prolonged starvation. Mol Microbiol **11:**1029-43.
224. **Wilson, M., McNab, R., Henderson, B.** 2002. Bacterial Disease Mechanisms. Cambridge University Press, Cambridge.
225. **Wu, T. H., J. A. Hutt, K. A. Garrison, L. S. Berliba, Y. Zhou, and C. R. Lyons.** 2005. Intranasal vaccination induces protective immunity against intranasal infection with virulent Francisella tularensis biovar A. Infect Immun **73:**2644-54.
226. **Wulff-Strobel, C. R., A. W. Williams, and S. C. Straley.** 2002. LcrQ and SycH function together at the Ysc type III secretion system in Yersinia pestis to impose a hierarchy of secretion. Mol Microbiol **43:**411-23.
227. **Zilinskas, R. A.** 1997. Iraq's biological weapons. The past as future? JAMA **278:**418-24.